Effects of lake trophic state and seasonal cycling on production and bioaccumulation of methylmercury in Te Arawa Lakes

A thesis

submitted in fulfilment

of the requirements for the degree

of

Doctor of Philosophy in Environmental Science

at

The University of Waikato

by

GRACE-LYNN CHONG

THE UNIVERSITY OF
WAIKATO
Te Whare Wānanga o Waikato

2025

Abstract

There are natural sources of Mercury in New Zealand, primarily derived from volcanic activity and geothermal vents. Mercury (Hg) and its organic derivative, methylmercury (MeHg), are highly toxic to both the environment and human health. Of particular concern is the ability of MeHg to bioaccumulate in aquatic food webs, leading to increased toxicity in higher trophic organisms. Given that fish constitute a significant component of the local diet, comprehensive monitoring of Hg and MeHg concentrations is essential for developing effective mitigation strategies. Such efforts are critical to controlling Hg contamination in the environment and aquatic biota, as well as informing the public about lakes with elevated mercury levels. Previous Hg studies in New Zealand have been limited in scope, with monitoring efforts focused on only a few lakes rather than a comprehensive assessment across multiple ecosystems. Additionally, most existing research has primarily examined elemental Hg, with limited investigation into the distribution and bioavailability of MeHg.

This study aims to comprehensively assess Hg and MeHg concentrations in 11 lakes of the Taupo Volcanic Zone. The study assessed Hg and MeHg concentrations in lake water and aquatic biota, including trout, crayfish (koura), and mussels (kakahi). To achieve this, Hg and MeHg in the water were measured using diffusive gradients in thin films (DGT) samplers, while tissue analyses determined Hg, MeHg and additional trace elements in the selected species. The findings of this study are expected to clarify the distribution and bioaccumulation of Hg and MeHg within lake ecosystems and to elucidate their transfer through the aquatic food web. These results will provide a scientific basis for assessing ecological and human health risks associated with mercury exposure, particularly for culturally and recreationally important species. The outcomes will inform lake management and monitoring strategies by identifying key pathways of mercury uptake and potential bioindicator species, and may guide the development of targeted mitigation measures, such as catchment management or advisories on species consumption. Collectively, this research will support evidence-based decision-making for freshwater ecosystem protection and long-term contaminant management.

The results of this study revealed that total mercury (THg) and MeHg concentrations in trout, koura, and kakahi from Lakes Rotorua, Rotoiti, and Rotomahana exceeded WHO recommended safety thresholds. This study also found

that a substantial proportion of THg was comprised of MeHg, which was predominantly accumulated in muscle tissue, whereas THg was primarily concentrated in the liver. The findings further indicated that eutrophication, lake stratification and hypolimnetic anoxia contribute to the enhanced production and bioaccumulation of Hg and MeHg within these aquatic systems. Additionally, selenium (Se) demonstrated a potential protective effect against MeHg toxicity in aquatic organisms.

Acknowledgements

First and foremost, I give all glory to God for giving me the strength to persevere through this long-suffering journey. I would also like to express my deepest gratitude to my partner, for your patience and unwavering support throughout the many years of my study. Thank you for standing by my side until the very end and for never giving up on me. I could not have done this without you. This thesis would not have been possible without your constant encouragement and assistance. I wholeheartedly dedicate the completion of my PhD journey to you.

I also want to express my gratitude to my parents for their encouragement and persistence in pushing me to the finish line, despite the countless times I wanted to give up. Thank you, Mummy and Daddy, for believing in me and for all your prayers throughout the years. I could never see the light at the end of this seemingly endless tunnel, but it was your guidance that led me through. This achievement is for both of you!

Finally, I would like to thank my supervisor, Nick Ling, for your patience, support, and understanding in helping me complete this thesis. Thank you for your guidance and direction throughout this research. Once again, I would not have reached this milestone without your help over these many years. So, from the bottom of my heart, thank you.

Nomenclature

Abbreviations

Δg	diffusive layer thickness
µg	microgram
µL	microlitre
3-MFSG	3-mercaptopropyl functionalized silica gel
A	sampler area exposed
AAS	atomic absorption spectroscopy
ACS	American Chemical Society
AFS	atomic fluorescence spectrometer
Ag	silver
AgI	silver iodide
Ag_2S	silver sulphide
Al	aluminium
AMP	ammoniummolybdophosphate
APA	polyacrylamide with agarose-derivative crosslinker
As	arsenic
B	boron
Ba	barium
BAF	bioaccumulation factor
Bi	bismuth
C	Celsius
CA	California
Ca^{2+}	calcium ion
Cb	porewater concentration coefficient
Cd	cadmium
CE	capillary electrophoresis
CFL	compact fluorescent lamps
Cl	chloride

Co	cobalt
Cr	chromium
Cs	cesium
CTD	conductivity, temperature, depth profiler
Cu	copper
CVAFS	cold vapor atomic fluorescence spectroscopy
Cys	cysteine
D	mercury/ MeHg diffusion
Dt	diffusion coefficient at temperature
D25	diffusion coefficient of ions in water at 25°C
DGT	Diffusive gradients in Thin-Films
DMA	direct mercury analyzer
DOC	dissolved organic carbon
DOM	dissolved organic matter
DW	dry weight
EQS	Environmental Quality Standard
FDA	Food and Drug Administration
Fe	iron
Ga	gallium
GPX	glutathione peroxidase
GST	glutathione-S-transferase
H_2O_2	hydrogen peroxide
HCl	hydrochloric acid
Hf	hafnium
Hg	mercury
Hg(0)	elemental mercury
HCO_3^-	bicarbonate ion
Hg^{2+}	mercury (II) cation
Hg(II)	mercury (II) cation
$HgCl_2$	mercury chloride

HgSe	mercury selenide
HNO_3	nitric acid
HgO	mercury oxide
HgS	mercury sulfide
HPLC	high performance liquid chromatography
HS-GC	head space gas chromatography
HVOD	hypolimnetic volumetric oxygen depletion
ICPMS	inductively coupled plasma mass spectrometer
ID-GC	isotopic dilution gas chromatography
IPCS	International Programme of Chemical Safety
K^+	potassium ion
kg	kilogram
km	kilometre
L	litre
LakeSPI	Lake Submerged Plant Indicators
LC	liquid chromatography
Li	lithium
m	metre
M	Mass accumulated in resin
M	Molar
MBL	mixed binding layer
MDL	method detection limits
MeHg	methylmercury
mEq	milliequivalent
mg	milligram
Mg^{2+}	magnesium ion
ml	millilitre
mm	millimeter
mM	millimolar
Mn	manganese

Mn (III)	manganese trivalent
MnO_2	manganese dioxide
Mo	molybdenum
n	sample size
Na^+	sodium ion
NaCl	sodium chloride
$NaNO_3$	sodium nitrate
Nb	niobium
ND	not detected
ng	nanogram
Ni	nickel
NIWA	National Institute of Water and Atmospheric Research
P	phosphorus
Pb	lead
Ppb	parts per billion
PQL	practical quantitation limits
PVC	polyvinyl chloride
pH	potential of hydrogen
QQQ	triple quadrupole
Rb	rubidium
ROS	reactive oxygen species
S	sulfur
S^{2-}	sulphide ion
Sb	antimony
Se	selenium
SeCys	selenocysteine
SeMet	selenomethionine
SH-CNP	thiol-modified carbon nanoparticle
Si	silicon
Sn	tin

SO_4^{2-}	sulphate ion
SOD	superoxide dismutase
SPR-IDA	suspended particulate reagent-iminodiacetate
Sr	strontium
SRB	sulphate-reducing bacteria
t	time exposed
t	temperature
Ta	tantalum
Te	tellurium
TEMED	tetramethylethylenediamine
Th	thorium
Ti	titanium
THg	total mercury
Tl	thallium
TLI	trophic level index
TMAH	Tetramethylammonium hydroxide
TMF	trophic magnification factors
TP	total phosphorus
TU	thiourea
TVZ	Taupo Volcanic Zone
TXNRD	thioredoxin reductase
U	uranium
UK	United Kingdom
USA	United States of America
UN	United Nations
UNEP	United Nations Environment Programme
UV	ultraviolet
V	vanadium
v/v	volume per volume
W	tungsten

WW	wet weight
WHO	World Health Organization
Zn	zinc
Zr	zirconium

List of Figures

List of Tables

Table of Contents

1 Introduction

1.1 Background

The mercury poisoning disaster in Minamata Bay, Japan, during the 1950s marked a pivotal moment in global recognition of the severe human health and environmental risks posed by mercury pollution (Basu et al., 2023). This event ultimately led to the adoption of the Minamata Convention on Mercury in 2013, an international treaty aimed at protecting human health and the environment through the reduction of anthropogenic mercury emissions and releases ("Minamata Convention on Mercury: Text and Annexes," 2024). The Convention underscores the widespread occurrence of mercury, a naturally occurring element that has been extensively used in industrial processes and consumer products, including batteries, fluorescent lamps, and artisanal gold mining (UN Environment, 2019). Ongoing releases from these activities have contributed to mercury's global dispersion and long-term persistence in the environment, reinforcing the need for coordinated international management (UN Environment, 2019). A central provision of the Minamata Convention is the regulation of mercury across its entire lifecycle. This includes measures to minimize its use in products and processes, phase out unnecessary applications, and control emissions from major industrial sources such as coal combustion and cement production. The Convention further emphasizes the environmentally sound management of mercury waste and seeks to curb mercury use in artisanal and small-scale gold mining, one of the largest sources of mercury pollution (UN Environment, 2019).

The preamble to the Minamata Convention on Mercury frames mercury as a chemical of global concern, reflecting its distinctive environmental behaviour and toxicological risks. It acknowledges mercury's ability to undergo long-range atmospheric transport, its persistence in ecosystems, and its capacity to bioaccumulate in ogranisms, resulting in significant adverse effects on both human health and biodiversity. By 2024, 151 countries had become parties to the Convention, demonstrating widespread international commitment to mitigating mercury's harmful impacts. The Minamata Convention represents a critical step in advancing global cooperation and implementing comprehensive strategies to address mercury pollution and its associated risks. ("Minamata Convention on Mercury: Text and Annexes,"

2024).

The toxicity of mercury poses significant risks to both human health and the environment, making its monitoring and management a critical global necessity. The measurements of mercury concentrations and its various chemical forms within local ecosystems are essential for understanding the extent of contamination and mitigating its adverse effects. While mercury pollution in many parts of the world is predominantly anthropogenic, New Zealand presents a unique case where natural sources are the primary contributors (Nriagu, 1989; Timperley & Hill, 1997). In New Zealand, volcanic and geothermal activities are responsible for most of the mercury emissions into the environment, distinguishing it from regions where human-made emissions dominate (Chrystall & Rumsby, 2009). Natural emissions from sources such as geothermal activities are not part of the Minamata Convention. However, New Zealand signed the Minamata Convention on Mercury in 2013 but it has not yet ratified it. As such, this signing is not binding on the country as yet. The New Zealand government is still consulting on proposals with the Ministry of Environment to strengthen its controls on mercury (Ministry for the Environment, 2020).

The natural release of mercury in New Zealand occurs through volcanic eruptions and geothermal vents, which introduce mercury into the atmosphere and aquatic systems. Atmospheric mercury deposition takes place near volcanic areas as gaseous mercury is emitted from volcanic fumaroles and geothermal features (Pan et al., 2024). Similarly, geothermal vents release mercury directly into lakes, creating localized hotspots of mercury contamination in water bodies. This distinct environmental context necessitates targeted monitoring strategies to assess mercury levels in areas affected by geothermal and volcanic activity (Weissberg & Zobel, 1973).

One of the primary regions of focus for mercury monitoring in New Zealand is the Taupo Volcanic Zone, an area characterized by high geothermal and volcanic activity. As an island nation surrounded by the Pacific Ocean, New Zealand faces significant concerns regarding mercury contamination in seafood, particularly in marine fish occupying higher trophic levels. Given the importance of seafood and freshwater fish in the New Zealand diet (Young, 2009) and the potential health risks associated with mercury exposure, monitoring and understanding mercury levels in marine fish is crucial for safeguarding public health and ensuring the sustainability of

marine resources (Sadhu et al., 2015).

Research in this region has investigated mercury concentrations in lake waters as well as in aquatic organisms (Brooks et al., 1976, Kim and Burggraaf, 1999, Verburg et al., 2014). Monitoring mercury in aquatic systems is particularly important because mercury exists in multiple forms, including elemental mercury, inorganic mercury, and MeHg, each with different degrees of toxicity and environmental persistence. MeHg, a highly toxic organic form of mercury, is of particular concern due to its propensity to bioaccumulate in aquatic organisms and biomagnify through the food web (Verburg et al., 2014). As mercury moves up the trophic levels, its concentration increases, posing significant health risks to predators, including fish-eating birds, mammals, and humans who consume contaminated fish (Dragan et al., 2023).

To gain a comprehensive understanding of mercury pollution and its ecological and human health implications, it is not sufficient to measure mercury concentrations in water alone, as such measurements do not capture mercury bioavailability, uptake by organisms, or its potential for biomagnification within aquatic food webs. Monitoring mercury levels in aquatic biota provides critical insights into the bioavailability of mercury and bioaccumulation. Studies that examine mercury content in fish, shellfish, and other aquatic organisms offer a clearer picture of the ecological and health implications of mercury contamination. Such research also informs risk assessments and the development of guidelines for safe fish consumption, helping to protect both wildlife and human populations from mercury exposure.

In summary, New Zealand's mercury emissions are driven largely by natural geothermal and volcanic processes, creating a distinctive environmental scenario that requires specialized monitoring approaches. The focus on lake water systems in regions like the Taupo Volcanic Zone has provided valuable but limited data on mercury concentrations and its behaviour in aquatic ecosystems. These studies that have been undertaken generally examined a small number of lakes such as Kim and Burggraaf in 1999 had examined five Te Arawa Lakes while Verburg (2014) only investigated three lakes. Continued research and monitoring are needed for a more accurate risk assessment of naturally occurring mercury in a majority of the Te Arawa Lakes and for developing strategies to limit its adverse impacts.

1.2 Thesis Aim

The primary aim of this research was to investigate the cycling, bioavailability, and bioaccumulation of mercury species, including total mercury (THg) and MeHg, within the Rotorua lakes ecosystem, with the goal of enhancing understanding of ecological and human exposure risks. A key focus was on quantifying mercury concentrations in lake water across multiple sites using Diffusive Gradients in Thin-films (DGT) samplers. These passive samplers allow continuous monitoring, offering a more comprehensive temporal and spatial representation of mercury dynamics compared to traditional grab sampling, and provide simultaneous measurement of inorganic and organic mercury forms to assess total bioavailable mercury and the fraction present as MeHg.

A second objective was to develop and validate robust laboratory methodologies for the analysis of THg and MeHg using High-Performance Liquid Chromatography coupled with Inductively Coupled Plasma Mass Spectrometry (HPLC-ICPMS). Establishing reliable analytical protocols was essential for accurately quantifying low-level mercury species, ensuring reproducibility of measurements and enabling the potential standardization of DGT-based monitoring approaches. This methodological foundation supported the broader goal of producing high-quality data to understand mercury dynamics in complex freshwater systems.

The study also examined mercury bioaccumulation across multiple trophic levels by analyzing tissues of key aquatic species, including freshwater mussels, crayfish, rainbow trout, and brown trout. Tissue-specific measurements of THg and MeHg allowed assessment of biomagnification patterns, while liver analysis provided insights into detoxification and storage processes. This approach aimed to elucidate how mercury is absorbed, transported, and retained within organisms, and how differences in species, trophic level, and feeding behavior influence overall exposure and ecological risk. As past studies only examined a handful number of lakes, this research aimed to investigate as many of the Te Arawa lakes as possible (11 lakes) to give a fuller, complete data to our mercury lake studies.

In addition to mercury analysis, the research explored the interactions of selenium and manganese with mercury in aquatic systems. Selenium was investigated for its potential protective role, forming stable complexes with mercury and reducing

its bioavailability and toxicity in organisms. Manganese was examined for its influence on mercury mobility and methylation in lake water, with a focus on redox-dependent adsorption and release processes. These analyses aimed to clarify how chemical interactions within the environment modulate mercury cycling, bioavailability, and ecological impact.

Finally, this study evaluated the influence of environmental factors, particularly eutrophication and other water quality parameters, on mercury dynamics. Nutrient enrichment and resulting anoxic conditions can enhance microbial methylation, increasing MeHg production, while biomass dilution may alter apparent concentrations in biota. By integrating water column measurements, biotic tissue analysis, and environmental assessments, this research adopted multifaceted approach to characterize mercury cycling and bioaccumulation in the Rotorua lakes, providing insights critical for environmental management, risk assessment, and protection of both ecosystem and human health.

1.3 Thesis Outline

Chapter 2 thoroughly reviews the key literature of mercury and its various cycling pathways in the environment that are relevant to the thesis aim. The literature review first overviews the fundamentals of mercury and MeHg species. It then depicts how mercury and MeHg are bioaccumulated in aquatic organisms, with a clearer explanation of its distribution and transformation in biological tissues. This is followed by looking into various lakes' trophic states that would influence the production of Hg and MeHg. Additionally, the literature review explores the diffusive gradient thin-films (DGT) technique that is used in this study.

The subsequent three chapters summarize the findings of this study, whereby chapter 3 discussed on method development to accumulate MeHg in an aquatic environment by using a passive sampler such as the DGT, while also delving into the separation and identification of MeHg using a combination high performance liquid chromatography – inductively coupled plasma mass spectrometer (HPLC-ICPMS) which is a first in New Zealand for both DGT and HPLC-ICPMS.

Chapter 4 details the major mercury and MeHg results obtained in 11 lakes.

The chapter summarises the concentration of THg and MeHg found in water and also in kakahi, koura and trout. It then delves deeper into the comparison of THg and MeHg in tissues and liver of the three sampled aquatic species. Finally, it looked into how mercury bioaccumulates up the food chain.

Chapter 5 expounds on the lakes trophic states and its impact on THg and MeHg. Various factors such as anoxic hypolimnion and eutrophication create the perfect environment to methylate elemental mercury into MeHg. It also investigates the relationship of trace elements such as selenium and manganese have with mercury. Chapter 6 summarises the major findings of the research and provides recommendations for areas of future work.

2 Literature Review

2.1 Mercury

Mercury, named after the swiftest planet in our solar system due to its rapid orbit around the Sun, is an element with unique properties that have captivated human interest throughout history. Its chemical symbol, "Hg," originates from its ancient Greek name ‘hydrargyrum’, signifying "liquid silver" owing to its reflective and silvery appearance. This elemental form of mercury possesses an atomic number of 80 and a relative atomic mass of approximately 200.592. Notably, mercury is the only metal that remains liquid at standard temperature and pressure conditions, setting it apart from other elements in this regard. Historically, mercury was extracted by heating cinnabar ore (mercury (II) sulfide or HgS), a source of vivid red pigment, to temperatures around 580°C, resulting in the separation and collection of elemental mercury as a liquid residue (Britannica, 2025).

Mercury has been extensively utilized throughout history for various applications, particularly in gold and silver extraction processes due to its capacity to form amalgams with these metals as well as zinc and cadmium (Lacerda & Salomons, 1998). Amalgamation techniques involve heating mercury to separate precious metals from their ores, followed by the distillation of mercury to yield refined metal. Beyond mining, amalgam alloys have been employed in dentistry for tooth fillings because they are malleable, durable, and cost-effective (Bates, 2006).

Mercury's ability to form stable compounds with numerous elements has led to its incorporation into diverse industrial products. For instance, inorganic mercury such as mercury chloride ($HgCl_2$) was formerly used as a disinfectant; mercury sulfide (HgS), known for its bright red color, is utilized in pigments; and mercury oxide (HgO) is an essential component in certain battery types. Additionally, elemental mercury (Hg(0)) has been commonly employed in scientific instruments such as thermometers and barometers, while its vapor form contributes to the functionality of fluorescent light bulbs.

Mercury exists in organic forms, notably MeHg and ethylmercury. These compounds are primarily formed by the binding of mercury to methyl or ethyl groups. While both exhibit similar cellular behavior, ethylmercury has a shorter excretory half-

life in humans compared to MeHg (Berlin et al., 2007). MeHg stands out as the most toxic form due to its propensity for bioaccumulation and biomagnification in aquatic ecosystems, leading to significant human exposure through consumption of fish. There has been extensive research on MeHg which underscores its detrimental effects, highlighting the necessity for stringent regulatory measures and public awareness regarding mercury exposure risks.

Despite its widespread use across industrial and medical fields, the toxic effects of mercury have garnered significant attention due to adverse health outcomes among individuals exposed to mercury compounds. Ingestion or inhalation of mercury can result in severe neurological damage, manifesting as coordination issues, blindness, numbness, and potentially leading to paralysis and death. Research has further implicated mercury poisoning in chronic degenerative diseases like Parkinson's disease and Alzheimer's disease, as well as cardiovascular disorders (Johnson & Atchison, 2009; Monnet-Tschudi et al., 2006; Mutter et al., 2010).

2.1.1 Mercury in the environment

Mercury, an environmental contaminant, exists as a stable chemical element that cannot be created or destroyed. The quantity present on Earth has remained constant since its formation. Natural production from the Earth's crust occurs at an estimated rate of 10,000 tons per year (Ehrlich & Newman, 2008).

The cycling of mercury in the environment involves complex interactions between natural and anthropogenic activities. Natural sources include volcanic emissions, wind-borne dust, geysers, thermal fluids, and sea-spray. Anthropogenic contributions are significant, with coal combustion being a major source, responsible for a substantial portion (two-thirds) of global atmospheric mercury emissions (Pirrone et al., 2010). Estimates of annual global mercury emissions (from all sources) range from 2,000 to 6,000 tons, reflecting the uncertainty associated with natural emission rates (Fergusson, 1990; Morel et al., 1998; Morita et al., 1998).

Mercury undergoes a series of biological, chemical, and physical transformations as it cycles through the atmosphere, land, and water. This cycling results in widespread exposure to mercury for humans, plants, and animals, leading to various ecological and human health impacts (Keating et al., 1997). Mercury cycling has been significantly altered by human activities since the onset of the industrial era.

Estimates suggest that approximately 4,000 tons of mercury are released into the atmosphere annually due to anthropogenic sources (Mason et al., 1994). Mercury and its compounds have been extensively used in various industries, including electrical goods production, catalysis, pulp and paper manufacturing, pigments, dental applications, and pesticide formulations. Notably, about half of anthropogenic mercury emissions stem from the electrolysis of brine to produce caustic soda and chlorine (Arrighi et al., 2024). Due to its wide application and volatility, mercury has become a global pollutant found even in remote regions such as deep oceans, atmospheres, Antarctic regions, and Arctic environments (Fergusson, 1990).

Recent research has focused on the biogeochemistry of mercury within these systems. In the atmosphere, mercury predominantly occurs as elemental mercury vapor (Hg0), which can remain airborne for up to a year, facilitating long-range transport across thousands of miles from emission sources ((Driscoll et al., 2013)). Oxidized forms like Hg(II) and MeHg typically constitute less than 2% of atmospheric mercury concentrations (Fitzegerald, 1989; Si et al., 2022).

Mercury methylation involves the conversion of inorganic mercury to mono- and diMeHg by microorganisms, though abiotic processes also play a role (Compeau and Bartha, 1985; Weber, 1993; Hintelmann et al., 1995; Lin et al., 2021). This process is primarily observed in soils and sediments under both aerobic and anaerobic conditions, favoring neutral to acidic pH levels. Factors influencing methylation include temperature, sulfide concentration, organic and inorganic ligands, pH, and redox conditions. In aquatic environments, mercury predominantly exists as inorganic species (Hsu-Kim et al., 2013). While rocks, sediments, water, and soils naturally contain trace amounts of mercury, certain geological formations and thermal springs can have elevated levels. For instance, groundwater near the surface in remote areas of Wisconsin has been measured to contain total mercury concentrations ranging from 2–4 ng/L (Krabbenhoft & Babiarz, 1992). In California, lake and river samples showed total mercury concentrations between 0.5 and 104 ng/L (Gill & Bruland, 1990).

Overall, the biogeochemical cycling of mercury is influenced by various environmental factors and anthropogenic activities, leading to its widespread presence and bioaccumulation in terrestrial and aquatic ecosystems.

2.1.2 Mercury speciation into Methylmercury

Mercury undergoes methylation, a biogeochemical process that converts inorganic mercury into MeHg, the most toxic and bioaccumulative form of the element. This transformation plays a central role in controlling mercury mobility, persistence, and ecological risk within aquatic environments. Atmospheric deposition introduces mercury primarily as elemental mercury (Hg^0), inorganic divalent mercury (Hg^{2+}), and, to a lesser extent, MeHg, with Hg^{2+} representing the dominant deposited species (Fitzgerald and Clarkson, 1991). Once deposited, Hg^{2+} serves as the principal substrate for microbial methylation, linking atmospheric inputs to the formation of MeHg and its subsequent bioaccumulation in aquatic food webs.

Upon entering surface water bodies, mercury engages in a complex cycle where it can undergo various transformations. Mercury attached to particles may settle into sediments, from which it can diffuse back into the water column or be resuspended by hydrodynamic forces. Additionally, sediment-bound mercury can be buried under newer layers of sediment or undergo methylation, facilitated primarily by microbial activity (Fitzgerald & Clarkson, 1991). MeHg generated through these processes can enter the aquatic food chain and bioaccumulate in higher trophic levels, posing significant risks to human health via consumption of contaminated fish. Conversely, MeHg can also be released back into the atmosphere through volatilization (Baya et al., 2015). Exposure to sunlight, particularly ultraviolet (UV) radiation, has a detoxifying effect on mercury compounds. UV light can catalyze the breakdown of MeHg into inorganic forms such as Hg^{2+} or elemental mercury (Hg°), which are then more likely to volatilize and re-enter the atmosphere as gases (Baya et al., 2015). This photodegradation process highlights the dynamic nature of mercury cycling between aquatic environments and the atmosphere, influenced by both biological and photochemical mechanisms.

The transport and speciation of mercury in aquatic environments are significantly influenced by its interactions with various ligands, including dissolved organic matter (DOM). These interactions affect the chemical properties and mobility of mercury, particularly in sediment systems where concentrations of both mercury and complexing ligands can be high (Coulibaly et al., 2016).

Dissolved Organic Matter (DOM) plays a particularly important role in

controlling mercury speciation. Dissolved organic matter is found in higher concentrations in sediment porewater than in surface water, strongly binding with mercury and often outcompeting other strong ligands such as sulfide (Ravichandran, 2004). This complexation can reduce the concentration of freely dissolved mercury below its solubility limit with solids, influencing solid-phase partitioning. Furthermore, DOM enhances the solubility and mobility of mercury in river systems (Mierle and Ingram, 1991), and its concentrations have been shown to correlate with the solid-liquid partitioning coefficient for mercury (Bloom et al., 1999).

Mercury methylation is particularly influenced by sediment redox conditions and dissolved mercury speciation. Aquatic systems play a critical role in this process, as they act as long-term sinks for deposited mercury while simultaneously providing redox conditions that promote both the production and degradation of MeHg (Fitzgerald et al., 2007). Within these systems, mercury methylation commonly occurs as a by-product of microbial sulfate reduction, requiring bioavailable inorganic mercury, suitable reducing conditions, and sufficient organic carbon to support microbial activity (Compeau and Bartha, 1985; Gilmour et al., 1992).

In sediment systems, steady-state MeHg concentrations are maintained through a balance between methylation and demethylation processes. Methylation is predominantly controlled by biological activity, while demethylation involves both chemical and biological mechanisms (Warner et al., 2003). DOM has been shown to either enhance or inhibit mercury methylation (Weber, 1993; Miskimmin, 1991), with enhancement likely due to increased bioavailable mercury and microbial activity from the presence of organic matter. However, high concentrations of DOM can also reduce the availability of the most bioactive forms of mercury.

The ratio of MeHg to total mercury provides critical insights into the balance between methylation and demethylation processes within sediment systems. High methylation rates relative to demethylation result in higher percentages of MeHg, whereas low methylation rates lead to lower MeHg percentages (Kannan et al., 1998). In sediment environments, absolute MeHg concentrations are important for assessing risk and biota exposure; however, the percentage of dissolved porewater mercury that is MeHg serves as a more direct indicator of MeHg productivity within the system (Li et al., 2010). Solid-bound mercury is generally considered less available for methylation compared to its aqueous counterpart. Consequently, the ratio of MeHg to

total mercury in porewater more accurately reflects the active methylation processes occurring in sediment systems. In productive systems, MeHg can comprise between 10 and 80% of the total mercury present in porewater, while solid-phase mercury typically contains less than 5% MeHg. This significant difference in partitioning behavior between organic (MeHg) and inorganic mercury species has substantial implications for the relative composition of mercury in both aqueous and solid phases. Due to these differences, solid-phase sampling may not accurately estimate the amount of MeHg present within a sediment system. The variability in MeHg percentages across different systems is influenced by the unique biological and chemical conditions present in each porewater environment (Kannan et al., 1998).

In summary, the percentage of MeHg relative to total mercury in porewater offers a more reliable indicator of methylation productivity compared to solid-phase measurements (Coleman Wasik et al., 2012). This emphasizes the importance of considering both partitioning dynamics and environmental factors when assessing MeHg concentrations and potential risks in sediment systems.

2.1.3 Mercury mobility (redox reactions)

The speciation of mercury in sediment systems is further complicated by redox conditions. In reducing environments where sulfide is present, it dominates mercury speciation; whereas in oxic or less strongly reduced environments lacking sulfide, other ligands such as chloride, hydroxide, thiols, and DOM control mercury speciation (Benoit et al., 1999). In non-steady-state redox conditions, changes in pH and other parameters can further alter the availability and mobility of mercury (Cappuyns & Swennen, 2005).

Mercury often occurs in precipitated solids such as sulfides under reducing conditions, where it can either complex directly with sulfides or adsorb onto metal-sulfide surfaces. The mobilization of mercury from these solid phases is primarily influenced by changes in redox conditions; specifically, the oxidation of reduced sediments can lead to significant increases in mobile mercury concentrations. This phenomenon has been extensively studied, particularly focusing on mercury-sulfide speciation and solubility constants (Paquette and Helz 1995). However, much of this research (Benoit et al., 1999, 2001) has concentrated on higher sulfide concentrations (>50 mM), which are indicative of strongly reducing environments.

Although there is substantial literature on metal release due to the oxidation of reduced sediments (Simpson 1998; Atkinson 2007), mercury-specific studies remain limited. Nonetheless, parallels can be drawn from broader research on metal mobilization during sediment resuspension under oxidizing conditions. For instance, not all resuspended anoxic sediments are fully oxidized within short timeframes (Burgess and Kester 2002). As a result, changes in redox conditions during sediment resuspension can alter mercury speciation and solubility, directly affecting the fraction of mercury that is mobile or bioavailable.

Research on arsenic release has demonstrated that dissolved organic carbon (DOC) and iron concentrations play significant roles in arsenic mobilization (Reza et al. 2010), a relationship likely applicable to mercury as well. Mercury's fate within an ecosystem is heavily influenced by pH and DOC levels, with higher acidity and increased DOC content enhancing mercury mobility and facilitating its entry into the food chain (Sophie et al., 2014; French et al., 2014).

The kinetics of metal dissolution from redox changes vary significantly depending on the mineral phase. Studies comparing various metal sulfides reveal that certain minerals, such as manganese sulfide, iron sulfide, nickel sulfide, and copper sulfide, can dissolve within an hour (Simpson et al., 1998). In contrast, zinc sulfide, cadmium sulfide, and lead sulfide may not fully dissolve even after prolonged periods (up to 8 hours).

Dynamic hydrologic systems also influence metal mobilization through changes in water chemistry. While some studies have examined these effects over longer timescales—ranging from months to years—(Vangriethuysen et al., 2005), the immediate release of metals following oxidation can spike within days and stabilize within weeks (Hong, Kinney, and Reible 2011). This is particularly relevant in environments subject to rapid water chemistry changes, such as tidal areas or flood-prone rivers. Despite potential long-term equilibrium, short-term metal releases can occur repeatedly, highlighting the importance of understanding temporal dynamics in mercury mobilization. In summary, the fate and mobility of mercury are influenced by a complex interplay between redox conditions, mineral phases, DOC levels, pH, and dynamic hydrological changes.

2.1.4 Bioaccumulation of mercury and methylmercury

The mechanisms governing mercury's entry into aquatic food chains remain largely understudied and exhibit significant variability across different ecosystems (Wood et al., 1968; Choi et al., 1994). A critical role is played by certain anaerobic bacteria that reduce sulfate and iron, subsequently converting inorganic mercury to MeHg through metabolic processes (Compeau and Bartha, 1985; Gilmour et al., 1992; Fleming et al., 2006). This conversion process is particularly pronounced in oxygen-depleted aquatic environments, where the concentration of MeHg tends to be higher due to the bacteria's anaerobic metabolic activity (Pak and Bartha, 1998; Blum et al., 2013).

Methylmercury is of particular concern in aquatic ecosystems due to its tendency to bioaccumulate and biomagnify through food webs. MeHg is readily taken up by lower trophic organisms such as plankton and then transferred to higher trophic levels, resulting in increasing mercury concentrations at each successive step (Cabana and Rasmussen, 1994). Consequently, top predators and larger fish typically exhibit the highest mercury burdens, which also represents the main route of human exposure through fish consumption. Mercury accumulation depends on the balance between uptake and elimination (Fisher et al., 1995; Wang et al., 1998; Bowles et al., 2001; Lawrence and Mason, 2001), and MeHg is particularly prone to retention due to its high bioavailability and slow elimination, with tissue half-lives ranging from months to years.

Research by Kim and Burggraaf (1999) revealed that the concentration of MeHg in zooplankton, smelts, bullies, and trout correlated linearly with total mercury levels in water. This suggests a rapid cycling of MeHg within these ecosystems. Both total mercury and MeHg chloride contribute to determining MeHg concentrations in these organisms.

In summary, the transformation of inorganic mercury into MeHg by anaerobic bacteria is a critical step that influences the bioaccumulation dynamics across trophic levels within aquatic ecosystems. These processes highlight the potential risks to human health through dietary exposure to contaminated fish and seafood. Further research into the ecological pathways and mechanisms driving these transformations is essential for understanding and mitigating mercury's impacts on both environmental

and public health.

2.1.5 Distribution of mercury and methylmercury in tissues

Understanding the distribution of mercury and MeHg within biological organisms is crucial for assessing both human health risks and ecological impacts. Monitoring tissue-specific concentrations can inform fish consumption advisories and guide recommendations on the relative safety of consuming different parts of fish, such as muscle versus liver. MeHg is particularly significant due to its high bioaccumulation potential and efficient absorption in fish tissues (Wolfe et al., 1998). Once ingested, MeHg readily binds with cysteine-rich proteins, forming complexes that facilitate its distribution throughout the organism. This results in higher concentrations of MeHg in critical organs such as the liver and muscle tissue. The formation of these complexes allows MeHg to cross biological barriers, including the human blood-brain barrier (Roos et al., 2010). Consequently, MeHg can accumulate in brain tissues, posing serious neurological risks. This characteristic underscore the importance of monitoring MeHg levels in fish and developing consumption guidelines that account for its tissue-specific distribution.

The distribution of mercury species within fish tissues, particularly between muscle and liver, remains a complex and poorly understood phenomenon due to inconsistent findings across various studies. Houserova (2006) reported that the highest concentrations of total mercury were found in the muscle tissues (out of organs tested such as gills, liver, kidney and skin) of all tested freshwater fish in his study; muscles contained cysteine rich-proteins where mercury has strong binding affinity (Boening, 2000; Anonymous, 2002). This observation has been corroborated by other researchers such as Anonymous (1999, 2002) and Dusek et al. (2005), who also noted elevated total mercury levels in muscle tissues. John Harley's (2015) study further supported this trend by reporting significantly higher concentrations of total Hg in muscle compared to liver. Most studies (in marine fish) focusing on mercury species in fish muscle support the conclusion that MeHg constitutes more than 80% of the mercury present (Jewett et al., 2003). However, Vigh et al. (1996) reported contrasting findings, noting higher total mercury concentrations in the kidneys of grass carp with lower levels found in gills and skin. Houserova et al. (2006) observed a decreasing trend in total mercury content across different tissues of chub: muscle >> kidney ≈ liver > skin ≈ gills.

Havelkova (2008) observed that the distribution pattern of mercury varied depending on contamination levels along the River Elbe. In lightly contaminated localities as studied by Hvalkova (2008), the pattern was generally muscle > kidney > liver > gonads; however, in heavily polluted areas, this trend was reversed to liver > muscle. Similar variability has been reported by other researchers (Abreu et al., 2000; Berg et al., 2000; Farkas et al., 2000; Kennedy, 2003; Gonzalez et al., 2005; Marsalek et al., 2007). Wang et al. (2005) reported an average of 50% higher mercury concentration in the liver than in muscle from both polluted and non-polluted sampling areas. Honda et al. (1983) found that Hg concentrations were twice as high in the liver compared to muscle in Pagothenia borchgreinki, a species from the Antarctic, an area free of significant anthropogenic pollution with heavy metals. Chen et al. (2004) also concluded that liver mercury concentrations were generally higher than those in muscle tissues across different levels of contamination.

Balshaw et al. (2008) investigated the distribution of mercury in farmed southern bluefin tuna (*Thunnus maccoyii*), found that total mercury composition was inversely related to lipid content, with variation as much as 36% (mean = 0.35 mg/kg vs. mean = 0.23 mg/kg) in different location of muscles taken. This variability could be attributed to differences in octanol-water partitioning dynamics between inorganic and organic species of Hg. Additionally, the lipid composition of muscle tissue can influence the availability of binding sites for mercury on proteins in which a decrease in muscle protein concentration could lead to lower THg concentrations due to reduced availability of cysteine residues (Balshaw et al., 2008).

In summary, while there is general agreement that total mercury levels are higher in fish muscle compared to liver, significant variability exists depending on the specific species, environmental contamination levels, and tissue lipid content. These findings underscore the complexity of mercury bioaccumulation dynamics within different tissues of fish.

2.1.6 Mercury and Methylmercury in New Zealand

Mercury emissions in New Zealand can be broadly categorized into natural and anthropogenic sources. Natural mercury emissions primarily arise from geological activities such as volcanic and geothermal activity, while anthropogenic emissions stem from industrial, medical, dental, electrical, and domestic applications, including

the use of mercury-containing lighting equipment. Based on the 2005 draft of the UNEP Mercury Toolkit, New Zealand's total annual mercury emissions were estimated at approximately 3,000 kg in 2008, with roughly equal contributions from both natural and anthropogenic sources (Chrystall & Rumsby, 2009).

The Mercury Inventory for New Zealand 2008 reported that volcanic emissions represent the most significant natural source, contributing 54% of natural emissions and 28% to the overall emission rate. Anthropogenically, the combustion of fossil fuels (accounting for 440 kg/year) and geothermal power generation (350 kg/year) are major contributors, representing 29% and 23%, respectively, of anthropogenic mercury emissions. Additional significant sources include wastewater biosolids (180 kg/year) and mercury-containing batteries (170 kg/year). Mercury-containing lamps contribute a minor share, emitting approximately 50 kg/year, which constitutes only about 3% of total anthropogenic emissions or less than 2% of the overall mercury emissions. Compact fluorescent lamps (CFLs), comprising roughly one-third of potential emissions from mercury-containing lamps in 2009, are expected to maintain a constant contribution under a high-use scenario if the mercury content per lamp remains unchanged. However, their relative contribution is projected to halve due to increases in total mercury emissions.

On a per capita basis, anthropogenic mercury inventories for New Zealand, Ireland, Canada, the United States, and the United Kingdom are comparable at approximately 10-4 kg/person/year. In contrast, Denmark and Australia exhibit inventories an order of magnitude greater at about 10-3 kg/person/year. Notably, excluding Australia's unquantified mercury releases from roads, its reported emissions are roughly twice those of New Zealand. This discrepancy is largely attributed to differences in primary metal production activities between the two countries (Chrystall & Rumsby, 2009).

New Zealand's unique geological setting at the convergence of the Australian and Pacific tectonic plates provides a significant natural source of mercury emissions through its geothermal activity. Notable sources include White Island and Mt Ruapehu, along with numerous other geothermal areas throughout the country, particularly those located within the Taupo Volcanic Zone (TVZ) in the Waikato and Eastern Bay of Plenty regions. The TVZ (Figure 1) encompasses an area of approximately 6000 km^2 and is characterized by a diverse range of lake water

compositions, possibly unique among global freshwater systems. In this region, sodium (Na+) and potassium (K+) ions often dominate over calcium (Ca2+) and magnesium (Mg2+), reflecting the predominance of rhyolitic rocks in the area. Additionally, small catchments and geothermal fluid contributions create a spectrum of water types ranging from precipitation-like waters to those rich in salts and dilute sulphuric acid. Deep geothermal waters within the TVZ contain significant amounts of sulphide (S^{2-}) rather than SO_4^{2-}. During steam separation, this sulphide is carried as H_2S, which upon contact with air forms sulphuric acid which is the primary ionic component in condensed steam. The presence of naturally occurring geothermal sulphides can elevate mercury concentrations in these waters. Given the unique geochemical characteristics and potential elevated mercury levels, the lakes within the TVZ are targeted locations for this research. These lakes vary significantly in terms of their trophic status (ranging from supertrophic to oligotrophic) as defined by algal biomass concentrations and exhibit marked differences in physicochemistry (Table 8-10).

Limited research exists on the presence of MeHg in fish and its bioaccumulation within aquatic food webs influenced by geothermal emissions. Early studies in New Zealand have reported elevated total Hg concentrations in trout inhabiting lakes affected by geothermal waters (Weissberg & Zobel, 1973; Brooks et al., 1976). Subsequent investigations have examined MeHg levels in trout across various New Zealand lakes with differing degrees of geothermal input (Kim, 1995; Phillips et al., 2009; Verburg et al., 2016). Additionally, variations in MeHg levels between lakes can be attributed to the extent of geothermal water input. For more information, Kim and Burggraaf (1999) reported varying geothermal input (%) into five lakes Okareka (6%), Okaro (6%), Tarawera (37%), Rotorua (43%) and Rotomahana (53%) with varying MeHg (0.09, 0.51, 0.21, 0.23 and 0.36 ng/L) and THg levels in water (0.92, 1.90, 0.57, 1.47 and 4.58 ng/L). He found that MeHg concentrations in zookplanton, smelts, bullies and trout exhibited linear increases with THg in water but not with MeHg.

In summary, although early studies have reported elevated Hg concentrations in trout from geothermally impacted lakes, more recent research has further elucidated the influence of geothermal activity on MeHg bioaccumulation. Factors such as fish size and age, alongside variations in geothermal input, play significant roles in

determining MeHg levels within these aquatic ecosystems.

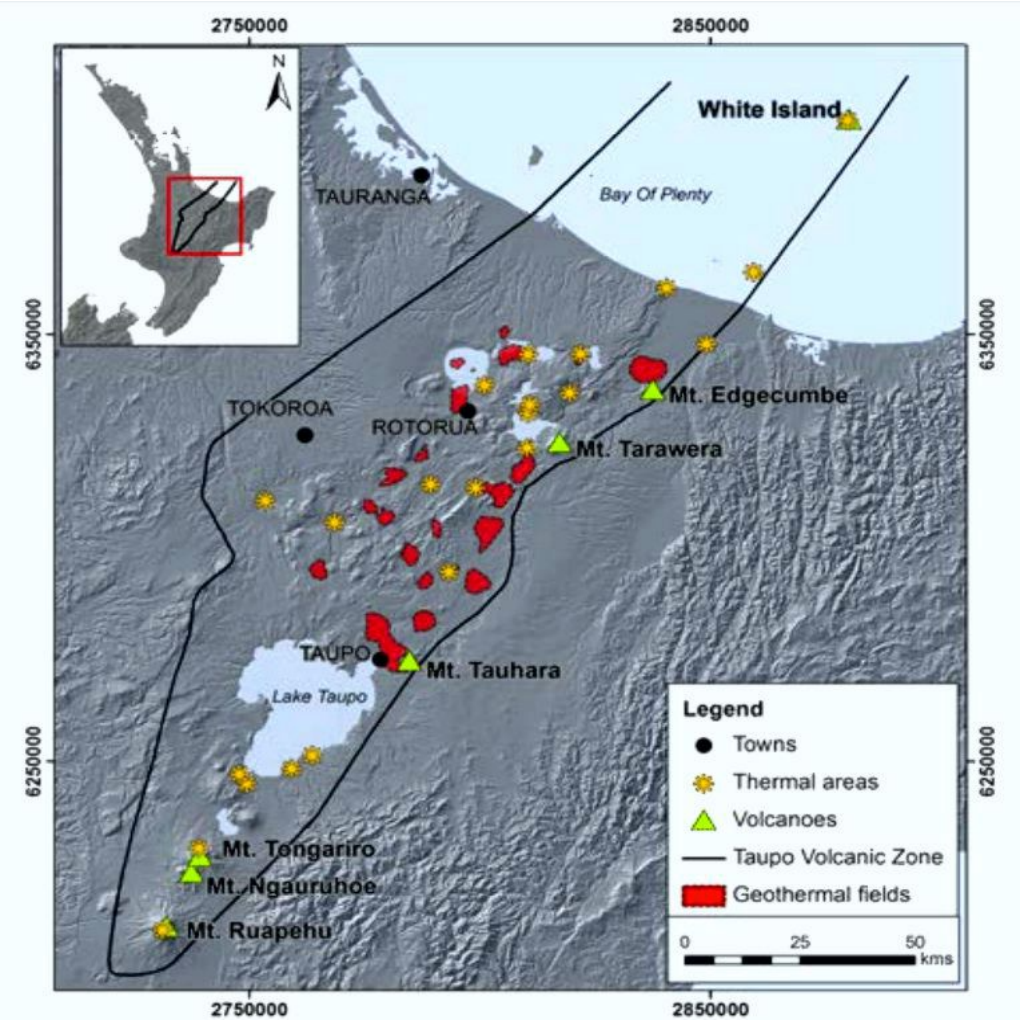

Figure 1: Map of geothermal systems in the Taupo Volcanic Zone [1]

2.1.6.1 Trophic state influence

In a series of multi-lake studies across the United States, researchers have identified various physical, chemical, and ecological factors that influence Hg bioaccumulation and trophic transfer within lake ecosystems. These studies indicate positive correlations between Hg accumulation and both lake size and watershed area, as well as negative associations with human land use, nutrient levels, pH, alkalinity, phytoplankton abundance, and zooplankton biomass (Watras et al., 1998; Kamman et

[1] https://www.researchgate.net/profile/Melissa-Climo-2/publication/316919696/figure/fig3/AS:873621580959745@1585299024543/Map-of-geothermal-systems-in-the-Taupo-Volcanic-Zone_Q640.jpg

al., 2004; Chen et al., 2005; Driscoll et al., 2007; Yu et al., 2011). Contrary to expectations, eutrophic lakes—characterized by high nutrient levels and productivity—are found to harbor lower Hg concentrations in top trophic level fish compared to oligotrophic or mesotrophic lakes. This phenomenon can be partially attributed to biodilution effects where higher zooplankton biomass reduces the concentration of bioavailable mercury (Chen and Folt, 2005; Chen et al., 2005).

The chemical and ecological characteristics of eutrophic lakes may contribute to reduced bioaccumulation and food web transfer of Hg relative to oligotrophic environments. Higher lake water pH and alkalinity levels can reduce the availability of MeHg for bioaccumulation within aquatic food webs (Driscoll et al., 2007). Additionally, abundant food sources in eutrophic conditions can lead to growth dilution effects in fish, further reducing tissue concentrations of Hg compared to their counterparts in oligotrophic settings (Essington and Houser, 2003; Ward et al., 2009). Nutrient enrichment in eutrophic lakes fosters algal blooms that distribute the pool of dissolved inorganic mercury and MeHg across a greater biomass of algal cells. This distribution effect dilutes Hg and MeHg concentrations within algae and their zooplankton consumers (Pickhardt et al., 2002; Luengen and Flegal, 2009). Moreover, elevated algal biomass can alter biogeochemical factors that influence the production of MeHg or enhance its uptake through absorption or ingestion of non-living particulate organic matter.

Verburg et al. (2014) observed discrepancies in Hg biomagnification and trout tissue concentrations between eutrophic and oligotrophic lakes. Their findings, based on trophic magnification factors (TMFs) and biotic ratios, suggested that the most significant degree of biomagnification occurred in the eutrophic lake, contrary to expectations derived from prior research advocating biomass dilution due to high plankton abundance as a mechanism for reducing Hg bioaccumulation. For biomass dilution to effectively mitigate Hg biomagnification in eutrophic environments, Hg concentrations would need to decrease more proportionally in higher trophic level organisms compared to those at lower trophic positions. Verburg's research indicated that the predictive models of Hg biomagnification based solely on phytoplankton densities should be approached with caution.

The study's results highlight those differences in physicochemical properties (pH, dissolved oxygen, alkalinity, anions, temperature) between lakes play a more

significant role in determining Hg biomagnification and concentrations in fish than variations due to biomass dilution from trophic state distinctions (Verburg et al., 2014). This can partly be attributed to the prevalence of low oxygen conditions in bottom waters, conducive to higher MeHg production rates, characteristic of highly productive systems. Additionally, elevated temperatures at the sediment-water interface, common in eutrophic environments, enhance methylation processes and may independently increase Hg concentrations in fish tissues.

Considering the ongoing challenges posed by global climate change, which is likely to exacerbate low oxygen conditions in aquatic ecosystems, the implications for enhanced MeHg production and resultant higher mercury levels in fish are significant. As a result, future research should continue to evaluate these complex interactions under changing environmental scenarios to better understand and mitigate Hg bioaccumulation risks within aquatic food webs.

2.1.7 Toxicological effects

Mercury pollution has long been recognized as a significant environmental health issue due to its toxic effects and the ease with which it bioaccumulates in aquatic ecosystems and subsequently affects human populations. One of the most infamous instances of mercury poisoning occurred in Minamata, Japan, where MeHg contamination of seafood led to severe neurological disorders among local inhabitants (Kiyoura, 1964). Minamata disease was first recognized in 1956 after residents of Minamata, a small city on the southwestern coast of Japan, began exhibiting symptoms such as numbness, tremors, and difficulty speaking. This condition was traced to severe MeHg poisoning, which stemmed from industrial wastewater discharged by Chisso Corporation’s chemical factory into Minamata Bay. The factory's waste contained mercury compounds that were converted into MeHg by microorganisms in the marine environment. As a result, fish and shellfish in the bay became contaminated with high levels of MeHg. This incident highlighted the need for comprehensive biogeochemical assessments that consider all forms of mercury to accurately evaluate its toxicity and bioaccumulation potential.

Mercury pollution has garnered global attention due to its widespread distribution and detrimental health impacts. Short-chain alkyl mercury compounds,

particularly MeHg, have been implicated in poisoning incidents affecting marine life and humans in various locations worldwide (Kiyoura, 1964; Johnels and Westermark, 1969; Morita et al., 1998). Scientific evidence indicates that all mercury species can induce adverse health effects at sufficiently high doses (Friberg and Vostal, 1972; Keating et al., 1997). Organic mercury compounds, especially MeHg, are particularly concerning due to their efficient bioaccumulation in tissues, high stability, and ease of crossing biological membranes (Westoo, 1973; Boudou and Ribeyre, 1985; Friberg et al., 1986; Bloom and Effler, 1990). Once inside cells, mercury can interfere with numerous biochemical processes by binding to thiol-containing biomolecules (Craig, 1986).

Human exposure to MeHg primarily occurs through fish consumption; however, other pathways such as inhalation, ingestion via drinking water and non-fish food sources, and dermal contact with contaminated soil and water can also contribute to toxicity (Keating et al., 1997). MeHg is particularly neurotoxic in humans, with the developing fetus being more susceptible than adults. Consequently, mercury and its organic forms are subject to strict monitoring under national and international regulations, including European Commission Directives (Quevauviller, 1996) and the Minamata Convention of 2013.

World Health Organization/International Programme on Chemical Safety (WHO/IPCS) guidelines provide recommended limits for mercury exposure. For adults, a daily MeHg intake of up to 0.48 mg/kg body weight is considered safe (WHO/IPCS, 1990). A higher intake level between 3 and 7 mg/kg body weight/day has been associated with a 6% increase in paresthesia incidence among adults (WHO/IPCS, 1990). Given individual variability, precise exposure limits are challenging to establish. In response to the Minamata and Niigata poisonings, the U.S. established an administrative guideline of 0.5 μg/g for mercury content in fish and shellfish sold across state lines (FDA, 1969). This limit was adjusted over time; it was elevated to 1.0 μg/g in 1979 and later converted from a total mercury standard to one based solely on MeHg content in 1984 (FDA, 1984).

In conclusion, the widespread distribution and severe health impacts of mercury pollution necessitate stringent monitoring and regulation efforts at both national and international levels. The identification of various exposure pathways and the development of comprehensive guidelines are essential for mitigating risks associated

with MeHg bioaccumulation in aquatic ecosystems and subsequent human consumption. Continued research is vital to refine our understanding of mercury's environmental fate, toxicity, and impact on public health.

2.2 DGT (What is DGT? Binding layers, Uses of DGT, Mechanisms of binding)

Diffusive Gradients in Thin-films (DGT) samplers are widely employed for measuring the bioavailable fraction of contaminants in aquatic environments (porewater, sediment-water interface, sediment and open water). Diffusive gradient in thin-film gel (DGT) was originally developed by Davison and Zhang (Davison, 1999) in order to measure cation concentrations in bulk seawater. Figure 2 shows the conceptual model used in DGT samplers.

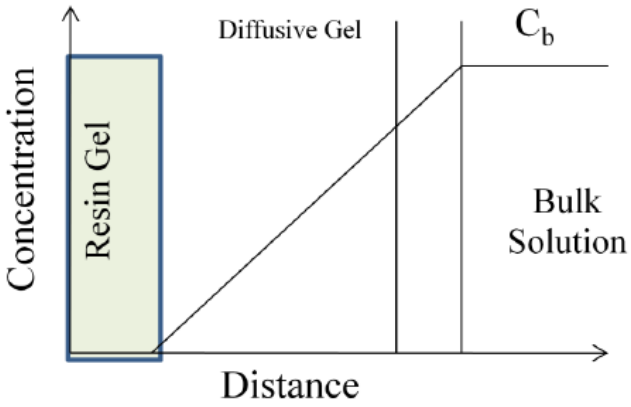

Figure 2: Conceptual model of DGT sampler

The equation describing the mass uptake is:

$$J = \frac{M}{At} = -D\frac{\delta y}{\delta x} = \frac{DC_b}{\Delta g} \rightarrow C_b = \frac{M\Delta g}{DtA}$$

C_b = Water Concentration coefficient

M = Mass accumulated in resin

Δg = Diffuse layer thickness

D = Hg/MeHg diffusion

t = Time exposed

A = Sampler area exposed

The DGT technique captures analytes through a series of diffusional and chemical processes, which require understanding and validation of several fundamental assumptions to ensure accurate measurements. DGT samplers operate under the principle that analytes diffuse through a diffusive gel into a binding layer (resin gel). The diffusive gel acts as a semi-permeable membrane, allowing dissolved species to pass while impeding particulate matter. The resin gel then captures these diffused species through chemical interactions.

Resin gels have a pivotal role in assessing mercury contamination levels within aquatic environments by absorbing significant quantities of dissolved mercury from the surrounding water. Over extended deployment durations—typically several days—the concentration of mercury within the gel matrix approaches an equilibrium state that is practically zero. This state simplifies subsequent calculations aimed at determining the concentration of mercury present in the porewater.

The objective of this methodology is to establish the conditions where diffusion through the resin gel constitutes the principal resistance governing the uptake process, thereby facilitating straightforward correlations between the quantity of mercury absorbed and its concentration in water. The calculation of the water concentration necessitates consideration of several key parameters: the mass of mercury accumulated by the resin gel over time, the diffusion length (a physical characteristic specific to the dimensions of the sampler), the diffusion coefficient (reflecting both dissolved inorganic and organic forms of mercury such as MeHg), the exposed surface area of the resin gel, and the duration of exposure.

The diffusion coefficient is a critical parameter that can be approximated using values for diffusion through water or determined experimentally at the specific site to account for local environmental conditions. It is noteworthy that temperature significantly influences the rate of diffusion; consequently, any diffusion coefficients utilized in porewater concentration calculations must be adjusted according to prevailing temperatures during the sampling period (Chess 2010). This adjustment ensures that the calculated concentrations accurately reflect the conditions under which mercury uptake occurs.

Davison and Zhang 1995 proposed the temperature correction for the diffusion coefficient shown below;

$$\text{Log } D_t = \frac{1.37023\,(t-25)+8.36\,x10^{-4}(t-25)^2}{109+t} + \log \frac{D_{25}(273+t)}{298}$$

D_t = diffusion coefficient at temperature t (cm^2/sec)

D_{25} = diffusion coefficient of ions in water at 25 °C (cm^2/sec)

t = temperature (°C).

DGT samplers rely on several assumptions (Davison and Zhang, 2012) to calculate the bulk concentration of the analyte being measured. The main assumptions are;

1) the geometric values of exposure area and diffuse thickness are well known,

2) analyte interaction with the diffusive layer and filter are negligible,

3) analyte binds to the resin layer at the surface instantaneously,

4) time to steady- state diffusion is negligible relative to deployment time, and

5) colloid-associated analyte species contribute negligibly to DGT uptake

One of the primary assumptions in DGT technology is that the effective exposure area of DGT samplers can exceed their geometric area by up to 20%, as demonstrated by Warnken, Zhang, and Davison (2006). This phenomenon is attributed to the lateral diffusion of analytes into the sampler in addition to perpendicular diffusion. Consequently, this expanded exposure area might result in an overestimation of concentration levels. The effective diffusion thickness encompasses not only the diffusion gel and filter but also incorporates the influence of a diffuse boundary layer, which has been approximated at approximately 0.2 mm (Davison & Zhang, 2012). Despite the larger exposure area and increased diffuse thickness, these factors tend to offset each other, leading to an error margin less than 10% in concentration estimation (Davison & Zhang, 2012).

Another assumption is that the kinetics of analyte binding with the resin layer are sufficiently fast so as not to significantly impact measurement accuracy for deployment times greater than two hours. Experimental evidence indicates that binding kinetics can be on the order of minutes, rendering this assumption generally valid for most deployments (Davison and Zhang, 2012). For example, at higher analyte

concentrations found in contaminated sites, the binding kinetics become even faster. The time to reach steady state is crucial. The time to 95% of steady state is approximated by $\Delta g2/2D$ and time to 99% of steady-state by $\Delta g2/D$. (Garmo, Davison, and Zhang, 2008). For typical DGT samplers, these times are approximately 13 and 27 minutes. These values indicate that deployment times of several hours or more are sufficient to ensure minimal error due to kinetic effects.

Another critical assumption is the negligible impact of colloid-bound species on DGT measurements. This assertion requires careful examination because colloidal complexes can exhibit varying degrees of labilization and diffusion coefficients, affecting the overall uptake kinetics. Labile complexes readily disassociate or diffuse at similar rates as free dissolved species. Common examples include metal complexes with inorganics such as carbonates, hydroxides, sulfates, and chlorides (Davison and Zhang, 2012). These labile species are effectively captured by DGT samplers. Semi-labile complexes present a more complex scenario. They partially disassociate within the diffusion gel but not entirely in solution. This partial disassociation can lead to overestimation of solution concentrations (Mongin et al., 2011). Modeling these effects requires detailed characterization of the binding ligands and their interactions. The interaction between DGT samplers and organic ligand complexes is intricate. In some cases, organic ligands themselves can be taken up by the diffusion gel, increasing the potential for metal-metal interactions (Garmo, Davison, and Zhang, 2008). This phenomenon further complicates the interpretation of uptake kinetics.

The properties of the diffusion gel also play a critical role in DGT performance. For instance, low ionic strength within the gel can enhance interactions between analytes and the resin layer (Zhang and Davison, 1999). At higher ionic strengths (greater than 1 mM), these effects diminish, suggesting that optimal conditions for minimal interference are established at elevated ionic concentrations (Davison & Zhang, 2012). The pore size of diffusion gels is another key factor. The mean pore diameter in agarose gels, commonly used in DGT samplers, has been estimated to be around 74 nm (Fatin-Rouge, Starchev, and Buffle, 2004). These pores serve as the primary pathway for analyte diffusion into the binding layer. However, detailed characterization of pore sizes remains incomplete. Nanoparticulate matter presents unique challenges due to their small size and potential for altered diffusion rates compared to free species. Theoretical estimates based on the Stokes-Einstein equation

suggest that particles around 5 nm would diffuse at approximately one-tenth the rate of freely dissolved analytes (Lead et al., 1994). However, experimental observations indicate that nanoparticle diffusion can be up to ten times slower than theoretical predictions in DGT gels (Scally, Davison, and Zhang, 2006). Given these findings, it is reasonable to assume that particles larger than 100 nm are likely excluded from the binding layer. Studies with lead nanoparticles have shown no direct uptake but suggest indirect effects on analyte uptake (Van Der Veeken, Pinheiro, and Van Leeuwen, 2008). Further research into nanoparticulate impacts is necessary to fully understand their influence.

Comparative studies between colloidal and free species demonstrate that the impact of colloids can vary widely depending on their chemical composition and labilization rates. For example, metal complexes with inorganics generally behave similarly to free species due to rapid disassociation (Davison and Zhang, 2012). The kinetic effects are less pronounced for deployments exceeding several hours. The steady-state approximations provide reliable estimates for the time required to achieve near-equilibrium conditions, validating this aspect of DGT operation. Laboratory experiments have confirmed that under controlled conditions with high ionic strengths, interference due to colloidal complexes is minimal (Zhang and Davison, 1999). These studies support the assumption that proper gel properties can mitigate potential biases introduced by colloids. Field applications of DGT samplers in various environmental settings have shown consistent results with laboratory predictions. For instance, deployments in heavily contaminated sites demonstrate rapid binding kinetics and minimal interference from nanoparticulates (Davison and Zhang, 2012).

2.2.1 DGT with 3-MFSG and agarose as resin and diffusive gels

The choice of resin within a DGT sampler is critical as it directly influences the efficiency and accuracy of the measurement. Different resins have been described for capturing specific species:

1. Ferrihydrite for Phosphates: Ferrihydrite has been utilized effectively to capture phosphates (Zhang & Davison, 1995). This iron oxide-based resin is known for its high affinity towards phosphate ions, making it a suitable choice in environments where the accurate measurement of phosphate concentrations is essential.

2. AG50W-X Cation-Exchange Resin: For cesium (Cs) and strontium (Sr), AG50W-X cation-exchange resin has been shown to be effective (Chang et al., 1998). This resin selectively binds cations, facilitating the accurate measurement of these elements in aquatic systems. The use of this resin highlights its versatility in capturing a range of monovalent and divalent cations.
3. Silver Iodide for Sulphides: Silver iodide has been employed to capture sulphide ions (Teasdale et al., 1999). This resin forms stable complexes with sulphide, making it an ideal choice for environments where sulphide pollution is a concern.
4. Thiol-Functionalized Resins for Mercury Species: Thiol-functionalized resins have gained prominence in capturing mercury and its various species (Docekalova & Divis, 2005; Clarisse & Hintelmann, 2006; Divis et al., 2009). These resins possess thiol groups that form strong bonds with mercury ions, enhancing their capture efficiency. Chelex 100 for Metal Ions: Chelex 100 is commonly used for the capture of divalent and trivalent metal ions (Garmo et al., 2003). This resin has a high affinity towards metals due to its chelating properties, making it suitable for environments with complex metal ion compositions.

Recent advancements have focused on improving the efficacy of DGT samplers for Hg^{2+} and MeHg. Fernández-Gómez et al. (2011) developed a specialized sampler designed specifically to measure these compounds, addressing critical environmental concerns related to their bioavailibility. One notable advancement involves the use of 3-mercaptopropyl functionalized silica gel (3-MFSG) as a resin material within DGT samplers for mercury and MeHg. Clarisse and Hintelmann (2006) highlighted that this thiol-functionalized resin exhibits a very high affinity for both Hg and MeHg. The efficiency of 3-MFSG has been extensively evaluated, with Chess (2010) reporting that the resin can absorb up to 91.6% of available Hg^{2+} and MeHg from solution, with an elution efficiency of approximately 96.5%. These high uptake and elution efficiencies underscore the suitability of this material for use in DGT samplers. The rapid binding kinetics associated with 3-MFSG further enhance its utility, as it ensures that analytes are captured efficiently within a short time frame. The resin's ability to quickly bind mercury species is crucial in ensuring accurate and timely measurements in aquatic environments where these compounds can rapidly transform or be diluted.

The diffusive layer in DGT samplers plays a critical role by facilitating the diffusion of analytes into the sampler. Traditionally, agarose gel has been used as the

diffusive layer material due to its minimal interaction with many analytes, allowing for linear diffusion through it without significant interference. This property is particularly advantageous when measuring mercury and MeHg, as the diffuse layer's non-reactive nature ensures that these metals can be effectively captured by the underlying resin. The effectiveness of agarose gel in minimizing interactions with mercury is well-documented (Clarisse & Hintelmann, 2006). By preventing strong interactions between the diffusive layer and the analytes, the gel allows for a consistent diffusion gradient to form over time. This linear diffusion profile ensures that the concentration measured by the DGT sampler accurately reflects the concentration of mercury or MeHg in the surrounding environment.

2.2.2 Applications and Limitations

One of the primary applications of the DGT technique is to measure the bioavailable fraction of metals in environmental samples such as water bodies, soils, and sediments (Davison & Zhang, 1994; Zhang et al., 2004). By capturing only those metal species that are present in dissolved or labile forms, DGT provides a measure of metal fractions that are more likely to be available for biological uptake (Zhang & Davison, 1995; Lombi et al., 2005). The DGT technique is widely used for continuous monitoring of metal pollution in aquatic systems and enables time-integrated measurements over deployment periods ranging from days to weeks, offering improved representation of temporal variability compared to discrete sampling methods (Zhang & Davison, 1999; Harper et al., 1998). Because DGT quantifies the bioavailable metal pool, its data are increasingly applied in ecological risk assessments and evaluations of potential human health impacts, supporting the development of environmental quality guidelines and management strategies (Lombi et al., 2005; Panther et al., 2014). In research settings, DGT is also employed to investigate the behaviour and speciation of metals under varying environmental conditions, including changes in pH, temperature, redox state, and organic matter content, thereby enhancing understanding of metal–ligand interactions in natural systems (Panther et al., 2014; Davison et al., 2000).

The effectiveness of DGT can be compromised by the complexity of the sample matrix, as inorganic particles, colloids, and dissolved organic matter may interfere with metal diffusion through the gel, leading to inaccuracies in measured concentrations (Zhang & Davison, 1995; Davison et al., 2000). These interferences

are particularly pronounced in highly turbid or polluted water bodies, where strong metal–particle or metal–organic associations can limit the availability of labile metal species for diffusion into the device (Luo et al., 2010; Panther et al., 2014). The diffusion rate of metals through the gel layer is a critical factor governing DGT performance, and metals present in large complexes or strongly bound to ligands may diffuse too slowly to be effectively captured by the resin, resulting in underestimation of concentrations (Zhang et al., 2004; Tusseau-Vuillemin et al., 2003). DGT measurements also rely on the assumption that equilibrium between the sample solution and the diffusive gel is rapidly established; however, this assumption may not always hold for metals with slow diffusion kinetics or complex speciation, further contributing to measurement uncertainty (Davison & Zhang, 2012). In addition, the deployment and interpretation of DGT devices require specialized expertise and laboratory infrastructure, and the cost of consumables such as binding resins and diffusive gels can limit accessibility for smaller laboratories or resource-constrained field studies (Panther et al., 2014). Although DGT is well suited for measuring low metal concentrations, its sensitivity may be insufficient for ultra-trace analysis of certain elements, restricting its applicability in environments where metals occur at extremely low levels (Zhang & Davison, 1999).

3 Development of Diffusive Gradient Thin Films (DGT) for methylmercury and mercury using HPLC-ICP-MS analysis

3.1 Introduction

Diffusive Gradients in Thin-films (DGT) technology was first introduced by Zhang and Davison (1999) as an in-situ technique for measuring dissolved metal concentrations in aquatic environments. Since its development, DGT has been widely adopted in environmental research due to its capacity to provide time-integrated, time-weighted average concentrations of bioavailable analytes (Table 1), rather than instantaneous measurements derived from discrete sampling events. This characteristic represents a major advantage over traditional grab sampling methods, which capture only short-term conditions and may fail to represent temporal variability caused by diurnal cycles, episodic inputs, or fluctuating physicochemical conditions.

The fundamental strength of DGT lies in its ability to control and quantify solute transport through a well-defined diffusion layer prior to accumulation on a binding resin. The technique is based on Fick's first law of diffusion, whereby a steady-state concentration gradient is established between the bulk solution and the binding layer. As dissolved, labile species diffuse through the diffusive gel, they are continuously sequestered by the resin, allowing solute fluxes to be integrated over deployment periods ranging from hours to several weeks. This time-integration capability enables DGT to smooth short-term fluctuations in concentration, producing a more representative measure of average exposure relevant to ecological processes and biological uptake (Zhang & Davison, 1995; Davison & Zhang, 2012).

Optimisation of DGT deployments requires careful consideration of exposure duration to ensure accurate measurements while avoiding resin saturation or degradation of device components. Deployment time is primarily constrained by the binding capacity of the resin layer and the stability of the diffusive gels. For most aquatic applications, DGT samplers can be deployed for periods of days to several weeks, depending on analyte concentration, temperature, and water chemistry (Zhang et al., 2004). Prolonged deployments under harsh environmental conditions, such as high temperatures, strong biofouling pressure, or prolonged anoxia, may lead to

changes in gel integrity, microbial colonisation, or altered diffusion characteristics, potentially affecting measurement accuracy (Davison et al., 2000). As a result, deployment durations are often optimised through preliminary trials or informed by published diffusion coefficients and resin capacities to ensure linear uptake and reliable quantification. In contrast to grab sampling, which requires repeated field visits and may be prone to contamination or handling, DGT provides a robust and low-maintenance approach for monitoring dissolved and bioavailable metal fractions over extended periods. The inclusion of a membrane filter between the diffusive and resin layers further enhances selectivity by excluding particulate matter and high-molecular-weight complexes, ensuring that only dissolved and labile species contribute to measured concentrations. Collectively, these features make DGT a powerful tool for assessing long-term metal dynamics, exposure risks, and biogeochemical processes in complex aquatic systems.

The concentration of Hg in environmental samples is often at trace levels, necessitating the use of sensitive sampling techniques for accurate quantification. Diffusive Gradients in Thin-films (DGT) passive samplers have emerged as a promising tool for accumulating Hg^{2+} over extended periods, providing valuable insights into its temporal and spatial distribution. However, the establishment of a standardized DGT method for the accumulation of Hg^{2+} remains inconsistent due to several factors. One significant challenge lies in sample preparation, which encompasses the selection of appropriate resins used within the DGT devices. Various types of resins are employed to accumulate Hg^{2+}, each with distinct binding affinities and capacities. Traditionally, Chelex-100 has been the most commonly used ion exchange resin in DGT for cation binding (24 elements as demonstrated by Garmo et al., 2003), while ferrihydrite serves as a resin for phosphorus. However, these resins have limited affinity towards organic metals such as MeHg and elemental mercury (Hg2+). To address this limitation, recent advancements have led to the development of DGT samplers with 3-MFS resin gel specifically tailored for measuring MeHg and Hg2+ concentrations (Fernández-Gómez et al., 2011). Nonetheless, variations in resin choice can lead to differing accumulation rates and thus affect the comparability of results across studies.

Besides finding a suitable resin for the accumulation of MeHg and Hg^{2+}, the separation and detection methods used in the speciation analysis of Hg^{2+} further

contribute to inconsistencies in DGT method standardization. Different analytical techniques, such as atomic absorption spectroscopy (AAS), inductively coupled plasma mass spectrometry (ICP-MS), and cold vapor atomic fluorescence spectroscopy (CVAFS), offer varying levels of sensitivity and specificity. The choice of detection method can significantly influence the precision and accuracy of Hg^{2+} measurements, thereby impacting the reliability of DGT-derived data (Suárez-Criado et al., 2022).

The inconsistency in sample preparation and analytical techniques underscores the need for a standardized approach to ensure the comparability and reproducibility of DGT results across different laboratories and environmental settings. Standardization efforts should focus on defining uniform protocols for resin selection, handling procedures, and detection methods, thereby minimizing variability and enhancing the reliability of Hg^{2+} accumulation data obtained through DGT samplers.

Furthermore, comprehensive validation studies are essential to assess the performance of DGT under various environmental conditions, including pH levels, ionic strength, and the presence of interfering species. Such studies can provide critical insights into the applicability and limitations of DGT as a tool for monitoring trace Hg^{2+} concentrations in aquatic environments.

While DGT passive samplers offer a potential avenue for accumulating and quantifying trace levels of Hg^{2+} over extended periods, the establishment of standardized methods remains challenging due to inconsistencies in sample preparation and analytical techniques. Addressing these challenges through rigorous validation studies and the development of uniform protocols will be crucial in enhancing the reliability and comparability of DGT-derived data, ultimately advancing our understanding of mercury dynamics in environmental systems.

The primary objective of this study was to validate a DGT-based approach for the simultaneous measurement of total Hg and methylmercury (MeHg) using a thiol-binding resin, 3-mercaptopropyl functionalised silica gel (3-MFSG). The study tested the hypothesis that coupling mercury-specific DGT samplers with chromatographic separation prior to detection would enable accurate, time-integrated quantification of MeHg in freshwater systems. To achieve this, high-performance liquid chromatography (HPLC) was integrated with inductively coupled plasma mass

spectrometry (ICP-MS) to separate MeHg from inorganic mercury species, allowing direct assessment of mercury speciation rather than reliance on bulk concentration measurements. By validating the performance of 3-MFSG-based DGT samplers and evaluating the analytical reliability of HPLC-ICP-MS, this research sought to enhance methodological robustness for mercury speciation analysis and demonstrate the advantages of time-integrated DGT sampling over conventional grab sampling in environmental studies.

3.2 Literature Review

DGT samplers have been utilized since the 1990s primarily for accumulating and measuring cations, particularly trace and heavy metals, in aqueous environments and expanded to include sediments and soils (Zhang & Davidson, 1995; Feng et al., 1997; Zhang et al., 1998). Additionally, DGT has been adapted as a tool for determining analyte speciation and assessing the bioavailability of solutes (Garmo et al., 2003; Mason et al., 2005; Clarisse & Hintelmann, 2006). Initially, DGT was primarily used to measure cationic metals such as Ni, Zn, Mn, Fe, Cu, and Cd, with Chelex-100 resin serving as the binding layer (Zhang & Davison, 1995). However, subsequent modifications involving alternative resins like ferrihydrite, thiol-modified silica, Spheron-Thiol, and silver iodide have broadened its applicability to a wider range of analytes. Table 1 provides an overview of past research on DGT using various binding resin layers for different analytes.

Table 1: Various resin layers tested in past DGT research.

Resin	**Analytes**	**Reference**
Chelex-100	Ni, Zn, Mn, Fe, Cu, Cd	Zhang et al. (1995)
Thiol-modified silica	Heavy metals and Hg	Feng et al. (1997)
AG50W-X	Cs, Sr	Chang et al. (1998)
Ferrihydrite	P	Zhang et al. (1998)
Silver iodide	S	Teasdale et al. (1999)
Ammoniummolybdophosphate (AMP)	Radionuclides Cs	Murdock et al. (2001)
Chelex-100	Co, Ni, Cu, Zn, Pb, Al, Mn, Ga, V, Cr, Fe, U, Mo, Ti, Ba, Sr, lanthanides, Li, Na, K, Rb, Mg, Ca, B, Tl, P, S, As, Bi, Se, Si, Sn, Sb, Te, Zr, Nb, Hf, Ta, W, Th, Ag	Garmo et al. (2003)
Ferrihydrite	As	Fitz et al. (2003)
Poly(4-styrenesulfonate) liquid binding layer	Cu, Cd	Li et al. (2003)
Suspended particulate reagent-iminodiacetate (SPR-IDA)	Co, Ni, Cu, Cd, Pb	Warnken et al. (2004)
Chelex + ferrihydrite (mixed binding layer)	Cd, Cu, Mn, Zn, P	Mason et al. (2005)
Spheron-thiol	Hg	Docekalova et al. (2005)
3-mercaptopropyl functionalized silica	MeHg	Clarisse & Hintelmann (2006)

As can be seen in Table 1, different resins had been tested depending on the species of interest. Chang et al. (1998) employed AG50W-X8, a general cation exchange resin, as the binding layer in DGT for measuring Cs and Sr. The embedded resin in polyacrylamide gel effectively removed these elements from solution. However, unlike highly selective resins such as Chelex-100 used for trace metals, AG50W-X8 becomes saturated due to continuous uptake of major cations present in the solution. Consequently, the theoretical response was only achieved for exposure times up to 20 hours in soft water environments. Feng et al. (1997) explored the use of functionalized organic monolayers (mercaptopropylsilane) on mesoporous silica to remove mercury and other heavy metals from both aqueous and non-aqueous waste streams. They demonstrated that these modified silicas were stable and could be regenerated and reused, highlighting their potential for practical applications in environmental remediation.

Teasdale et al. (1999) developed a DGT technique for measuring dissolved sulphide using a resin gel containing silver iodide (AgI). Sulphide reacts with pale yellow AgI to form black Ag_2S. The accumulated sulphide was quantified using a conventional purge-and-trap method followed by colorimetric measurement with methylene blue. This study demonstrated that sulphide can be measured quantitatively using the AgI-DGT technique. Silver iodide was chosen as the binding agent due to its low solubility in water, its ability to readily form highly insoluble Ag_2S, and the accompanying color change from pale yellow to black upon reaction with sulphide.

Subsequent work expanded DGT resins that were developed for anionic analytes. Zhang et al. (1998) prepared a binding layer containing ferrihydrite by adding 2 g of ferrihydrite slurry into 10 ml of gel solution. This work demonstrated that DGT can be used to measure phosphorus species in situ in natural waters. Murdock et al. (2001) employed ammoniummolybdophosphate (AMP) as the binding agent, which has been widely used for the adsorption and analysis of caesium in surface waters. Their experiments with known concentrations of ^{134}Cs showed that DGT measurements using AMP gels closely reproduced the immersion solution concentration with high accuracy and precision over sampling periods up to one day. This work implies that DGT can provide an accurate estimation of average caesium concentrations in natural waters over periods of up to a month. The technique is noted for its simplicity, involving minimal sample preparation, and offers several advantages over traditional sampling methods for monitoring radionuclides such as ^{134}Cs and ^{137}Cs.

Garmo et al. (2003) evaluated the Chelex-100 resin in DGT for 55 elements and concluded that it was useful for measuring the following 24: Pb, Zn, Co, Ni, Cu, Cd, Al, Mn, Ga, La, Ce, Pr, Nd, Sm, Eu, Gd, Tb, Dy, Ho, Er, Tm, Yb, Lu, and Y. In the same year, Li et al. (2003) pioneered a liquid phase binding layer combined with a dialysis membrane diffusive layer. The binding phase was a solution of poly(4-styrenesulfonate) (PSS), which binds to Cd^{2+} and Cu^{2+}, acting as a cation exchanger under competitive binding conditions. Warnken et al. (2004) experimented with a novel resin using suspended particulate reagent-iminodiacetate (SPR-IDA) as an alternative to Chelex-100. They demonstrated that SPR-IDA effectively binds Co, Ni, Cu, Cd, and Pb, yielding linear increasing concentrations. The analytes bound to the SPR-IDA were detected using laser ablation ICPMS.

Mason et al. (2005) developed a mixed binding layer (MBL) containing ferrihydrite for phosphate sorption and Chelex-100 for metal cation sorption, enabling simultaneous measurement of both anions and cations using DGT. This advancement broadens the applicability of DGT in environmental monitoring by accommodating diverse chemical forms present in natural waters.

Early mercury-specific DGT studies focused on evaluating the performance of different binding resins and diffusive gels to optimise mercury uptake and measurement accuracy. In their study, Docekalova et al. (2005) systematically evaluated two binding resins; Chelex-100, containing iminodiacetic acid groups, and Spheron-Thiol, containing thiol functional groups. They demonstrated that mercury accumulation using the thiol resin was approximately threefold higher than that achieved with Chelex-100. This enhanced performance was attributed to the strong affinity of thiol groups for Hg^{2+}, including mercury present in non-labile or weakly complexed forms, underscoring the importance of ligand–metal interactions in DGT resin design. These findings are consistent with broader materials research, such as the work by Feng et al. (1997) who developed thiol-functionalized monolayers on ordered mesoporous silica supports for heavy metal sequestration. Their study demonstrated exceptionally high mercury binding capacities, driven by the formation of strong covalent Hg–S bonds and the high surface area of the mesoporous support. Together, these studies highlight a common principle underpinning mercury sorbent development: the incorporation of sulfur-based functional groups and high-surface-area matrices substantially enhances mercury capture efficiency.

Further, Clarisse and Hintelmann (2006) devised a DGT technique for in situ sampling of dissolved MeHg in natural waters. Instead of utilizing Chelex-100, they employed a 3-mercaptopropyl functionalized silica gel resin specifically designed to complex mercury ions. This new binding medium was characterized and calibrated for use as a quantitative time-integrating monitoring tool for MeHg. Their study showed a low detection limit (1 pg MeHg, corresponding to approximately 30 pg/L for a 24 h deployment), with potential for even greater sensitivity through longer deployments or thinner diffusive gels. Previous research indicated that thiol-modified silica gel resins exhibit selective affinity towards mercury and silver ions (Vieira et al., 1997; Nooney et al., 2001), while other metal ions, such as Cd^{2+}, Pb^{2+}, Zn^{2+}, Co^{3+}, Cr^{3+}, Fe^{3+}, Cu^{2+}, and Ni^{2+}, exhibited minimal or no binding (Brown et al., 1999; Liu et al., 2000).

Consequently, it was concluded that these alternative metal ions do not compete with mercury for binding sites on the resin.

In summary, DGT has evolved significantly since its inception, with diverse binding resins tailored to specific analytes, enhancing its utility across various environmental monitoring contexts. The choice of resin critically influences the efficiency and selectivity of metal uptake, as exemplified by studies utilizing different materials such as Chelex-100, AG50W-X8, and mercaptopropylsilane-modified silica.

Previous literature has demonstrated various resins used for accumulating Hg and its species within diffusive gradients in thin films (DGT). A comprehensive summary of prior research on Hg DGT can be found in Table 2. The most frequently utilized resin for binding both Hg and MeHg in DGT is Spheron-Thiol and 3-mercaptopropyl functionalized silica. These resins are effective due to the strong affinity of thiol groups towards mercury ions. Researchers have introduced modifications to enhance the effectiveness of these resins, such as incorporating thiol groups with carbon nanoparticles (Wu et al., 2017), modifying metal double hydroxide with thiol groups (Yao et al., 2020), and integrating 3-mercaptopropyl functionalized ethenylene with periodic mesoporous organosilica (Gao et al., 2011).

In Hg speciation analysis, various chromatographic techniques are used for separating mercury species. Commonly employed methods include liquid chromatography (LC), gas chromatography (GC), and capillary electrophoresis (CE). Amde et al. (2016) have illustrated these separation techniques in Hg speciation analysis, as shown in

Figure 3. Non-chromatographic techniques for separating target Hg chemical species rely on their distinct chemical and physical properties. For instance, speciation analysis based on atomization modes relies on the principle that organic mercury species require more heat to volatilize compared to elemental mercury (Hg^0). Chen et al. (2011) demonstrated the reduction of Hg^{2+} through cold atomization followed by quantification using AFS.

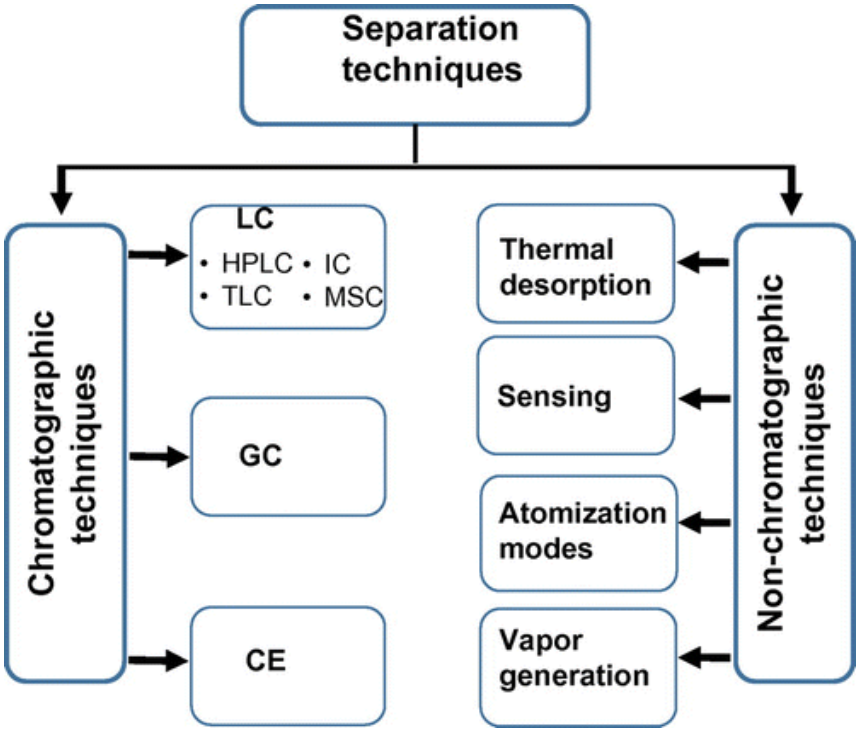

LC: Liquid Chromatography HPLC: High Performance Liquid Chromatography

GC: Gas Chromatography TLC: Thin Layer Chromatography

CE: Capillary Electrophoresis IC: Ion Chromatography MSC: Multisyringe Chromatography

Figure 3. Separation techniques that can be used in the speciation analysis of Hg.

The earliest method for quantifying Hg in water involved the use of (Table 2) atomic absorption spectrometry (AAS) as demonstrated by Hatch et al. (1968). Since then, numerous detection techniques have been utilized for analyzing mercury in environmental samples. The choice of detector depends on factors such as sensitivity, specificity, cost, analysis time, and sample characteristics. Commonly used detectors include AAS, atomic fluorescence spectrometry (AFS) and inductively coupled plasma mass spectrometry (ICP-MS). Among these techniques, AFS and ICP-MS are particularly favored for speciation analysis due to their high sensitivity and selectivity. Additionally, AFS is cost-effective, while ICP-MS can be employed in isotopic dilution analysis to improve the precision and accuracy of experimental results. Another notable advantage of the ICP-MS detector is its capability to provide isotopic information about the analyte.

Table 2. Past literature regarding types of resin used in DGTs to accumulate Hg and MeHg and method of analysis.

Resin	Separation/ Detection Methods	Reference
Spheron-Thiol	AAS[a]	Docekalova & Divis (2005)
Spheron-Thiol	HPLC-ICPMS[b]	Cattani et al. (2008)
3-MFS[c]	AFS[d]	Fernandez-Gomez et al. (2011)
3-MFS	HPLC-ICPMS	Hong et al. (2011)
P81 membrane	CV-AFS[e]	Colaco et al. (2014)
SH-CNP[f]	ICPMS	Wu et al. (2017)
3-MFS	ICPMS	Sierra et al. (2017)
Spheron-Thiol	ICPMS	Turull et al. (2018)
Spheron-Thiol	DMA[g]	Schintu et al. (2018)
3-MFS	HS-GC-CVAFS[h]	Bratkic et al. (2019)
3-MFS	ID-GC-ICPMS[i]	Bretier et al. (2020)
3-MFS	DMA	Marrugo-Madrid et al. (2022)

[a] AAS: atomic absorption spectrometer

[b] HPLC-ICPMS: high-performance liquid chromatography coupled with inductively coupled plasma mass spectrometer

[c] 3-MFS: 3-mercaptopropyl functionalized silica gel

[d] AFS: atomic fluorescence spectrometer

[e] CV-AFS: cold-vapour atomic fluorescence spectrometer

[f] SH-CNP: thiol-modified carbon nanoparticle

[g] DMA: direct mercury analyzer

[h] HS-GC-CVAFS: head space coupled with gas chromatography and cold-vapour atomic fluorescence spectrometer

[i] ID-GC-ICPMS: isotopic dilution coupled with gas chromatography and inductively coupled plasma mass spectrometer

3.3 Materials and Methods

The experimental methods were adapted from Hong et al. (2011).

3.3.1 General Techniques

Analytical reagent grade and/or equivalent analytical purity chemicals and trace metal grade acids were used in all experiments. All solutions were prepared by dissolving the chemicals in deionized water with a resistivity of 18 MΩ cm^{-1} obtained from a Milli-Q system (Millipore, Milford, MA). All glass and plasticware were prewashed in 10% HCl followed by rinsing in deionized water and then washed in 10% HNO_3 followed by rinsing with deionized water.

For the addition of Hg species to the experimental solutions, 1000 mg/L Hg^{2+} and 1.0 mg/L MeHg stock solutions were purchased from Sigma Aldrich. The 1000 mg/L Hg^{2+} stock solution was diluted to 1.0 mg/L in 1.0 M HNO_3 and 1.0 M HCl.

3.3.2 Ion Chromatographic Separation of MeHg and Hg^{2+}

High-pressure liquid chromatography (HPLC) was performed using an Agilent 1200 system to separate MeHg and mercury(II) (Hg^{2+}) complexes via a cation exchange column (IonPac CG5A, Dionex, Sunnyvale, CA, USA). The specific operating parameters for the HPLC are detailed in Table 3. The HPLC system was combined with a triple-quadrupole inductively coupled plasma mass spectrometry (QQQ-ICP-MS) unit (Agilent 8900) through a manually operated switching valve (Rheodyne, Rohnert Park, CA, USA), enabling the operation of the system either as HPLC-ICP-MS or in standalone ICP-MS mode.

To form cationic species such as MeHg(TU)+ and $Hg(TU)_4^{2+}$, an acidic thiourea solution (1.5% thiourea + 6.5% concentrated nitric acid + 10% glacial acetic acid) was employed as the mobile phase in conjunction with the cation exchange column. The analysis of MeHg and Hg^{2+} was conducted with a continuous flow rate of the mobile phase at 1.0 mL/min and an injection volume of 100 µL, resulting in a total run time of 7 minutes. The retention times for each mercury species were validated by injecting blanks that had been spiked separately with MeHg and Hg^{2+}. All calibration curves and concentrations were calculated using the ICP-MS MassHunter software provided by Agilent Technologies.

Table 3. Working parameters for HPLC

HPLC (Agilent series 1200)	
Column	Cation exchange column (IonPac CG5A)
Mobile phase	1.5% thiourea + 6.5% concentrated HNO3 + 10% glacial acetic acid
Flow rate	1.0 mL/min
Injection volume	100 μL

3.3.3 Preparation of DGT Probes

The DGT probes utilized in this experiment adhered to the standard configuration comprising a diffusive layer, a membrane filter, and a resin layer housed within plastic enclosures procured from DGT Research Ltd. (Lancaster, UK). The diffusive layer was composed of 1.5% agarose, chosen for its lower interference and affinity towards Hg^{2+} compared to alternative diffusive gels such as polyacrylamide (Docekalova & Divis, 2005; Divis et al., 2010; Amirbahman et al., 2013). The resin layer consisted of beads of 3-mercaptopropyl-functionalized silica gel (3-MFSG, Sigma Aldrich), which possess thiol functional groups. A 0.45 μm polysulfone membrane filter was utilized as the membrane filter. The probes were prepared following the procedures established by Hong et al. (2011) with minor modifications.

To prepare the 1.5% agarose diffusive layer, 0.45 g of agarose was mixed with 30 mL of deionized water and heated to 90°C while stirring on a heated magnetic stirrer until it became clear. Concurrently, molds were prepared by positioning spacers with a thickness of 0.5 mm between two glass plates and preheating them in an oven at 50°C. Once the agarose solution reached 90°C, it was pipetted into the mold and allowed to solidify at room temperature (20°C) for one hour. The prepared agarose diffusive gels were subsequently stored in a 0.01 M NaCl solution until further use.

For the resin layer, 2 g of 3-MFSG beads were weighed and placed in 10 mL of cross-linked acrylamide (APA) solution containing 15% polyacrylamide and 0.3% patented cross-linker (DGT Research, Lancaster, UK). The APA solution was prepared by mixing 7.5 g of DGT cross-linker with 23.75 mL of deionized water, followed by the addition of 18.75 mL of acrylamide solution and thorough stirring to produce a total volume of 50 mL. This APA solution could be stored in a refrigerator for up to six months. After adding the 3-MFSG beads to the APA solution and mixing

well, polymerization was initiated by incorporating 60 µL of ammonium persulfate and 15 µL of tetramethylethylenediamine (TEMED) into the mixture. The solution was then pipetted into pre-cooled glass plate molds with spacers to maintain a thickness of 0.5 mm. The glass plates were allowed to sit at room temperature (20°C) for one hour to solidify. Following this, the resin layer was carefully retrieved from the glass plates using plastic forceps and subjected to multiple rinses with deionized water to facilitate easy removal. Subsequently, the resin layer was hydrated in a buffer solution (0.01 M $NaNO_3$, pH 8) for more than one day, with the rinsing solution being changed over three times within 24 hours to remove impurities such as residual TEMED.

Both the resin and diffusive layers were cut to fit into the plastic DGT housings procured from DGT Research Ltd. (Lancaster, UK). The assembly of the probe involved placing the 3-MFSG resin layer with its bead side facing upward onto the DGT probe, followed by the agarose diffusive layer, and finally a 0.45 µm pore size polysulfone membrane filter. The entire assembly was then encapsulated using the plastic housing provided with the DGT probe.

3.3.4 DGT laboratory experiments

The linear accumulation of MeHg over time was initially evaluated using 12 DGT probes immersed in a solution containing 1.0 µg/L MeHg. The exposure durations were set at 2, 3, 4, 5, 6, and 7 hours. Each probe with its replicate were placed within a 2L Sistema container that was air-tight and filled with 0.01M $NaNO_3$ solution spiked with the aforementioned MeHg concentration. Subsequently, the containers were sealed with parafilm and subjected to agitation on a platform shaker at 20°C for 2, 3, 4, 5, 6, and 7 hours. Post-exposure, 10 mL of water was collected from each container using a syringe and filter into a 10 mL digitube for MeHg concentration measurement via ICP-MS analysis. The resin layers from the DGT probes were then excised and soaked in 1.0 mL of acidic thiourea solution within 1.5 mL tubes for a period of 24 hours. The extracted MeHg was quantified using HPLC-ICP-MS. This preliminary experiment aimed to validate that the 3-MFSG resin within DGT probes could effectively accumulate MeHg even at trace concentrations.

Upon confirming the successful accumulation of MeHg by the 3-MFSG resin, a subsequent experiment was conducted to further assess the linear uptake kinetics

over time using 40 DGT probes exposed to both 1.0 μg/L MeHg and 1.0 μg/L Hg^{2+} in two synthetic lake water systems. Each bucket contained 20L of synthetic lake water with 5 DGT probes and their replicates. The synthetic lake waters were prepared based on anion data from the Bay of Plenty Regional Council, replicating Rotomahana and Blue Lake environments. Lake Rotomahana was chosen due to the high geothermal input and salts coming from the vents to reflect the actual DGT field test while Blue Lake was chosen due to its non-geothermal input. For Rotomahana, the solution was formulated with Cl^- at 3.97 mEq/L, SO_4^{2-} at 3.33 mEq/L, and HCO_3^- at 3.79 mEq/L; for Blue Lake, the concentrations were set to Cl^- at 0.016 mEq/L, SO_4^{2-} at 0.024 mEq/L, and nil for HCO_3^-. The DGT probes were immersed in these synthetic waters for durations of 1, 2, 3, 6, and 12 days to examine the effects of MeHg and Hg^{2+} complexes with dissolved organic matter (DOM) on DGT performance. Post-exposure, 10 mL of water was collected from each container using a syringe and filter into a 10 mL digitube for MeHg concentration measurement via ICP-MS analysis.

Additional experiments were conducted by incorporating Suwannee River DOM at a concentration of 10 mg/L into two buckets of synthetic Rotomahana and Blue lake waters, with 1.0 μg/L MeHg and 1.0 μg/L Hg^{2+} concentrations. Ten probes were deployed in each bucket with two being retrieved on each sampling day for the durations of 1, 2, 3, 6, and 12 days. The volumes of Hg solutions and DGT deployment times were optimized to minimize depletion of Hg species during experimentation. Buckets were securely sealed with lids and parafilm tape throughout the exposure periods. At the conclusion of the experiment, water samples from each bucket were analyzed for residual Hg concentrations using ICP-MS, revealing that less than 10% of Hg was lost through evaporation. The resin layers from all DGT probes were then removed, placed in 1.5 mL tubes containing 1.0 mL of acidic thiourea solution, and soaked overnight. Extracted MeHg and Hg^{2+} levels were subsequently quantified via HPLC-ICP-MS analysis.

3.3.5 DGT field test

Twelve DGTs were deployed in three fresh water lakes in Rotorua known for relatively high concentrations of mercury based on Kim and Burggraaf (1999). They were Lake Okaro, Rotoiti and Rotomahana. Three DGTs were suspended 5 meters above the lake bed (the hypolimnion) and another three DGTs were suspended 5 meters below the surface (the epilimnion). The DGTs were tied inside a perforated

PVC pipe (Figure 4) together with temperature loggers and then attached to a rope that was anchored to the bottom and a buoy on the surface. The DGTs were deployed at Lake Okaro in October 2017, Lake Rotoiti and Rotomahana in November 2017. The DGTs were also deployed at Lake Okaro for 17 days (9th of March – 25th of March 2019) and Lake Rotoiti for 22 days (26th of March – 16th April 2019). The dates were chosen during summer because the lakes were stratified during this season. During retrieval, the DGTs were rinsed with deionized water and stored in an air-tight container filled with deionized water. Once the DGTs reached the laboratory, the plastic housing was removed with a screwdriver and the resin layer immersed in 1.0 mL of acidic thiourea solution for 24 hours to extract the MeHg and Hg^{2+}. They were then stored in the refrigerator at 4◦C until analysis using HPLC-ICP-MS. Water samples were collected from each lake using a Van Dorn sampler at the hypolimnion and the epilimnion at the beginning and the end of the experiment to determine total Hg by ICP-MS and major anions by ion chromatography (DX-120, Dionex, Sunnyvale, CA, USA). Temperature, depth, salinity and dissolved oxygen were measured at the time of DGT deployment using a CTD (conductivity, temperature and depth profiler, SBE 19 plus V2 SeaCAT profiler, Sea-Bird Electronics Inc., Washington).

Figure 4. DGTs housed in a PVC pipe with temperature loggers to be suspended 5 meters above sediment and 5 meters below water surface

3.3.6 Calculations for DGT accumulation of ions

The concentration of labile metals in the bulk solution can be estimated based on the total quantity of metal ions accumulated in the resin layer, as outlined below:

$$Cb = \frac{M \times \Delta g}{D \times \mathrm{t} \times A}$$

Where:

Cb is the metal concentration in bulk solution (ppb)

M is the accumulated metal in the resin (ng)

t is the deployment time (sec)

D is the metal's diffusion coefficient in the hydrogel ($cm^2\ s^{-1}$)

A is the exposed interfacial area (cm^2)

Δg is the total thickness of the diffusion layer including the diffusive boundary layer, filter membrane, and diffusive layer (mm)

3.4 Results and Discussion

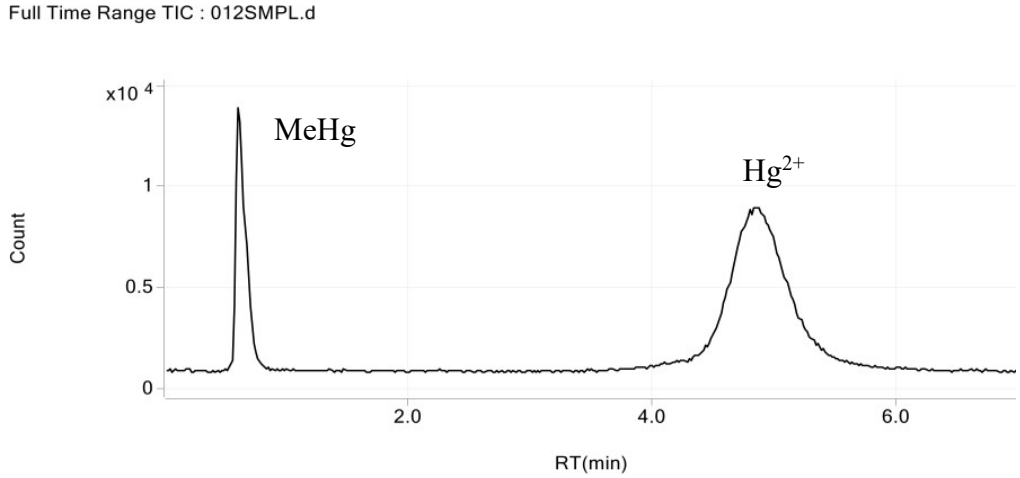

Figure 5. Chromatogram depicting 0.05 mg/kg MeHg and 0.05 mg/kg Hg^{2+}

Clear separation of Hg species was achieved through HPLC-ICPMS analysis of standards, as evidenced by Figure 5. The retention times for each peak did not overlap, indicating well-resolved peaks with minimal baseline noise relative to the standards used. Specifically, MeHg eluted at a retention time of 1.2 minutes, while

Hg^{2+} eluted at a retention time of 4.5 minutes. These results confirm that the separation of Hg species is consistent with previous findings (Hong et al., 2011).

For context, Cattani et al. (2009) reported different retention times for MeHg and Hg^{2+}, with MeHg eluting at 3.21 minutes and Hg^{2+} at 4.65 minutes. The discrepancy in retention times between the current study and that of Cattani et al. (2009) can be attributed to differences in flow rates; specifically, a lower flow rate of 0.35 mL/min was used by Cattani et al., compared to the 1.0 mL/min utilized here. The observed separation confirms that HPLC-ICPMS is an effective technique for distinguishing between different forms of Hg species in aqueous solutions, providing reliable and reproducible results when appropriate experimental conditions are maintained. This methodological consistency ensures accurate quantification of both MeHg and Hg^{2+}.

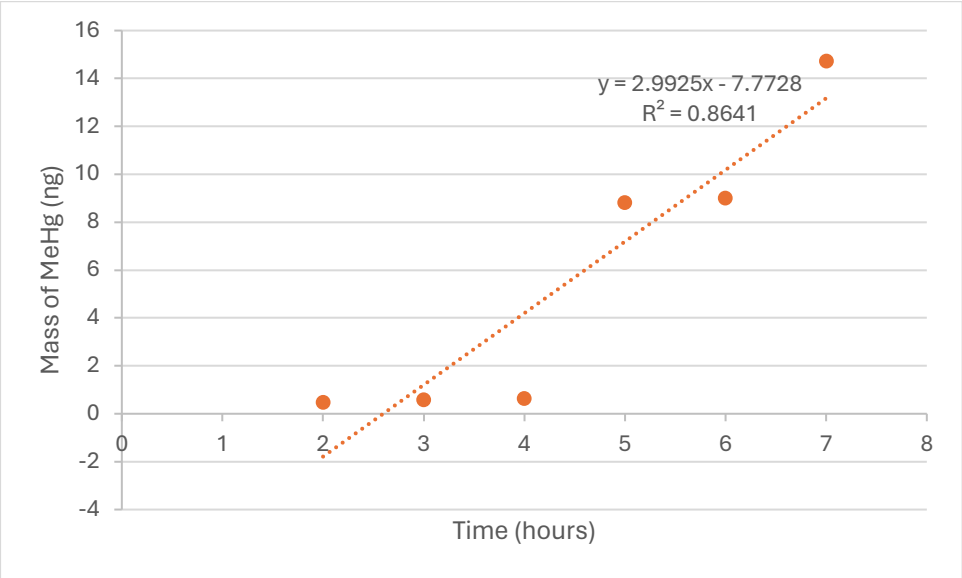

Figure 6. Time dependent MeHg accumulated in the 3-MFSG resin layer. DGT probes immersed in a solution containing 1.0 µg/L MeHg. The exposure durations were set at 2, 3, 4, 5, 6, and 7 hours.

Methylmercury accumulation within the DGT devices increased linearly over the seven-hour deployment period. DGT samplers incorporating the 3-MFSG resin exhibited a consistent, time-dependent increase in accumulated MeHg mass, indicating linear uptake kinetics as seen in Figure 6. Results from the DGT deployed showed 3-MFSG resin effectively adsorbed more than 99% of the MeHg from the water with a concentration range spanning from 111 ng/L to 2655 ng/L (equivalent to 0.4 – 14.7 ng/cm² in the resin layer). These findings are consistent with previous

research by Hong et al. (2011), who reported that their 3-MFSG resin was capable of adsorbing both MeHg and Hg^{2+} from water within a concentration range of 20 ng/L to 2000 ng/L, corresponding to 0.6 – 17 ng/cm² Hg over the resin layer. The high capacity for adsorption of various Hg species observed in this study is also supported by earlier work (Shade & Hudson, 2005; Clarisse & Hintelmann, 2006; Shade, 2008). The combination of high uptake efficiency and elution efficiency makes the 3-MFSG resin an ideal material for use in DGT samplers. This robust performance underscores its suitability for accurately quantifying MeHg concentrations in environmental samples.

Overall, the linear relationship between time and MeHg accumulation, as well as the high adsorption capacity of the 3-MFSG resin across a broad range of concentrations, validates the effectiveness of this material for Hg species analysis. The consistency with previous studies further strengthens the reliability and applicability of DGT devices using 3-MFSG resin in environmental monitoring contexts.

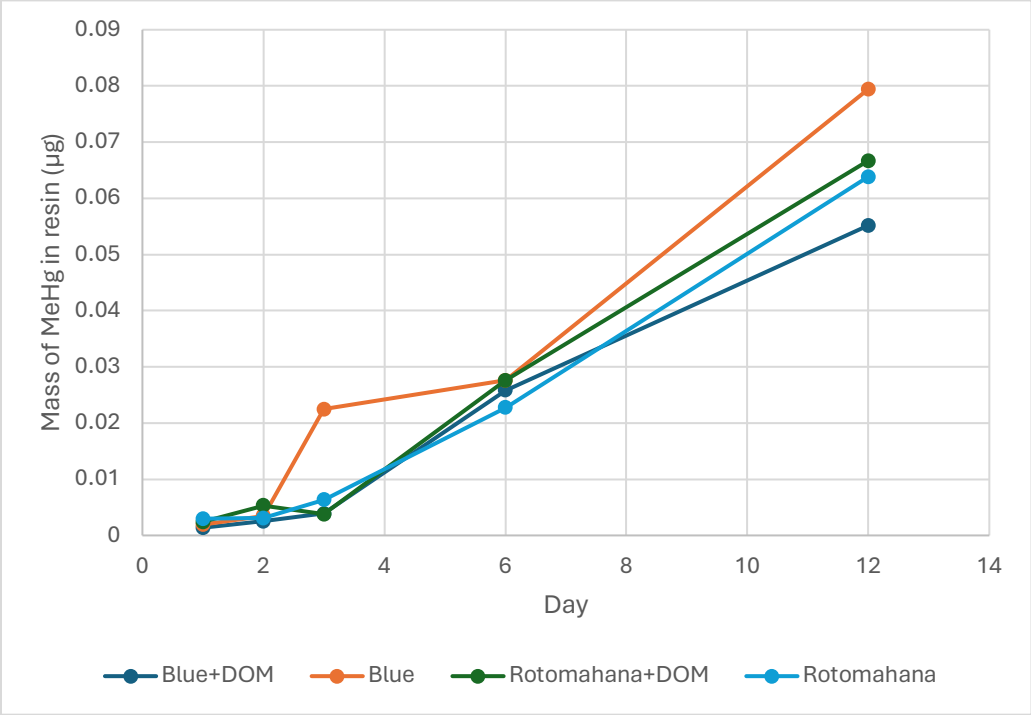

Figure 7. Time trialled DGT experiments (5 DGT probes per bucket for each day with replicates each) with 1.0 µg/L MeHg in synthetically made up Rotomahana Lake and Blue Lake in 20 L water buckets with 10 mg/L dissolved organic matter

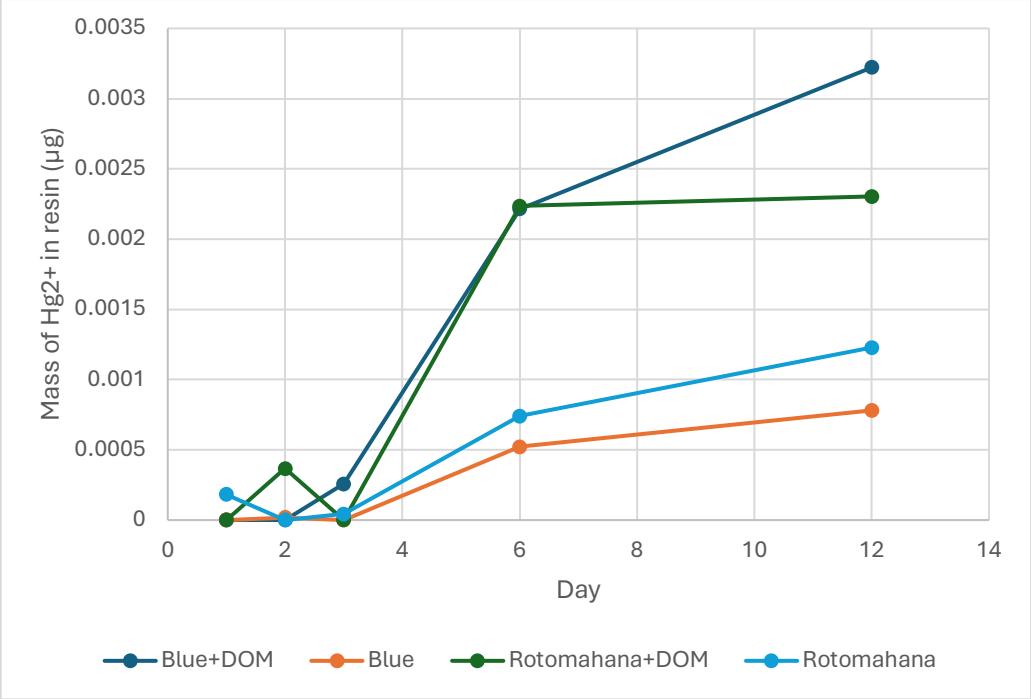

Figure 8. Time trialled DGT experiments (5 DGT probes per bucket for each day with replicates each) with 1.0 µg/L Hg^{2+} in synthetically made up Rotomahana Lake and Blue Lake in 20 L water buckets with 10 mg/L dissolved organic matter

The results for the concentration of MeHg and Hg^{2+} measured in the water at the beginning of the trial and taken after the trial showed a 0.4% difference. This is less than 10% of MeHg and Hg^{2+} loss through evaporation and other environmental factors in the lab.

In the time-trial DGT experiments conducted in synthetic lake waters spiked with MeHg, a linear increase in MeHg accumulation on the 3-MFSG resin was observed over time across all treatments (Figure 7). Overall, MeHg uptake occurred at a substantially higher rate than Hg^{2+}, with adsorption rates observed to be approximately 20 times greater than those observed for Hg^{2+}. The presence of dissolved organic matter (DOM) generally resulted in a reduced rate of MeHg accumulation, most notably in the Blue Lake treatment, where the MeHg + DOM condition exhibited the lowest uptake relative to the corresponding treatment without DOM. In contrast, no difference in MeHg accumulation was observed between DOM and non-DOM treatments in the Rotomahana Lake water. These results indicate that DOM exerted a variable influence on MeHg uptake depending on water chemistry, with its effect being minimal in the Rotomahana Lake system.

First of all, 3-MFSG resin binds strongly with any Hg species due to the thiol group in the resin. On the other hand, DOM has lots of thiol functional groups as well and easily forms complexes with MeHg and Hg^{2+}. DOM consists of both humic and fulvic acids, which range in size between 0.5 and 400 nm and have molar weights ranging from 200 to 10 5 g/mol or greater (Van de Weerd et al., 1999). MeHg is considered to have a lower affinity for the thiol functional groups in organic matter than Hg^{2+} because the attachment of the methyl functional group reduces the MeHg's affinity to thiols. This implies that MeHg - DOM complexes are more labile than Hg^{2+} - DOM complexes and have a higher dissociation rate constant. Similar behavior of metal DOM complexes was observed in a previous study (Warnken et al., 2007). As of such, MeHg-DOM would disassociate faster and be adsorbed unto the 3-MFSG resin quicker. It would also explain why MeHg had a greater uptake in concentration on the 3-MFSG resin compared to Hg^{2+} as Hg^{2+} had to compete with MeHg for binding spaces on the resin. With greater diffusion kinetics, it was predicted that MeHg would be greater over Hg^{2+} in waters where both Hg species are present. Due to the high lability of MeHg–DOM complexes, the presence of DOM had little influence on the rate of MeHg adsorption observed in the bucket experiments. Even so, the Blue Lake bucket test without DOM showed a greater MeHg adsorption compared to the one with DOM (Figure 7) as MeHg was able to be adsorbed freely onto the resin without any association and disassociation from DOM.

In the experiments involving Hg^{2+}, DGT samplers exhibited linear accumulation over the first six days of deployment, followed by a plateau phase that persisted until day twelve (Figure 8). Overall, Hg^{2+} uptake by the 3-MFSG resin was substantially lower than that observed for MeHg across all treatments. Variations in uptake behaviour between lake waters are likely linked to differences in ionic composition, as Rotomahana Lake waters contained higher concentrations of major anions (Cl^-, SO_4^{2-}, and HCO_3^-) compared with the Blue Lake waters, where anion concentrations were negligible. The addition of dissolved organic matter (DOM) produced a contrasting effect on Hg^{2+} accumulation relative to MeHg. After seven hours of DGT deployment, Hg^{2+} uptake in the Blue Lake treatment was observed to be approximately five times higher in the presence of DOM than in the DOM-free treatment, while the Rotomahana Lake treatment exhibited an observed twofold increase with DOM addition (Figure 8). These results indicate that DOM enhanced Hg^{2+} adsorption onto the 3-MFSG resin, likely by altering mercury speciation or

facilitating interactions between Hg^{2+} and the resin surface.

On the contrary, DOM binds strongly with Hg^{2+} to form a Hg-DOM complex. Similar to chloride, Hg^{2+} makes strong complexes with thiol functional groups in DOM. The complexation of Hg species to DOM often complicates the DGT performance because the diffusion coefficients of DOM are typically markedly lower than those of metals complexed with small inorganic ligands (Zhang & Davidson, 2000; Cattani et al., 2009). Hg-DOM complexes have a lower lability and are more stable when compared to MeHg-DOM complexes (Cattani et al., 2009). Due to a stronger Hg-DOM binding, Hg^{2+} would have a lower effective diffusion coefficient as Hg^{2+} would need a longer time to disassociate from DOM. Warnken et al. (2007) proposed that a thicker diffusive layer would allow Hg-DOM to have longer residence time for disassociation and therefore, allowing Hg^{2+} to move freely into the resin with a higher diffusion coefficient. The effective diffusion coefficients tended to decrease (become slower) by decreasing the thickness of the diffusion layer. Thinner diffusive layer would mean shorter residence time for Hg-DOM complexes, thereby not allowing dissociation of the complexes. Hong et al. (2011) came up with another probable explanation for Hg^{2+} slower adsorption rate when compared to MeHg. He postulated that Hg^{2+} combined with OH^- in the diffusive layer formed a metal complex which caused a Hg^{2+} retardation in the agarose layer. Docekalova and Divis (2005) observed that Hg^{2+} concentrations in agarose layer were 4.5 times greater when compared to Hg^{2+} concentrations in water after 8h equilibration. Strong sorption of Hg^{2+} to the agarose layer is not expected, but slight retardation of Hg^{2+} in the layer is possible. All of this explained the greater uptake of MeHg in the DGT as compared to Hg^{2+}. Even so, high concentrations of DOM in natural waters may reduce the most bioavailable forms of mercury.

With a greater binding between Hg-DOM complexes, it would also mean lesser loss of Hg^{2+} into the air. Free, unbound Hg^{2+} easily evaporate into the atmosphere through a process called evasion (Ariya et al., 2015). In Hg^{2+} buckets without DOM, Hg^{2+} had a smaller uptake in DGT which may be due to loss of Hg^{2+} into the air. In Hg^{2+} buckets with DOM, Hg^{2+} easily binds with DOM and gets trapped in the diffusive layer before being adsorbed onto the resin. As a result, the final Hg^{2+} concentration in DGT was much higher as compared to the buckets of Hg^{2+} without DOM.

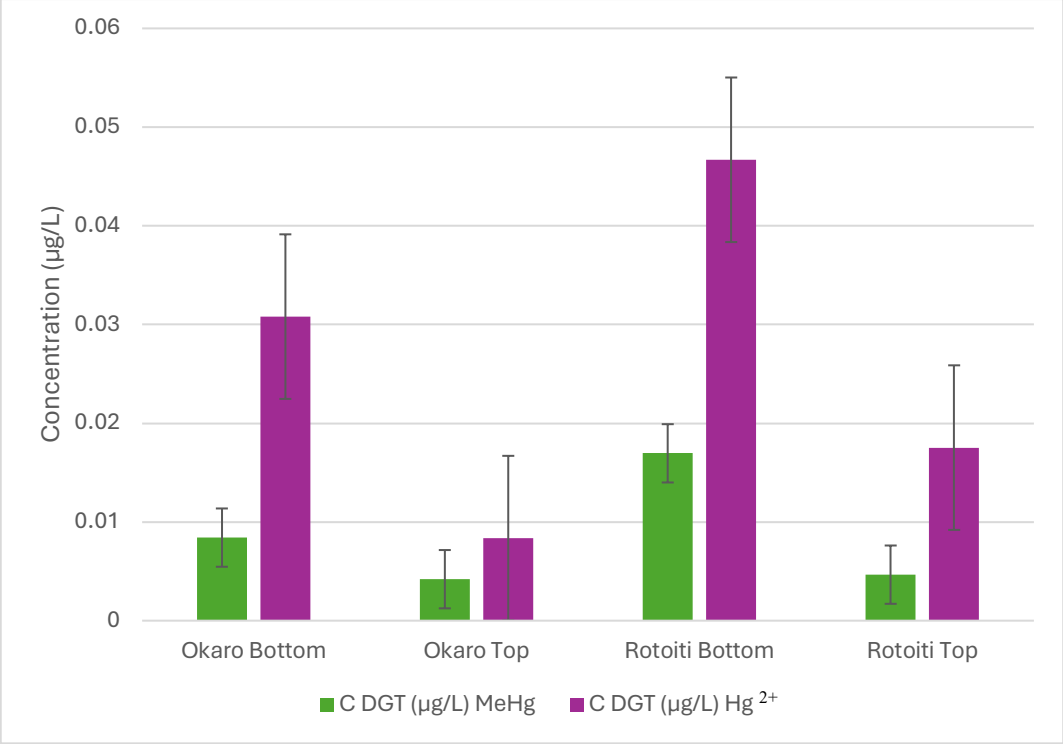

Figure 9. Concentration of Hg^{2+} and MeHg accumulated in DGTs deployed in triplicates in the epilimnion and hypolimnion of Lakes Rotoiti and Okaro during March and April 2019.

The MeHg DGT combined to HPLC-ICPMS technique was tested in three locations at Rotorua, namely Lakes Rotoiti, Okaro and Rotomahana. Earlier data of DGTs that were deployed in 2017 from the three lakes could not be used as the HPLC-ICPMS were having problems analysing MeHg. The ICPMS (Perkin Elmer) that was previously used at the University of Waikato had been upgraded to a triple quad in 2018 with a different manufacturer (Agilent). There were a few obstacles in setting up the method with a new software which contributed to a lapse time in analysing the DGTs. As such, data that were obtained did not accurately reflect the concentration of MeHg as the DGTs would have degraded over time.

As seen from Figure 9, levels of MeHg and elemental mercury were found to be highest in the hypolimnion of Lake Rotoiti with a concentration of 0.018 µg/L and 0.047 µg/L respectively. The epilimnion at Lake Rotoiti had 0.022 µg/L of elemental mercury and 0.006 µg/L of MeHg. The hypolimnion of Lake Okaro showed a MeHg concentration of 0.008 µg/L and a concentration of elemental mercury at 0.029 µg/L while the epilimnion showed a concentration of 0.005 µg/L MeHg and 0.011 µg/L elemental mercury. The results seen in Lake Okaro showed a similar pattern whereby the concentration of elemental mercury was much

higher than MeHg and the concentrations of both mercury levels were much higher in the hypolimnion as compared to the epilimnion.

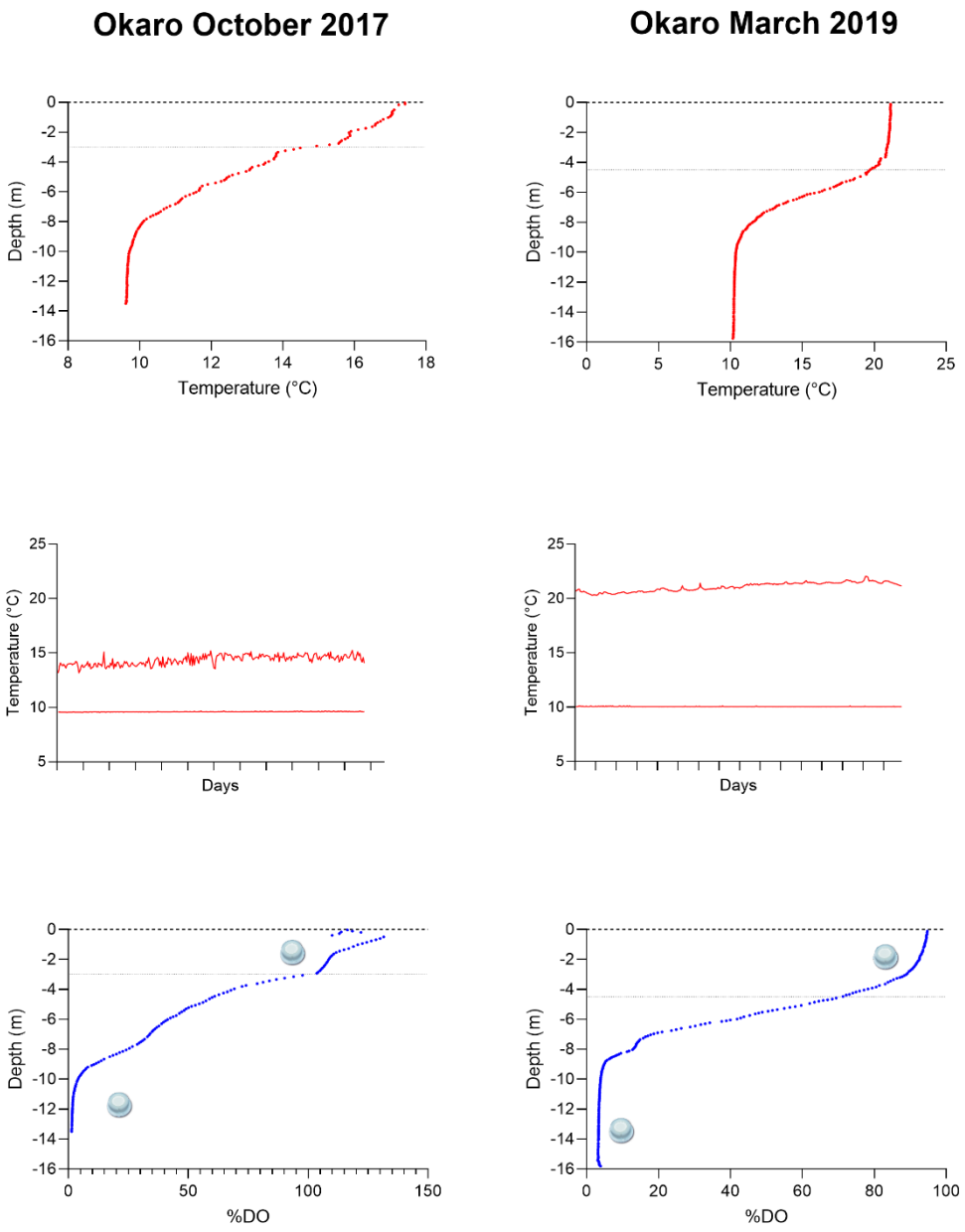

Figure 10. Temperature profile of the water column during DGT deployment and throughout the days when the DGT were deployed, dissolved oxygen profile (mg/L) in Lake Okaro in October 2017 and March 2019.

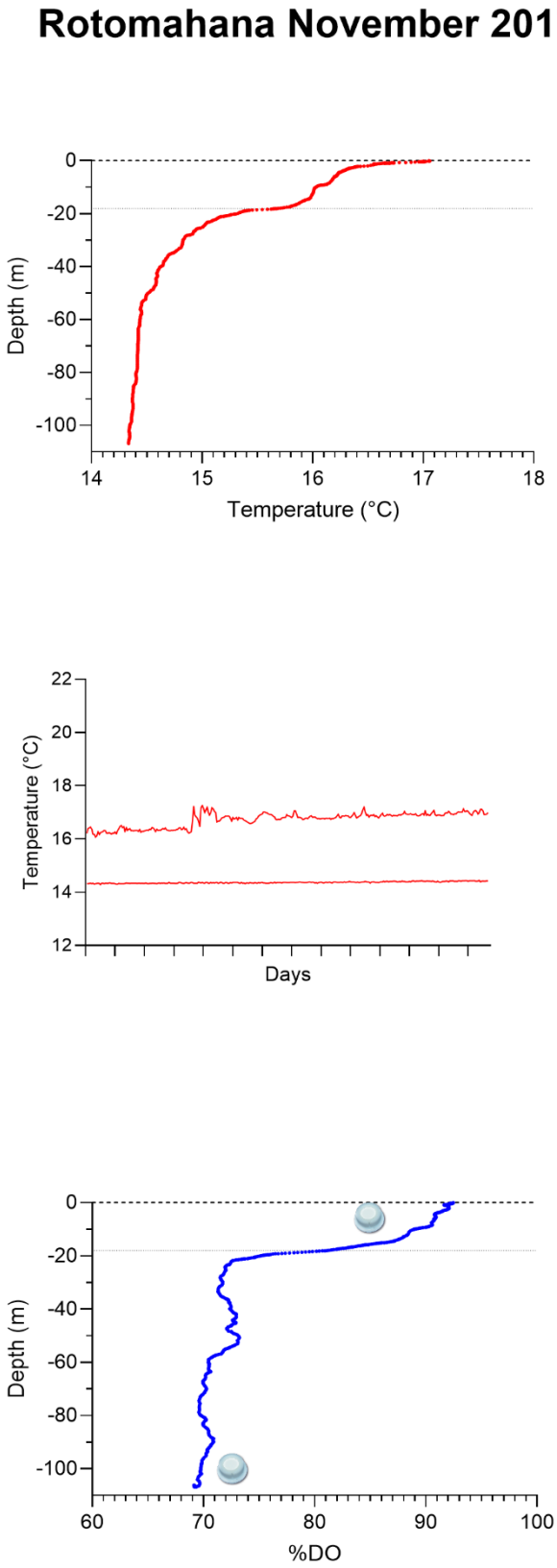

Figure 11. Temperature profile of the water column during DGT deployment and throughout the days when the DGT were deployed, dissolved oxygen profile (mg/L) in Lake Rotomahana in November 2017.

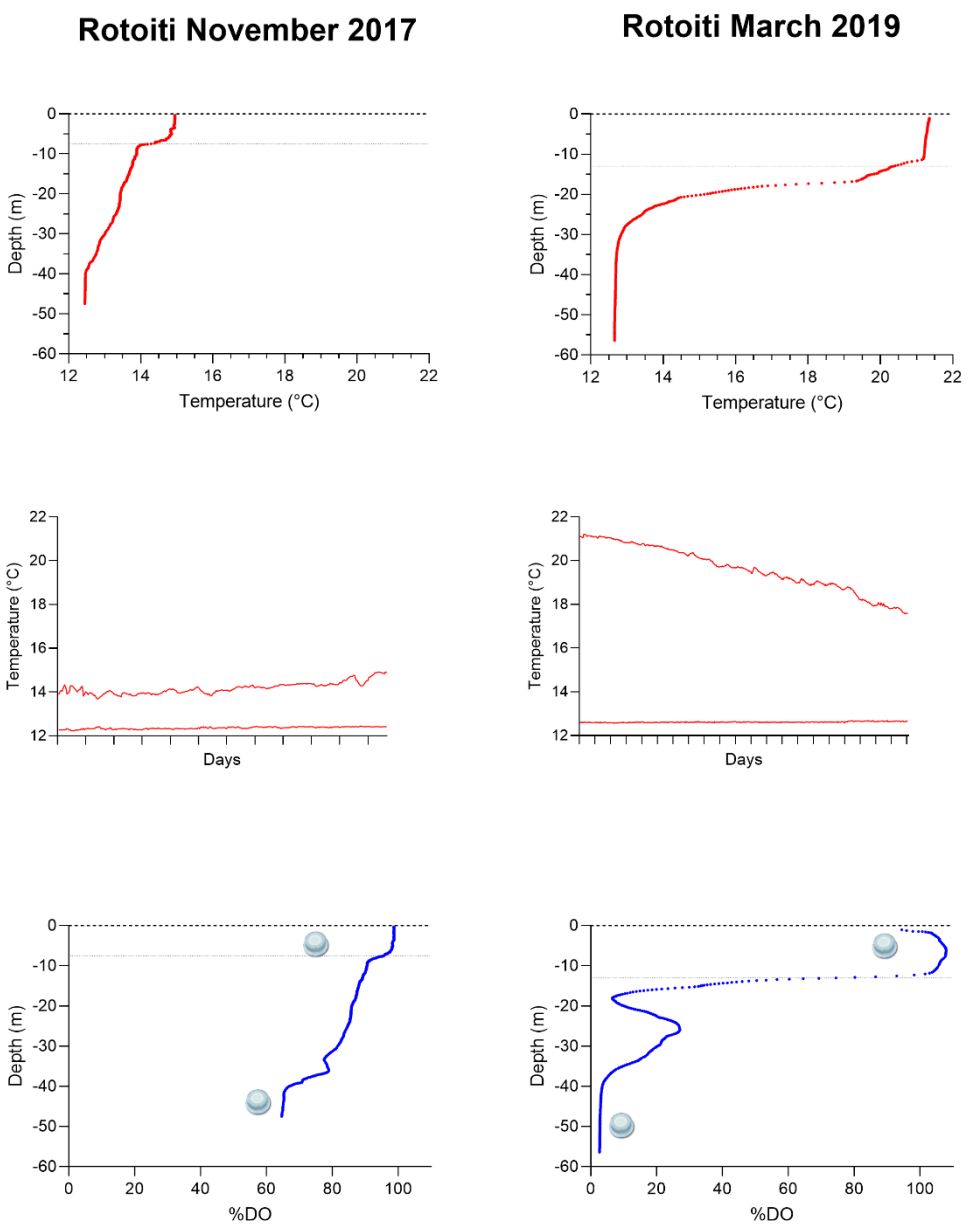

Figure 12. Temperature profile of the water column during DGT deployment and throughout the days when the DGT were deployed, dissolved oxygen profile (mg/L) in Lake Rotoiti in November 2017 and March 2019.

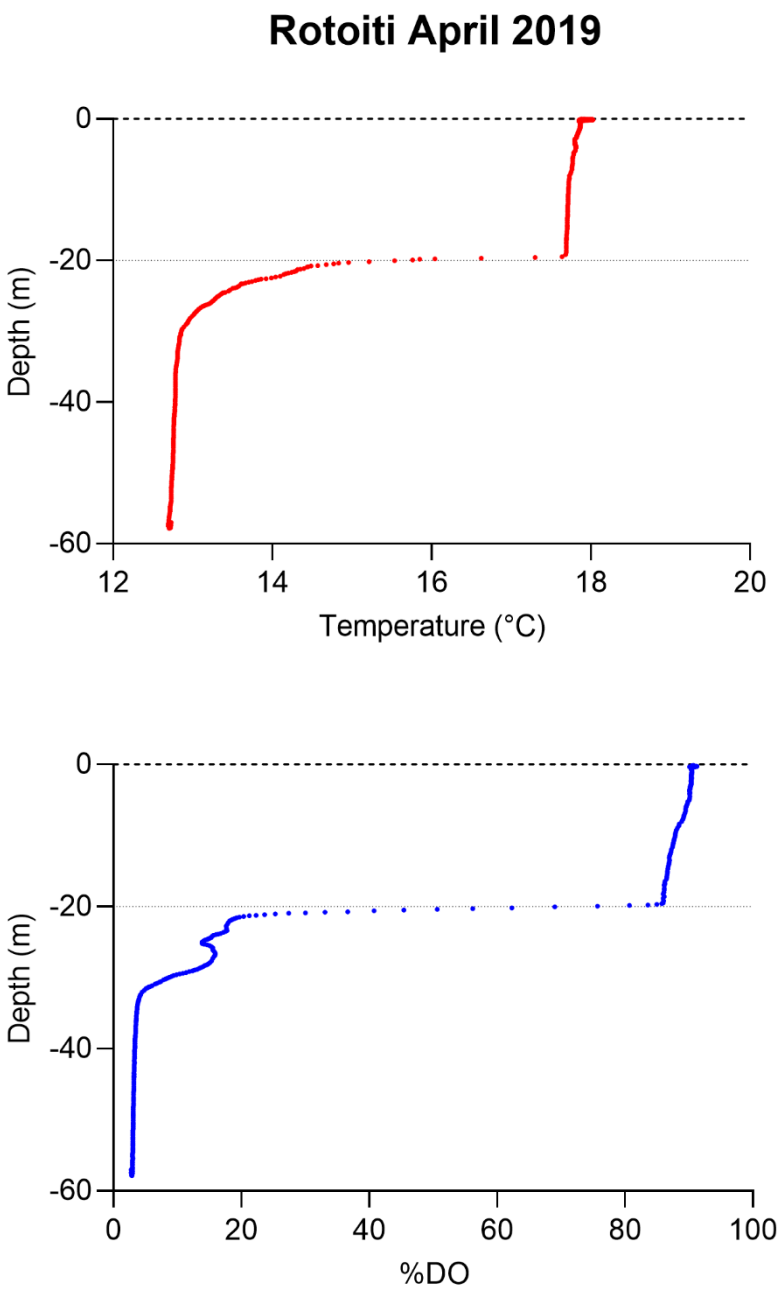

Figure 13. Dissolved oxygen profile (mg/L) and temperature (°C) vs depth (m) in Lake Rotoiti on the 16th of April 2019 during retrieval of DGTs.

As the DGTs were placed during the start of spring and at the end of summer for lakes Rotoiti and Okaro, there were obvious thermal stratification (Figure 10 to Figure 13) in the lake column. Even though the DGT data for MeHg and Hg were not useable for year 2017, the temperature profiles as well as the dissolved oxygen profiles provided additional data to compare in different seasons. As seen in Figure 8, Lake Okaro with a depth of 16 m, had clear thermal stratification in March 2019 as compared to October 2017 where the temperature drop was more gradual. The epilimnion layer where the DGTs were placed in Lake Okaro in 2019 showed a high temperature of 21°C while DGTs placed in Lake Okaro in 2017 showed a temperature of 14°C. Both the hypolimnion remained the same at about 10°C. In lake Rotoiti, thermal stratification was seen more distinctly (Figure 10) in summer as compared to lake Okaro due to a deeper depth in the lake. In the summer of 2019, the epilimnion where the DGTs were deployed in Rotoiti achieved a high temperature of 21°C and a low of 12°C in the hypolimnion. This was at the beginning of the DGT deployment. At the end of the deployment for lake Rotoiti, the epilimnion showed a decreasing temperature of 17°C while the hypolimnion remained the same. Due to the hypolimnion and the epilimnion not mixing, trace elements and MeHg remained at a higher concentration in the hypolimnion. It is interesting to note the dissolved oxygen levels showed similar patterns for lakes Rotoiti and Rotomahana during summer with high thermal stratification and in spring with no stratification. During spring where there were little to no stratification, dissolved oxygen was roughly 60-70% at the bottom of lake Rotoiti and Rotomahana while in summer with obvious thermal stratification occurring, lake Rotoiti showed anoxic conditions at the bottom of the lake. In spring when the lake turnover, dissolved oxygen from the epilimnion would be able to replenish the anoxic conditions at the bottom of the lake. The dissolved oxygen data above confirmed that thermal stratification and lake turnover affect mixing and distribution of not only oxygen but also other elements that are present at the hypolimnion. Lake Okaro exhibited lower dissolved oxygen levels and higher anoxia during spring compared to Lakes Rotoiti and Rotomahana, primarily due to its status as a highly eutrophic lake. Eutrophic conditions in Lake Okaro result in elevated nutrient concentrations, which promote excessive plant and algal growth. As these primary producers die and undergo decomposition, microbial activity increases, leading to heightened oxygen consumption in the water column. This process further depletes oxygen levels, ultimately resulting in anoxic conditions in the hypolimnion (Forsyth et al., 1988).

In a broader ecological context, the microbial conversion of Hg^{2+} into MeHg is

mediated by sulfate-reducing bacteria and iron-reducing microorganisms. These organisms take up Hg^{2+} during their metabolic processes in anaerobic conditions and convert it to MeHg (Compeau & Bartha, 1985; Fleming et al., 2006). The methylation process is intimately tied to the redox potential of the environment, which influences microbial activity. In water bodies, anoxic zones such as hypolimnion exhibit higher concentrations of MeHg compared to oxic regions like epilimnion (Pak & Bartha, 1998; Blum et al., 2013). This spatial distribution of MeHg can be attributed to the prevalence of anaerobic conditions that favor bacterial conversion in hypolimnion layers. In anoxic environments such as hypolimnion, the high concentration of MeHg can be attributed to increased microbial activities under anaerobic conditions. These environments support a diverse community of sulfate-reducing bacteria and iron-reducing microorganisms that are capable of methylating mercury (Fleming et al., 2006). Anaerobic zones often have lower redox potentials, which favor the reduction of sulfur compounds to sulfides and the reduction of Fe^{3+} to Fe^{2+}. These chemical transformations can influence the bioavailability of Hg^{2+} by altering its speciation in the environment (Gilmour et al., 1992).

Overall, it can be concluded that lake Rotoiti was stratified during the DGT deployment as it was during summer, and the hypolimnetic water was anoxic, thereby promoting conditions that would favour MeHg production. To elucidate the intricate mechanisms underlying mercury methylation, future research should focus on characterizing the specific functional groups in DOM that facilitate Hg^{2+} complexation and examining their influence on microbial activities (Weber, 1993). Additionally, investigating the spatial distribution of MeHg concentrations across different redox zones within aquatic systems can provide insights into the environmental factors driving methylation processes. By integrating these findings with ecological and chemical data, a comprehensive understanding of mercury cycling in aquatic environments can be achieved.

Furthermore, understanding the environmental conditions that favor or inhibit mercury methylation is crucial for predicting its occurrence and potential impacts on ecosystems (Drott et al., 2008). Factors such as temperature, pH, and nutrient availability can affect microbial activities and Hg^{2+} speciation, thereby influencing methylation rates. Investigating these relationships through field studies and laboratory experiments can provide valuable insights into the ecological processes

governing mercury transformations.

3.5 Conclusion

This chapter introduced an innovative methodology for quantifying MeHg and Hg^{2+} within aquatic ecosystems through the utilization of DGT technology equipped with a 3-MFSG resin. The 3-MFSG resin facilitated the selective accumulation and concentration of mercury species, including MeHg and elemental Hg, over an extended deployment period within the aquatic medium. A key advancement in this methodology was the development of a more precise extraction protocol for retrieving MeHg and Hg from the hydrogel matrix of DGT devices. This protocol ensured minimal loss of mercury through evaporation, thereby enhancing the accuracy and reliability of subsequent analyses. The analysis itself employed a combined High-Performance Liquid Chromatography Inductively Coupled Plasma Mass Spectrometry (HPLC-ICP-MS) technique, which offered exceptional sensitivity and specificity in detecting trace levels of MeHg and Hg within environmental samples.

The efficacy and applicability of this novel methodology were demonstrated through field deployments of DGT devices in Lakes Rotoiti and Okaro. The successful quantification of both MeHg and Hg concentrations in these lakes underscored the potential of this approach for monitoring mercury dynamics in aquatic systems, providing critical data for assessing environmental risks and informing management strategies aimed at mitigating mercury contamination.

This chapter represents a significant contribution to the field of environmental chemistry by offering an enhanced methodological framework for the precise measurement of MeHg and Hg concentrations in natural waters. By combining DGT samplers incorporating 3-MFSG resin with optimized extraction and analytical procedures, this study demonstrates a robust and highly sensitive method for mercury speciation. The ability to separate MeHg from total mercury at low detection limits enhances the utility of this approach for advancing understanding of mercury biogeochemical processes and informing environmental management in aquatic systems.

4 Comparison of bioaccumulation of methylmercury and mercury between tissues and species

4.1 Introduction

The Taupo Volcanic Zone (TVZ) in New Zealand is renowned for its recreational trout fishing, particularly with *Oncorhynchus mykiss* (rainbow trout). Prior to the introduction of recreational trout fishing, Māori communities utilized these freshwater lakes as a primary food source, a relationship that continues through ongoing customary use and harvesting. Indigenous fish species such as toitoi (*Gobiomorphus spp*.), inanga (*Galaxias maculatus*), kokopu (*Galaxias vulgaris* and *Galaxias brevipinnis*), koaro (*Galaxias cobitoides*), kakahi (mussels), and koura (freshwater crayfish) were commonly harvested (Hiroa, 1921; Kusabs and Quinn, 2009). Rainbow trout were introduced into Lake Rotorua in 1892 and Lake Taupo in 1897, and whilst recreational fishing became a popular pastime, it lead to a decline in the average weight of trout to approximately 2 kg by 1990 (McKinnon, 2007). To manage fishing pressure, daily catch limits were implemented which is a daily limit of eight trout. Today trout can be found in rivers and lakes throughout the region but the Te Arawa lakes, and Lake Taupō and its catchment, remain the most fished waters.

Bioaccumulation of mercury in aquatic organisms poses a significant environmental and public health concern due to its persistence, toxicity, and propensity to increase in concentration at higher trophic levels. Fish serves as a crucial dietary source of protein for Māori and other New Zealanders, making bioaccumulated Hg and MeHg a significant health concern. Although the presence of mercury in marine fish, particularly larger predatory species, is well-documented, there is relatively less awareness regarding its accumulation in freshwater fish in New Zealand. However, several studies have investigated Hg levels in lake water and aquatic organisms resulting from geothermal inputs into lakes within the Taupo Volcanic Zone (Brooks et al., 1976; Timperley and Vigor-Brown, 1986; Kim and Burggraaf, 1999; Verburg et al., 2014). Many chemicals are known to bioaccumulate, meaning their concentrations are higher within organisms compared to their surroundings. Hg^{2+} and MeHg exhibit both bioaccumulation and biomagnification, leading to increased tissue concentrations in biota as

they ascend the trophic levels of food webs (Kidd et al., 1995). Consequently, species at higher trophic positions face greater health risks due to exposure to biomagnifying chemicals. Therefore, regular chemical monitoring of fish populations is essential for assessing their potential risk to human health.

Exposure in humans to high levels of MeHg can lead to neurological damage. Infants *in utero* are especially at risk as their brains develop rapidly during this period. Certain studies focusing on populations with a heavy fish diet have found correlations between maternal consumption and subtle developmental delays in children, which can only be identified through specialized tests designed to evaluate learning and behavior (Budtz-Jørgensen et al., 2000; Grandjean et al., 1997). In adults, the initial manifestations of excessive MeHg exposure generally include sensory symptoms like numbness and tingling in the fingers, lips, and toes. It is important to note that the levels required to produce adverse effects in adults are significantly higher than those associated with fetal developmental issues stemming from maternal exposure (Clarkson, T.W., 2002).

The health impacts of MeHg have led governmental bodies to establish strict limits on permissible levels in commercially sold fish. For instance, the acceptable concentration in retail fish in the USA and specific predatory species in Australia and the European Union is 1 μg/g wet weight, while other retail fish in Canada are subject to a limit of 0.5 μg/g (Canadian Food Inspection Agency, 2002; The Commission of the European Communities, 2001; United Nations Environment Programme Chemicals, 2002; US Food and Drug Administration, 2007). Moreover, several government agencies have issued guidelines to limit mercury exposure through fish consumption. In Alaska, recommendations for different species have been formulated based on contaminant levels (Hamade, 2014), while New Zealand Food Safety has advised specific serving sizes for trout from Lake Rotomahana and other geothermal lakes to minimize MeHg intake, suggesting one serving every one to two weeks as safe (New Zealand Food Safety, 2023). These guidelines are referring to fish fillet and are particularly relevant to populations relying heavily on fish and marine mammals in their diet. Given that entire fish, not just the flesh, are often consumed, it is imperative to understand the distribution of THg and MeHg across various tissue types and species to accurately assess consumption risks and formulate appropriate dietary recommendations.

Several studies have been conducted on Hg concentrations in trout from the Taupo Volcanic Zone (TVZ), including those by Brooks et al. (1976), Kim and Burggraaf (1999), and Verburg et al. (2014). However, these investigations did not encompass all TVZ lakes (Table 4) that receive geothermal inputs as well as these studies have been conducted many years ago and do not reflect the current understanding of Hg and MeHg in fish. In this study, we examined THg and MeHg concentrations in selected macrofauna from the food webs of 11 lakes with geothermal Hg inputs around the Rotorua region. Building upon the work of Brooks (1976), Kim (1995), Ling (unpublished, 2007/2008), Philips et al. (2009), and Verburg et al. (2014), we have expanded our investigation to include lakes not previously covered by these studies. Furthermore, we have analyzed organs beyond muscle tissue and included MeHg analysis in addition to elemental and total mercury. The findings from this study aim to provide insights into the distribution of MeHg between flesh and liver tissues and the biomagnification processes within the food chain. The outcomes of this study are anticipated to support risk assessment efforts and the formulation of regionally appropriate guidelines for mercury concentrations in freshwater fish.

4.2 Literature Review

The toxicological implications of Hg have garnered significant international attention within public health circles following the widespread poisoning incident in Minamata Bay, Japan, which affected over 800 individuals, predominantly fetuses and infants (Powell, 1991). Consequently, monitoring Hg concentrations in both environmental settings and living organisms has become a critical component of human health risk assessment. However, to effectively engage in this monitoring, it is imperative first to comprehend the various chemical species of Hg. While numerous forms exist, for purposes of environmental surveillance, Hg can be broadly categorized into two primary groups: inorganic mercury (Hg^0, Hg^{2+}, Hg^+) and organic mercury (MeHg, CH_2Hg). According to Clarkson (1997), inorganic Hg is poorly absorbed by the vertebrate gastrointestinal tract and is rapidly excreted via urine and feces following ingestion. In contrast, organic mercury, particularly MeHg, poses a considerable risk to humans and top predators that predominantly consume fish-based diets. This is due to its high bioavailability, allowing for efficient absorption in the gut and subsequent distribution throughout various tissues such as muscle and liver, where it can accumulate over time (Wolfe et al., 1998). As MeHg is transferred through aquatic food webs, biomagnification can result in concentrations that may present a potential toxicological risk to humans. The transport of

MeHg within the human body is facilitated by complexes formed with cysteine groups (MeHg-S-R), which enable the crossing of the blood-brain barrier and accumulation in brain tissues (Clarkson et al., 2003). This characteristic makes MeHg a potent neurotoxicant, posing substantial risks to both infants and adults (Roos et al., 2010).

In New Zealand, natural geothermal discharges introduce Hg into lakes and streams. Initially, Hg is present in its inorganic form, settling in sediments while also circulating freely within the hypolimnion. Through a process known as methylation, inorganic Hg is converted to organic Hg, which poses greater risks to living organisms. Subsequently, Hg moves from sediments into the food chain (Park and Curtis, 1997). The concentration of Hg within an organism generally increases with its trophic level in the food web (Cizdziel et al., 2002; Dusek et al., 2005), as well as factors such as size, age, and duration of exposure (Honda et al., 1983). Additionally, there is a correlation between Hg concentrations and fish weight, whereby an increase in size and age would increase Hg concentrations (Abreu et al., 2000; Farkas, Salanki & Specziar, 2003).

Mercury levels in fish muscle are shaped by both the predominance of methylmercury and the biochemical composition of the tissue. Numerous studies have demonstrated that MeHg constitutes over 80% of total Hg (THg) concentrations in fish muscle (Jewett et al., 2003). A reduction in protein concentration could result in lower THg levels as a consequence of diminished binding site availability, particularly cysteine residues. Consequently, these biochemical interactions may contribute to differences in the percentage of MeHg relative to total mercury content (%MeHg).

In vertebrates, including mammals, birds, and fish, THg concentrations are often highest in liver tissues (Wagemann et al., 1998; Dietz et al., 2000; Moses et al., 2009). The liver plays a crucial role in metal sequestration, biotransformation, and elimination processes. Given its central importance in metal toxicokinetics, many Hg monitoring studies focus exclusively on hepatic tissues (Riget et al., 2005; Mieiro et al., 2009). Liver serve as key indicators of mercury bioaccumulation and toxicity. However, the percentage of MeHg in liver tissue exhibits considerable variability compared to other tissues (Palmisano et al., 1995; Eagles-Smith et al., 2009). This variability is partly attributed to demethylation processes that occur within the liver. Demethylation converts MeHg back into inorganic mercury, which can then be excreted more readily from the body (Lee et al., 2020; X. Wang & Wang, 2017).

Consequently, lower % MeHg levels observed in some fish livers may indicate active demethylation processes (Barkay & Gu, 2022; Polak-Juszczak, 2018; R. Wang et al., 2013). The biochemical pathways and regulatory mechanisms governing these transformations are complex and multifaceted. They involve enzymatic activities such as cytochrome P450-dependent monooxygenases and glutathione S-transferase (GST) enzymes, which play roles in both the methylation and demethylation of mercury compounds (Palmisano et al., 1995). Understanding these processes is crucial for developing effective strategies to mitigate the impacts of mercury pollution.

In New Zealand, Weissberg & Zobel (1973) conducted a study on the mercury content in muscle tissue from various rainbow trout (*Oncorhynchus mykiss*) inhabiting the Taupo Volcanic Zone (TVZ) lakes. Their findings indicated that mercury levels in these fish exceeded the limits deemed safe for human consumption as established by health authorities worldwide. Notably, Weissberg & Zobel (1973) discovered elevated Hg concentrations (0.020-3.220 mg/kg), which they attributed to natural emissions from geothermal areas while investigating high mercury levels in trout caught in Lake Maraetai, originally suspected to originate from a paper mill at Kinleith. Brooks et al. (1976) extended this research by examining the presence of mercury and other heavy metals across various organs and tissues of trout located around TVZ lakes. Their study revealed high concentrations of THg in the muscle tissue of rainbow trout from Lakes Rotorua, Rotoiti, Rotomahana, Maraetai, and a single specimen from Reporoa. Further research by Kim & Burggraaf (1999) demonstrated that MeHg concentrations accumulate and biomagnify through the food webs in Lakes Okareka, Okaro, Tarawera, Rotorua and Rotomahana. More recently, Verburg et al. (2014) established a positive correlation between MeHg levels in trout and the degree of eutrophication in their respective lakes. In summary, these studies underscore the significant bioaccumulation of mercury in rainbow trout within the TVZ region of New Zealand. The findings reported that elevated Hg concentrations in fish muscle tissue had surpassed safety thresholds established by health authorities globally. Additionally, biomagnification processes amplify these levels through the food webs, with eutrophic conditions exacerbating mercury accumulation in trout populations (Verburg et al., 2014).

Table 4. Range of total Hg (mg/kg wet weight) in muscles tissues of trout sampled from past studies.

Author (Year)	Lakes (n)	Trout THg (mg/kg)
Weissberg & Zobel (1973)	6	0.020-3.220
Brooks et al. (1976)	13	0.060-3.000
Kim & Burggraaf (1999)	5	0.220-1.840
Philips et al. (1999)	11	0.190-19.000
Verburg et al. (2014)	3	1.131-9.021

4.3 Materials and Methods

4.3.1 Study area

All eleven Te Arawa lakes located in the Bay of Plenty Region (Rotorua, Rotoiti, Rotoehu, Rotoma, Okataina, Okareka, Tikitapu, Tarawera, Rotomahana, Okaro, Rerewhakaaitu) were selected as part of the study area. These lakes lie within the Taupo Volcanic Zone (TVZ), which has existing natural geothermal activity. The geothermal waters in the TVZ are high in Hg compared to other natural waters in New Zealand (Weissberg, 1975; Weissberg and Rohde, 1978; Timperley, 1986; Kim, 1995). Lakes Okareka and Okaro have few geothermal sources (6% of total water input) while Lakes Tarawera, Rotorua and Rotomahana have greater geothermal inputs from hot springs and thermal vents estimated at 37%, 43% and 53% respectively (Donovan et al., 2003). Other lake characteristics are also shown in (Table 5), such as depth and lake volumes.

Table 5. Lake morphology of the study area in Rotorua (Donovan et al., 2003).

Lakes	Lake area (km2)	Catchment Area (km2)	Max. depth (m)
Okareka	3.3	19.6	33.5
Okaro	0.33	3.9	18
Okataina	10.8	59.8	78.5
Rerewhakaaitu	5.8	37	15.8
Rotoehu	8.1	49.2	13.5
Rotoiti	34.6	123.7	124
Rotoma	11.2	27.8	83
Rotomahana	9	83.3	125
Rotorua	80.8	508	45
Tarawera	41.7	143.1	87.5
Tikitapu	1.5	6.2	27.5

4.3.2 Sample collection

Fish sampling began in all 11 lakes during the spring and autumn seasons of 2017 and it was to continue during these seasons for 2018 and 2019 as well. However, due to unpredictable weather (cyclones, rain and storms), fish were collected throughout the years whenever possible. Most fishes were obtained with the help from Eastern Region Fish and Game Council, Rotorua. The overall targeted samples (n=10) per lake of rainbow trout (*Oncorhynchus mykiss*) were collected for total Hg and MeHg analysis, although this number varied with different lakes. They were captured using gill nets set from littoral margins. A 100 mm mesh size was used to effectively select fish that were two to three years old, between 40 and 60 cm long and weighing 1 to 3 kg. Nets were set for no longer than 3 hours and checked regularly to avoid overfishing. For some lakes, fish were supplied by anglers and in the case of Lake Okataina only muscle was provided without accompanying livers. The anglers recorded the weight and length of each fish before filleting the tissues and storing them in ice. Following capture, all fish were immediately killed by stunning and pithing according to SOP#6 of the University of Waikato Animal Ethics Committee (Euthanasia and Anaesthesia of Fish) and frozen (-20°C) until analysis in the laboratory. At the laboratory, fish lengths were recorded and trout were weighed. Trout were then dissected by cutting 5 cm of flesh from the epaxial

muscle immediately posterior to the position of the operculum (Figure 14), with a subsample of approximately 2 g wet weight used for analysis. The liver was also sampled with a subsample of approximate wet weight of 2 g as well. All samples were labelled and stored in sterile Whirl-Pak bags at -20°C until further analysis.

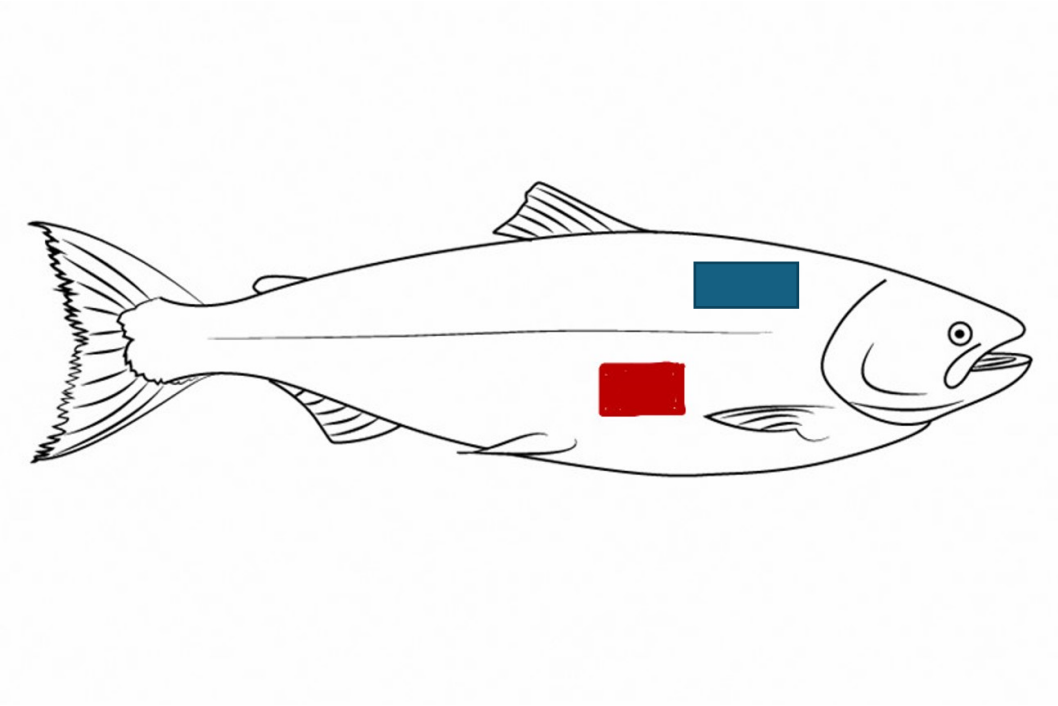

Figure 14. Location of flesh taken – the location of the flesh sample actually corresponds to the blue rectangle above – i.e. epaxial muscle forward of the dorsal fin.

Adult koura (*Paranephrops planifrons*) were collected by SCUBA divers from all of the Rotorua lakes that are known to support significant populations: Rotorua, Rotoiti, Rotoehu, Rotoma, Okataina, Tarawera, Tikitapu, Okareka, Rerewhakaaitu. Collections of koura from Lakes Okareka, Tikitapu and Rerewhakaaitu were undertaken as part of fish health monitoring associated with whole lake mineral treatments in 2006 and 2007. Other lakes were sampled in the winter of 2007 and late summer of 2008, with the exception of Lake Rotorua which was only sampled in late summer 2008. Koura were collected from under logs and boulders near the lake shore in lakes Rotorua, Rotoehu, Tikitapu and Rerewhakaaitu due to the relative scarcity of animals in open water. Koura were either anaesthetised in an ice/water slurry for 10 min or killed by freezing prior to dissection. Measurements were taken of total length (± 1 mm), ocular carapace length (± 1 mm) and total weight (± 0.01 g). Animals were dissected by cutting along the midline of the ventral cephalothorax (Figure 15) and along both sides of the

tail. The entire hepatopancreas (Figure 16) and approximately 1 – 2.5 g of tail flesh were removed and stored in cryovials at - 20°C for later analysis of metals by inductively-coupled plasma mass spectrometry (ICPMS). Tissue digests of the hepatopancreas and tail flesh of koura were undertaken at the time of collection and this study includes a reanalysis of those data. Elemental analyses were performed on both the tail flesh and the hepatopancreas (digestive gland). Attempts to reanalyse stored digested samples from koura were unsuccessful due to sample stability and preservation over time.

Adult individuals of the native freshwater unionid mussel (*Echyridella menziesii*) (local Māori name kakahi) were collected by snorkeling or SCUBA diving at depths up to 5 m. Kakahi and koura could not be found in Lake Rotomahana and are not known to occur in this lake due to the historical volcanic ejection of the lake's contents during the Tarawera eruption in 1886. Kakahi also do not occur in lakes Okataina, Okaro and Tikitapu. Only the digestive gland was analysed in kakahi. The entire digestive gland was dissected from the surrounding tissues and analysed for trace element composition using the same digestion and analysis procedures outlined for the tissues of koura and trout.

Figure 15. Koura - ventral dissection

Figure 16. Removal of the hepatopancreas

Surface water for Hg was collected in acid-cleaned polyethylene bottles by hand dipping and transferred to 50 ml tubes using a 50 ml syringe and filtered with 0.45 µm sterile membrane filter. The water samples were then stored in an ice box and brought back to the laboratory for further processing. Back at the laboratory, water samples were diluted by taking out 1 ml from the 50 ml tube and put into a 10 ml tube. It was then topped up with 8.8 ml H_2O and 100 µL HNO_3 and 100 µL HCl. The water samples were sent to the ICPMS laboratory for heavy metals analysis. Sediment data was obtained from Trolle, D. (2008). Trolle collected surface sediment (0-2 cm) from each lake using a cylindrical gravity corer.

To give a summary of the sampling timeline, trout, surface water and kakahi were collected from year 2017 to 2019, koura was collected from year 2007-2008 while sediment data provided from Trolle (2008) was collected from year 2006-2007.

Approvals to sample aquatic life were via our MPI special fisheries permit (SP698) which required consultation with iwi regarding sampling within their rohe. The taking of rainbow trout was permitted through Fish and Game new Zealand Eastern Region, and the sampling of the taonga species (koura and kakahi) was through consultation with the Te Arawa Lakes Trust and permitted through a puka whakamana issued by TALT under the Te Arawa Lakes (Fisheries) Bylaws 2020, including allowing the use of SCUBA to undertake that sampling.

4.3.3 Sample analysis

4.3.3.1 Sample digestion

The digestion method was taken from the standard operating procedure for metals, inductively coupled plasma – mass spectrometry in fish tissues (EPA, 200.11). All reagents used in this experiment were of ACS grade. A labelled 50 mL centrifuge tube with its cap on was placed in a 100 mL beaker and both containers were tared. The weight of both containers were recorded. An approximate 2 g wet weight sample of fish tissue was placed into this 50 mL centrifuge tube and the weight was recorded to the nearest mg. A standard was prepared using 0.2 g of dried fish certified reference material (DOLT-4, DORM-4 by National Research Council of Canada) was also placed into a labelled 50 mL centrifuge tube and the weight recorded. This reference was processed through the entire digestion with the fish samples. The samples were then sent for freeze drying. After the samples were freeze dried to constant weight, the weight of all samples together with the centrifuge tubes were recorded. A volume of 2 mL of Tetramethylammonium hydroxide (TMAH) (25% m/v, Sigma-Aldrich) were added into each sample. The cap was replaced and tightened securely. A method blank was prepared by transferring 2 mL of TMAH to an empty, labelled 50 mL centrifuge tube. This blank was processed through the entire digestion together with the fish samples. All samples, blank and references were placed in an open rack and heated for one hour at 60 ± 5°C in a water bath. After the first hour of heating, the samples were removed from the water bath, the caps were retightened if loosened, and the samples were mixed using a vortex mixer. The samples were returned to the water bath and heated for an additional hour. After the second hour of heating, each sample was vortex mixed and the rack of mixed samples was placed in an ice water bath for 30 min. Sample digests were partially oxidised by the addition of 0.5 mL of cold H_2O_2 (30% m/m, Sigma-Aldrich). The tube was immediately recapped and tightened securely. The capped samples were refrigerated overnight. The following day, the samples were vortex mixed and then 2 mL of 16M HNO_3 (65% v/v, Sigma-Aldrich) was added to each sample. The tube was recapped and vortex mixed again, each sample individually treated before proceeding to the next sample. The samples were returned to the water bath, and heated for 2 hours at 90°C with each sample vortex mixed after the first hour. The samples were cooled to room temperature, and made up to 50 mL with distilled water, and mixed well. Each sample was filtered using a 50 ml syringe and 0.45 µm sterile membrane filter into a clean, labelled 50 mL centrifuge tube. The samples were then diluted by taking 1 mL of digest from the 50 mL tube and placed into a 10 mL tube. In this 10 mL tube, a volume of 8.8 mL H_2O and 100 µL HNO_3 and 100 µL HCl

(37% v/v, Sigma-Aldrich) were added. This final 10 mL of diluted, digested sample was sent for ICPMS analysis for total Hg and a suite of other trace elements. For further CH_3Hg speciation, 1 mL of sample was taken from the 10 mL diluted, digested sample and placed into 1.5 mL HPLC tubes. A volume of 1 mL mobile phase was added and stored in the refrigerator till further analysis. Mobile phase consisted of 1.5% thiourea (Sigma-Aldrich) + 6.5% concentrated HNO_3 + 10% Acetic acid (Sigma-Aldrich).

4.3.3.2 Total mercury analysis

THg concentrations were determined by using inductively-coupled plasma mass spectrometry (ICP-MS). A suite of 28 elements, including physiologically regulated and non-regulated metals, were measured in tissue samples based on established methods (USEPA, 1997). The measured elements were: lithium (Li), boron (B), sodium (Na), magnesium (Mg), phosphorus (P), potassium (K), calcium (Ca), vanadium (V), chromium (Cr), iron (Fe), manganese (Mn), cobalt (Co), nickel (Ni), copper (Cu), zinc (Zn), arsenic (As), selenium (Se), strontium (Sr), silver (Ag), cadmium (Cd), indium (In), barium (Ba), lanthanum (La), mercury (Hg), thalium (Tl), lead (Pb), bismuth (Bi), uranium (U).

4.3.3.3 MeHg analysis

The samples that had been prepared for CH_3Hg analysis were analysed using high performance liquid chromatography (HPLC)/ inductively-coupled plasma mass spectrometry (ICP-MS). The mercury species concentrations that were determined were Hg^{2+} and MeHg and the experimental methods that were used were adapted from Hong et al. (2011). A high-pressure liquid chromatography (HPLC) system (Agilent 1200) was used to separate MeHg and Hg^{2+} complexes via a cation exchange column (IonPac CG5A, Dionex, Sunnyvale, Ca, USA). The HPLC unit was connected to a triple-quadrupole (QQQ) of a ICP-MS (Agilent 8900) through a manually switching valve (Rheodyne, Rohnert Park, Ca, USA) that allowed the system to be operated in either HPLC-ICP-MS mode or ICP-MS only mode. An acidic thiourea solution (1.5% thiourea + 6.5% concentrated nitric acid + 10% glacial acetic acid) was used to form the cationic charged species of Hg, such as $CH_3Hg(TU)^+$ and $Hg(TU)_4^{2+}$, and the complexes were then separated in a cation exchange column using the acidic thiourea solution as a mobile phase. With a continuous mobile phase flow rate of 1.0 mL/min and an injection volume of 100 µL, the total running time for MeHg and Hg^{2+} analysis was 7 minutes. The retention times of each Hg species were verified by injecting

blanks only spiked with MeHg and Hg^{2+}. MeHg was seen eluted at a retention time of 1.2 min and Hg^{2+} eluted at a retention time of 4.5 min. The HPLC-ICP-MS detection limits were able to show results of 1 ng/L, based on a signal to noise ratio 3:1.

4.3.4 Data analysis

All Quality Control criteria listed in the ICP-MS Standard Operating Procedure were followed. The fish reference material had the Quality Control recovery limits of 70 – 100%. The method detection limits (MDL) and practical quantitation limits (PQL) in μg/g were determined for each analyte using a natural fish matrix. The results were reported as μg metal / g wet fish tissue and were calculated as below:

$$\mu\mu g/g \text{ wet weight} = \frac{\mu\mu g / L * 0.05 L}{\text{wet weight fish(g)}}$$

If a dry-weight value was used, the dry weight was determined from a separate 2 g fish tissue freeze dried for >48 hours at -90°C.

Percent MeHg was calculated for each individual and tissue as mean [MeHg]/ mean [THg].

Bioaccumulation was determined from the slope of the linear regression of mean THg (trout) concentration against sediment THg concentration across lakes. The process was repeated with koura and kakahi against sediment THg concentration. Following Burgraaf et al. (1999), the bioaccumulation factor (BAF) was calculated as the antilog of the regression slope. Log transformed ratios were calculated for THg concentrations in trout-sediment, koura-sediment, kakahi-sediment, trout-kakahi, trout-koura and koura-kakahi (Watras et al., 1998). Such ratios were useful and were complimentary indicators of bioaccumulation of Hg in the food web. The 95% confidence limits of the regression slopes and BAF's were determined.

Statistical analyses were conducted using R. Differences in mean values were assessed using Student's *t*-tests, while relationships between variables were evaluated using Pearson's and Spearman's correlation coefficients, as appropriate.

4.4 Results and Discussion

Rainbow trout (*Oncorhynchus mykiss*) were selected for monitoring the bioaccumulation of THg and MeHg in the lakes ecosystem as they are the top predator in the food chain and are also commonly consumed by humans in recreational fishing. Mean concentrations of THg

found in the livers and flesh of trout sampled from 11 lakes in Rotorua are presented in Table 6. Data of koura and kakahi were taken from Ling, N. (unpublished, 2007-2008) as samples that were rerun once again in the ICP-MS did not corroborate with the original data. This could be due to degradation of the samples or loss of Hg in the tissues. In the 11 lakes sampled (Figure 19), fish from three lakes were found to exceed the WHO advisory recommendation for safe mercury levels consumption of 1 mg/kg wet weight of fish. THg were found to be highest in the flesh of trout from Lake Rotomahana with a mean THg of 3.195 mg/kg wet weight, ranging from 2.350-4.037 mg/kg wet weight, although only 3 fish were analysed from this lake. This was followed by trout from Lake Rotoiti with a mean THg concentration of 1.998 mg/kg wet weight flesh (range 1.603-2.812 mg/kg ww) and Lake Rotorua with a mean THg concentration of 1.763 mg/kg wet weight flesh (range 0.309-5.126 mg/kg ww). THg results at Lake Rotorua showed a wide range of THg concentration found in fish due to 3 individual fishes that had much higher concentrations of THg (4.937 mg/kg ww, 4.958 mg/kg ww, 5.126 mg/kg ww). This is particularly alarming given that the THg concentrations in these fishes were five times higher than allowed by the FDA and it would be of significant concern with regards to human consumption. FDA advisory allows a maximum mean mercury concentration of 0.678 mg/kg wet weight in trout (freshwater) for children and pregnant woman (FDA, 1991-2008). From the results shown, besides the three lakes mentioned earlier, all the other lakes (Rotoehu, Rotoma, Okataina, Okareka, Tikitapu, Tarawera, Okaro and Rerewhakaaitu) showed a mean THg concentration that is below the FDA safe levels, although there were several fishes that were higher than the FDA safe levels found in lakes Rotoma, Tarawera and Okaro.

When compared with results from past publications (Brooks et al., 1976; Kim, 1999; Ling, unpublished, 2007/8; Philips et al., 2009; Verburg et al., 2014), it is found that the THg concentrations of this study is consistent especially showing high concentrations above the WHO advisory safe mercury levels in lakes Rotorua, Rotoiti and Rotomahana. It is of grave concern as we looked at data from Brooks et al. who recorded the earliest mercury concentration in trout in 1976, we see an increase in total mercury concentrations in lakes Rotorua, Rotoiti and Rotomahana as compared to this study. Over a span of 43 years, total mercury levels have risen considerably: from a mean of 0.85 mg/kg to 1.763 mg/kg in Lake Rotorua, from 1.0 mg/kg to 1.998 mg/kg in Lake Rotoiti, and from 2.1 mg/kg to 3.195 mg/kg in Lake Rotomahana. Despite a plateau observed since Kim's study in 1995, the THg concentrations have nearly doubled over time. The increase in THg concentration might be attributed to an enhancement of the trophic state of these lakes. An increased trophic state leads

to greater hypolimnetic anoxia, which promotes higher MeHg production (Armstrong et al., 2025). According to the Rotorua Lakes Water Quality Report from 2000-2015, Lake Rotoiti fluctuated between eutrophic and mesotrophic states over a span of 15 years, while Lake Rotomahana remained mesotrophic and Lake Rotorua was consistently eutrophic. This trend is supported by Verburg et al. (2014), who found that the biomagnification of mercury and its concentrations in trout were enhanced by factors such as anoxia and other physicochemical properties associated with increased eutrophication.

As seen in Figure 17, Lakes Rotomahana, Rotorua and Rotoiti have a high percentage of geothermal fluids and steam coming into the lakes (Timperley & Vigor-Brown, 1986). Geothermal fluids often contain elevated concentrations of various metals and substances such as boron (B), arsenic (As), lithium (Li) in water, and hydrogen sulfide (H_2S), ammonium ions (NH_4^+), and mercury (Hg) in steam (Ellis & Mahon, 1977). Lakes Rotorua, Rotoiti, and Rotomahana are expected to have higher concentrations of Hg in water due to the influence of geothermal steam compared to lakes that do not receive any geothermal inputs. The high concentration of THg in trout from these lakes matched expectations and is consistent with the substantial amount of geothermal steam feeding into these water bodies. In contrast, Lakes Rotoma and Rotoehu exhibit a significant percentage of their inflows as geothermal waters; however, they have negligible amounts of geothermal steam. The THg concentrations in trout from these two lakes are notably lower, with an average of 0.412 mg/kg wet weight (ww) for Lake Rotoma and 0.336 mg/kg ww for Lake Rotoehu. These results align well with the presence or absence of geothermal steam. Therefore, it can be concluded that geothermal sources beneath these lakes play a critical role in contributing to higher THg concentrations in trout populations. In summary, the elevated THg concentrations observed in trout from Lakes Rotorua, Rotoiti, and Rotomahana are consistent with their exposure to geothermal steam. The lower levels of THg in trout from Lakes Rotoma and Rotoehu, despite substantial geothermal water inflows, suggest that steam is a key factor in the bioaccumulation of mercury. The influence of geothermal steam appears to be particularly significant in this context. Given the elevated mercury levels in trout from geothermally influenced lakes, caution should be exercised by anglers and consumers who may harvest or consume fish from these water bodies.

The analysis of THg concentrations in koura (freshwater crayfish) revealed significant variations across different lakes. Measurements of THg concentrations in kōura are of particular relevance due to their significance as a traditional Māori food source (mahinga kai)

and their ongoing consumption by communities living in the vicinity of these lakes. A total of 25 koura samples from Lake Rotoiti showed THg concentrations ranging from 0.393 to 2.460 mg/kg ww. In Lake Rotoiti, THg concentrations (Figure 19) were notably high, with a mean concentration of 1.211 mg/kg wet weight flesh (ww). This value exceeds the World Health Organization's (WHO) advisory recommendation for safe mercury levels, which is set at 1.0 mg/kg ww. Similarly, concerning levels of THg were observed in koura from Lakes Rotorua, Okareka, and Rerewhakaaitu. In these lakes, 40% from Lake Rerewhakaaitu, 15% from Lake Rotorua and 5.71% from lake Okareka exceeded the Food and Drug Administration (FDA) acceptable mercury level of 0.678 mg/kg. Specifically, the THg concentration ranges for Lake Rotorua were between 0.21 to 0.95 mg/kg ww, while koura from Lake Okareka exhibited concentrations ranging from 0.1 to 0.74 mg/kg ww. Notably, Lake Rerewhakaaitu recorded alarming levels of THg, with a range of 0.407 to 1.166 mg/kg ww. Conversely, koura samples from Lakes Rotoehu, Rotoma, Okataina, Tikitapu, and Tarawera exhibited low THg concentrations in their flesh (tail). These findings indicate that these lakes have relatively lower mercury contamination levels compared to the aforementioned sites. Upon comparison with THg concentrations in trout, the results from koura were consistent in Lakes Rotorua and Rotoiti which had high geothermal steam input. Unfortunately, no koura were found in Lakes Rotomahana and Okaro, limiting our ability to assess mercury levels in these environments.

Similar to koura, the analysis of THg concentrations in the digestive glands of kakahi (freshwater mussels) revealed considerable variations across different lakes. As depicted in Figure 19, notable concentrations were observed in Lakes Rotorua and Rotoiti, with mean THg levels of 1.323 mg/kg wet weight (ww) and 1.441 mg/kg ww, respectively. These values exceed WHO’s recommended safe threshold of 1.0 mg/kg ww. In contrast, kakahi sampled from other lakes such as Rotoehu, Rotoma, Okareka, Tarawera, and Rerewhakaaitu showed THg concentrations that were well below the WHO's safety limit. These lower levels indicate that consumption of kakahi from these lakes poses minimal risk to human health. Notably, no kakahi were found in Lakes Okataina, Tikitapu, Rotomahana, and Okaro, leading to an absence of data for mercury concentrations in these environments. This finding suggests that either the conditions in these lakes are not conducive to the survival or proliferation of kakahi, or there may be other ecological factors at play.

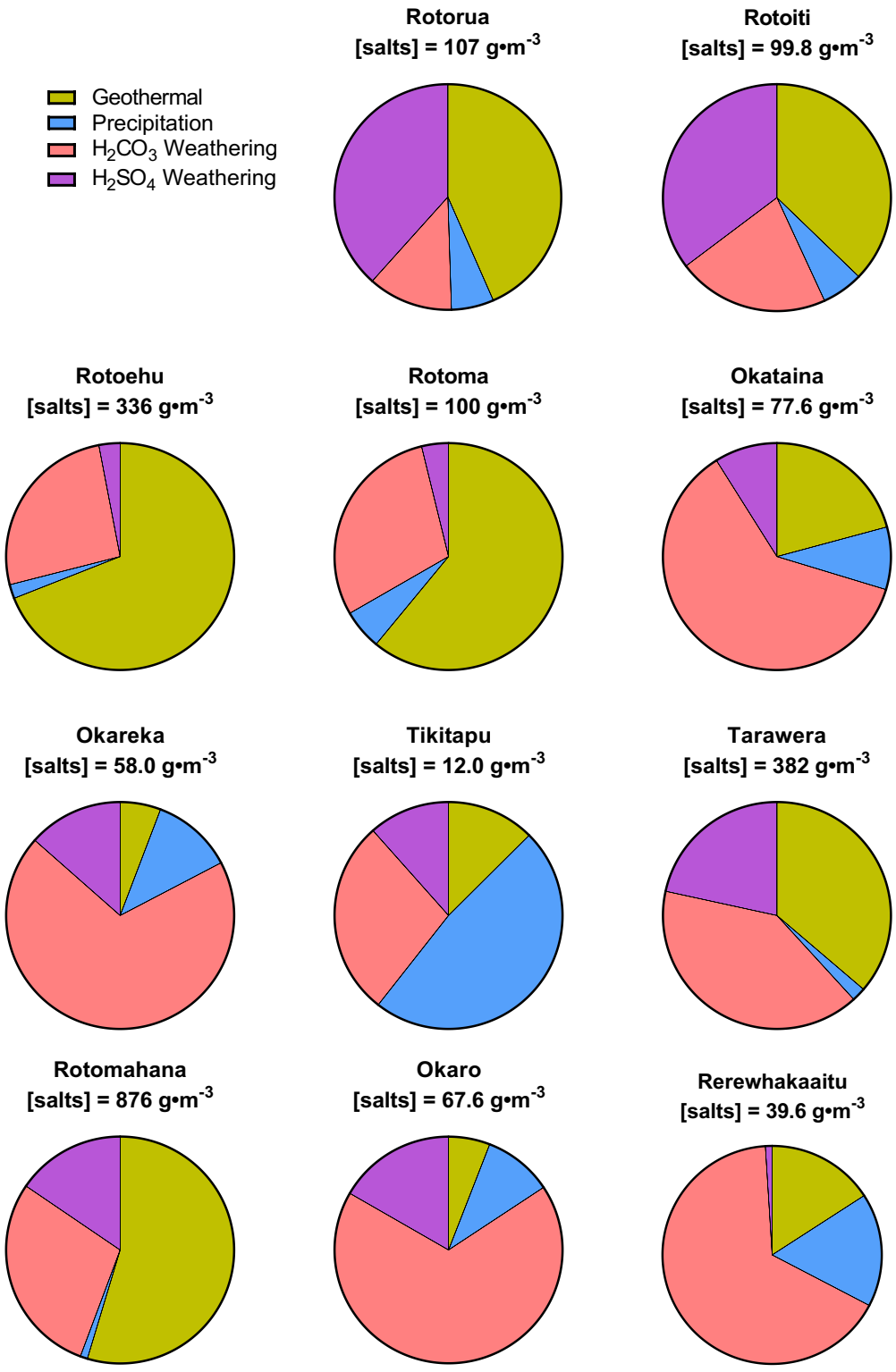

Figure 17. Diagrams depicting dissolved salts from geothermal sources, precipitation, carbonic acid and sulphuric acid weathering contribution to lakes (Timperley & Vigor-Brown, 1986).

Table 6. Mean concentrations (mg/kg, wet weight) of THg and the range of THg concentrations in livers and flesh of trout (2017-2019) , livers and flesh of koura (2007-2008) and digestive gland of kakahi (2017-2019) examined in 11 lakes at Rotorua, New Zealand.

	THg (mg/kg) Trout Liver			THg (mg/kg) Trout Flesh		THg (mg/kg) Koura Liver			THg (mg/kg) Koura Flesh		THg (mg/kg) Kakahi Digestive Gland		
Lake	**n**	**Mean**	**Range**	**Mean**	**Range**	**n**	**Mean**	**Range**	**Mean**	**Range**	**n**	**Mean**	**Range**
Rotorua	11	4.942	0.296-21.186	1.763	0.309-5.126	20	0.313	0.210-0.400	0.454	0.210-0.950	8	1.323	0.285-2.717
Rotoiti	10	3.811	2.892-5.831	1.998	1.603-2.812	25	0.461	0.115-1.220	1.211	0.393-2.460	9	1.441	0.417-3.667
Rotoehu	10	0.374	0.092-1.041	0.336	0.124-0.534	13	0.156	0.075-0.270	0.134	0.070-0.230	9	0.030	0.007-0.043
Rotoma	10	0.417	0.012-1.017	0.412	0.145-0.835	16	0.062	0.007-0.110	0.045	0.009-0.080	9	0.070	0.018-0.218
Okataina	10	0.116	0.085-0.186	NA	NA	19	0.089	0.007-0.360	0.063	0.016-0.140	0	NA	NA
Okareka	10	1.467	0.792-4.119	0.126	0.089-0.190	35	0.196	0.050-0.380	0.372	0.100-0.740	9	0.013	0.004-0.023
Tikitapu	10	0.354	0.300-0.477	0.328	0.243-0.417	22	0.113	0.070-0.190	0.136	0.060-0.460		NA	NA
Tarawera	10	0.655	0.122-2.436	0.322	0.122-1.596	30	0.030	0.004-0.160	0.073	0.018-0.390	9	0.019	0.007-0.041
Rotomahana	3	2.752	1.582-3.401	3.195	2.350-4.037	0	NA	NA	NA	NA	0	NA	NA
Okaro	10	0.497	0.004-1.007	0.392	0.194-0.673	0	NA	NA	NA	NA	0	NA	NA
Rerewhakaaitu	11	0.370	0.234-0.670	0.222	0.116-0.334	20	0.368	0.126-0.889	0.654	0.407-1.166	9	0.024	0.009-0.052

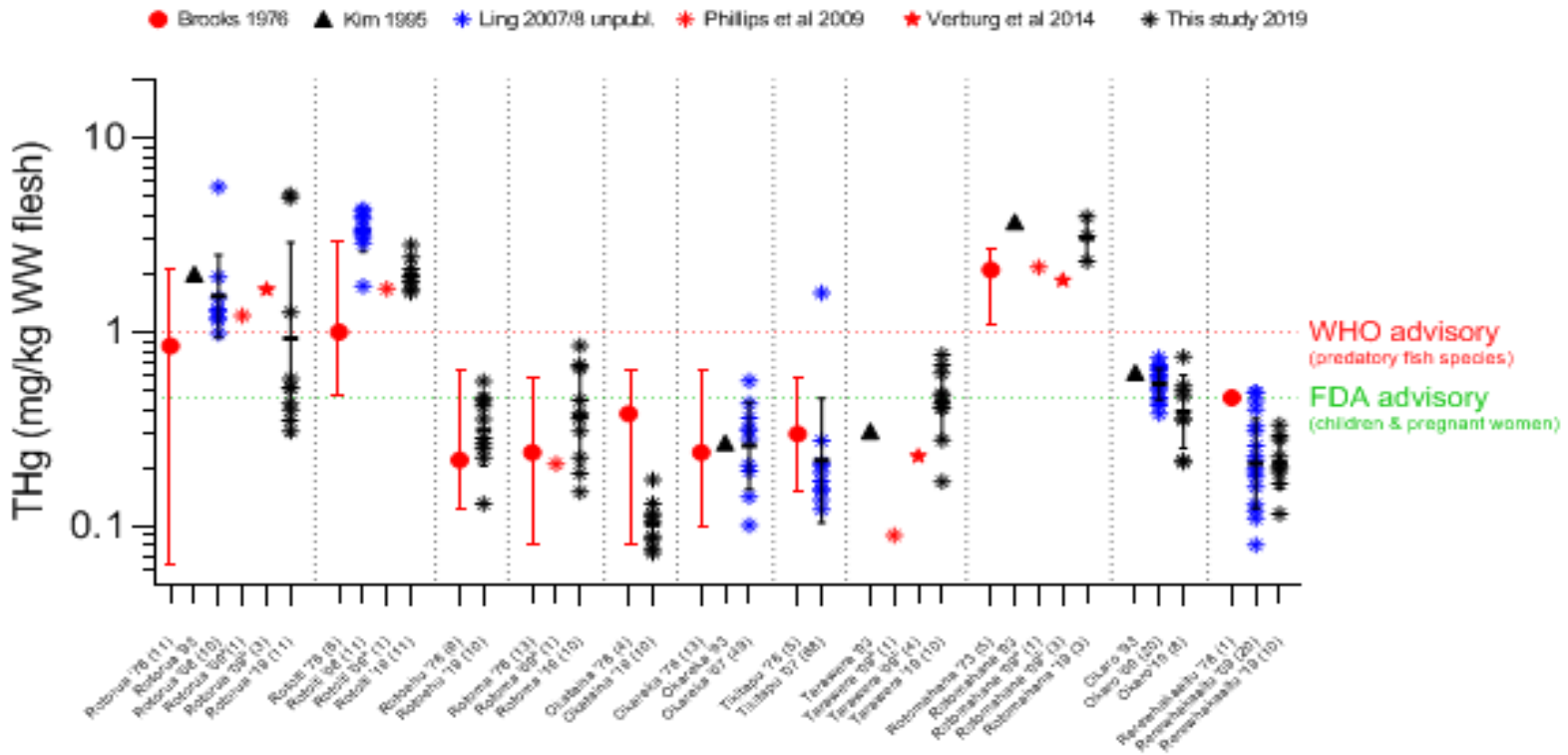

Figure 18. Comparison between previously published THg concentrations (mg/kg wet weight) in trout and those measured in this study from Rotorua lakes.

Sources: Brooks et al., 1976; Kim, 1999; Ling, unpublished, 2007/8; Philips et al., 2009; Verburg et al., 2014

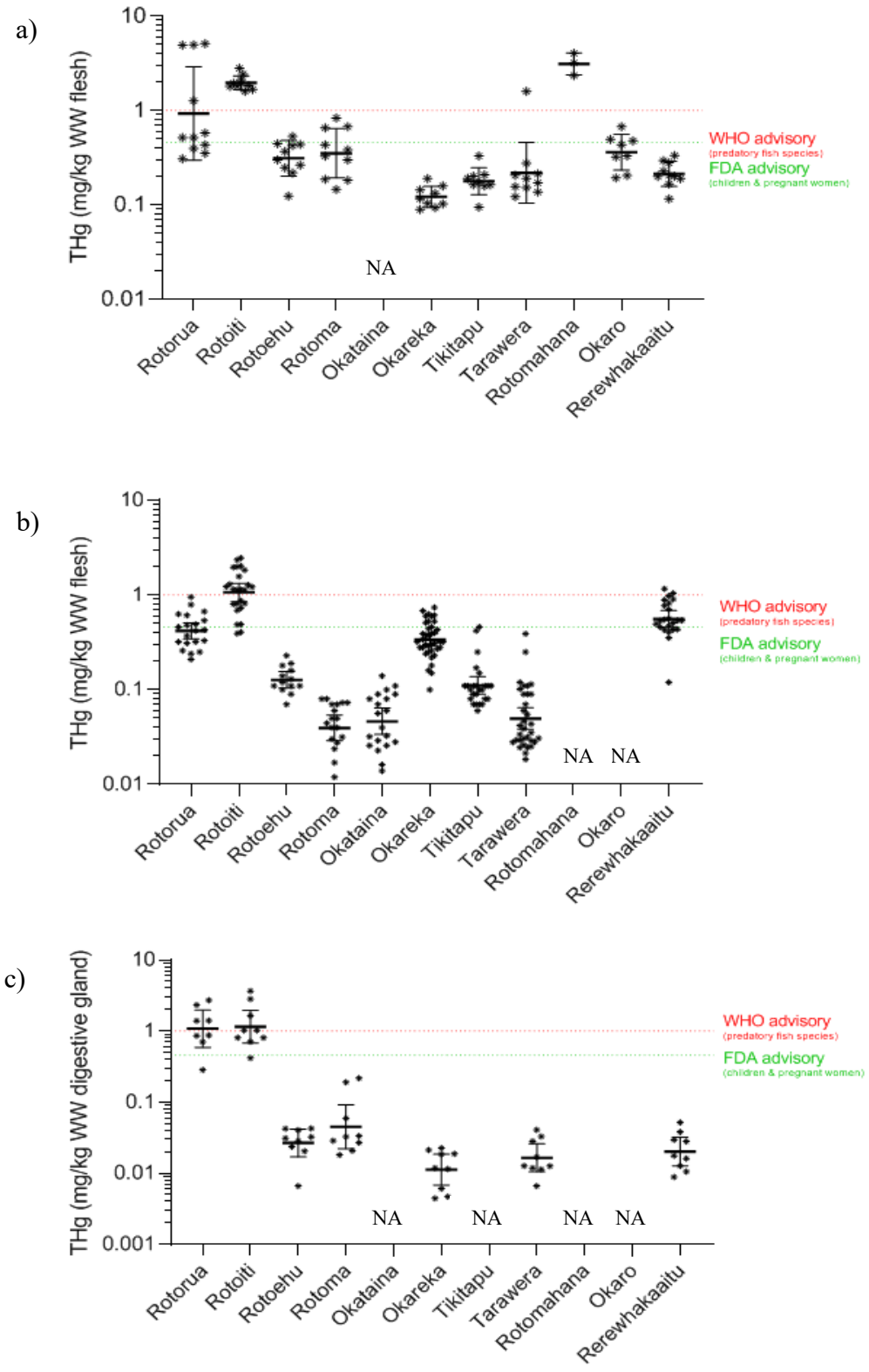

Figure 19. Total mercury concentrations (THg) (mg/kg ww flesh) measured in trout (a), koura (b) and kakahi (c) in 11 Rotorua lakes.

Across the sampled lakes and aquatic species, clear spatial and trophic patterns in THg accumulation were observed. Analysis of kakahi, koura, and trout revealed consistently elevated THg concentrations in Lakes Rotorua and Rotoiti, indicating these systems as hotspots for mercury accumulation. Although koura and kakahi were absent from Lake Rotomahana, the high THg concentrations measured in trout from this lake nevertheless suggest a substantial risk of mercury bioaccumulation within its food web. As illustrated in Figure 19, THg concentrations increased with trophic level, demonstrating a clear pattern of biomagnification. Trout, occupying higher trophic positions, generally exhibited the highest THg concentrations, with values in most lakes exceeding 0.1 mg/kg wet weight (ww). In contrast, kakahi showed lower THg concentrations across the majority of sampled lakes, exceeding above 0.1 mg/kg ww limited to Lakes Rotorua and Rotoiti. Mean THg concentrations in kakahi from Lake Rotorua (1.323 mg/kg ww) and Lake Rotoiti (1.441 mg/kg ww) exceeded the WHO guideline value of 1.0 mg/kg ww. Mercury concentrations in koura were more variable across lakes, with four lakes exhibiting THg concentrations above 0.1 mg/kg ww, three lakes below this threshold, and two lakes showing values close to 0.1 mg/kg ww. Although 0.1 mg/kg ww is well below international consumption guideline values, it is used here as a comparative reference point to evaluate trophic-level differences and early-stage biomagnification patterns across species and lakes, rather than as an indicator of human health risk. This variability suggests species- and site-specific differences in mercury exposure and accumulation pathways within the lake ecosystems.

Tissue-specific patterns of THg accumulation were examined by comparing concentrations in the liver and flesh of trout. The liver plays a central role in the redistribution, detoxification, and transformation of contaminants and is therefore a key site for inorganic mercury accumulation (Yamashita et al., 2005; Maršálek et al., 2007). As such, liver tissue provides a sensitive indicator of environmental mercury exposure. In contrast, flesh tissue is of primary relevance for human health assessments, as it represents the portion most commonly consumed. Across most lakes, trout exhibited higher THg concentrations in the liver than in the flesh (Figure 20), indicating preferential accumulation in detoxification tissues. This pattern was particularly pronounced in highly contaminated lakes such as Rotorua and Rotoiti, where liver THg concentrations were approximately twice those measured in muscle. This finding is consistent with previous studies reporting that when muscle THg concentrations exceed 1 mg/kg, mercury levels in the liver are several-fold higher (Goldstein et al., 1996). Conversely, in lakes with lower overall mercury contamination (Rotoehu, Rotoma, Tikitapu, Tarawera,

Okaro, and Rerewhakaaitu), THg concentrations in trout liver and flesh were broadly comparable, approaching a 1:1 ratio. Similar liver-to-muscle relationships have been widely documented in both freshwater and marine fish species (Jewett et al., 2003; Burger et al., 2007). Several authors have suggested that Hg distribution in fish tissues differs between heavily contaminated and less contaminated environments (Abreu et al., 2000; Farkas et al., 2003; Marsalek et al., 2007; Berg et al., 2000; Gonzalez et al., 2005). Havelková et al. (2008) corroborated this finding by demonstrating that the liver-to-muscle index for Hg concentration was significantly higher in fish from heavily contaminated areas compared to those from lightly contaminated locales. The liver is recognized as the primary target organ for Hg accumulation in fish from heavily contaminated sites due to its role in demethylation of organic mercury to a less toxic inorganic form and subsequent storage and metabolism. Conversely, in lightly contaminated environments, the main target organ for Hg accumulation appears to be the muscle (Havelková et al., 2008). This difference underscores the liver's critical function in detoxification processes. An exception was observed in Lake Rotomahana, where the THg concentration in the flesh exceeded that in the liver. However, this difference was not statistically significant ($p = 0.593$) and may be attributed to a small sample size of only three trout compared to other lakes. This finding highlights the importance of larger sample sizes for robust statistical analysis.

The analysis of MeHg accumulation patterns in trout from various lakes revealed that the highest concentrations were consistently observed in the flesh tissue across all sampled populations (Figure 21). The relative concentrations of MeHg (%) in trout flesh were in the range of 86.% to 96.9% MeHg of THg. These findings are consistent with previous literature, which has reported similar proportions of MeHg in fish muscle tissues (Boening, 2000; Landaluze et al., 2004; Havelková et al., 2008). Additionally, Kannan et al. (1998) have noted that the MeHg concentration in fish flesh typically exceeds 80% of total mercury content.

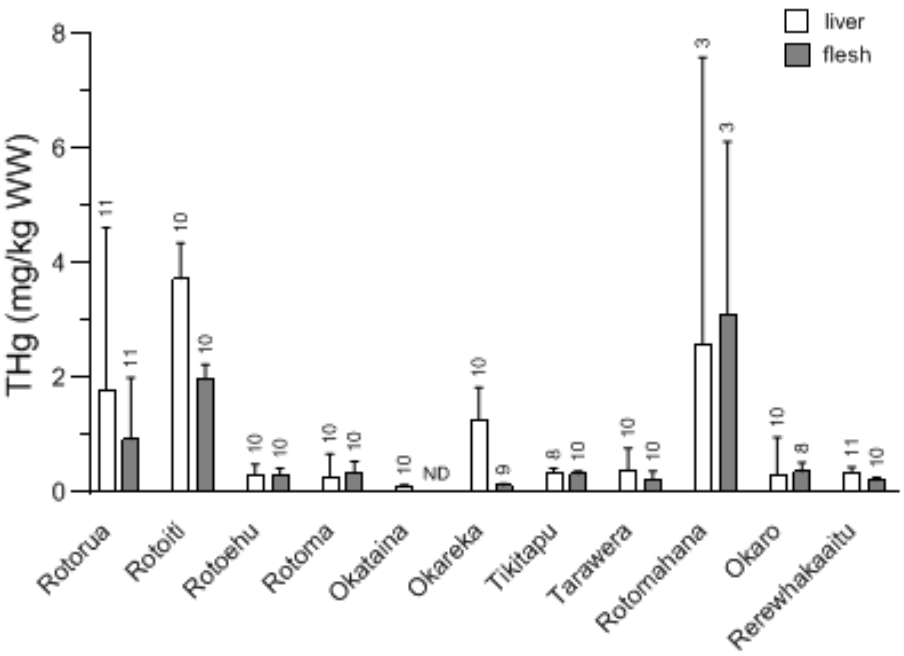

Figure 20. Total mercury concentrations in liver and flesh for trout (brown and rainbow) reported in 11 Rotorua lakes (2017-2019). Individual numbers represent sample size (n). ND – no liver samples were provided for Lake Okataina fish.

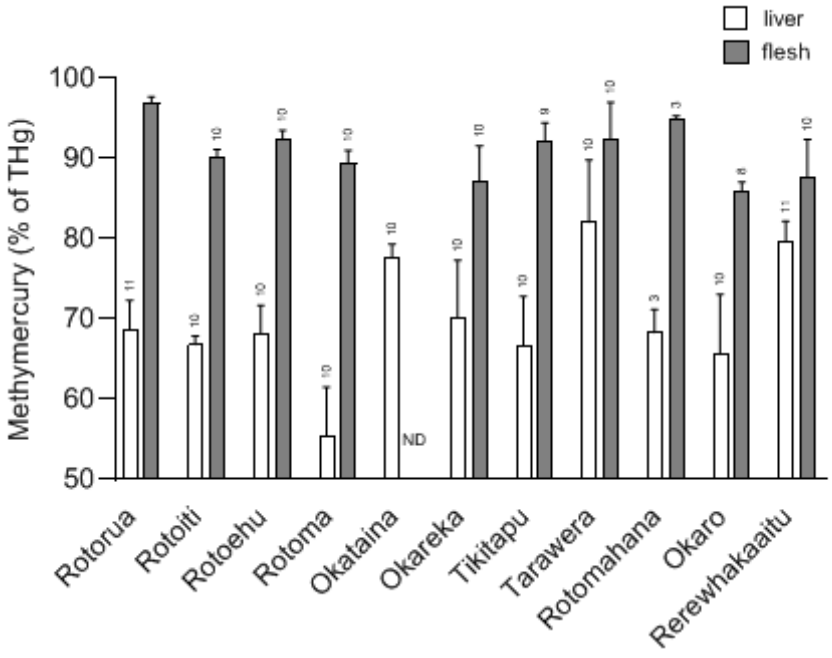

Figure 21. Percent MeHg of THg in liver and flesh for trout reported in 11 Rotorua lakes. Individual numbers represent sample size (n). ND – no liver samples were provided for Lake Okataina fish.

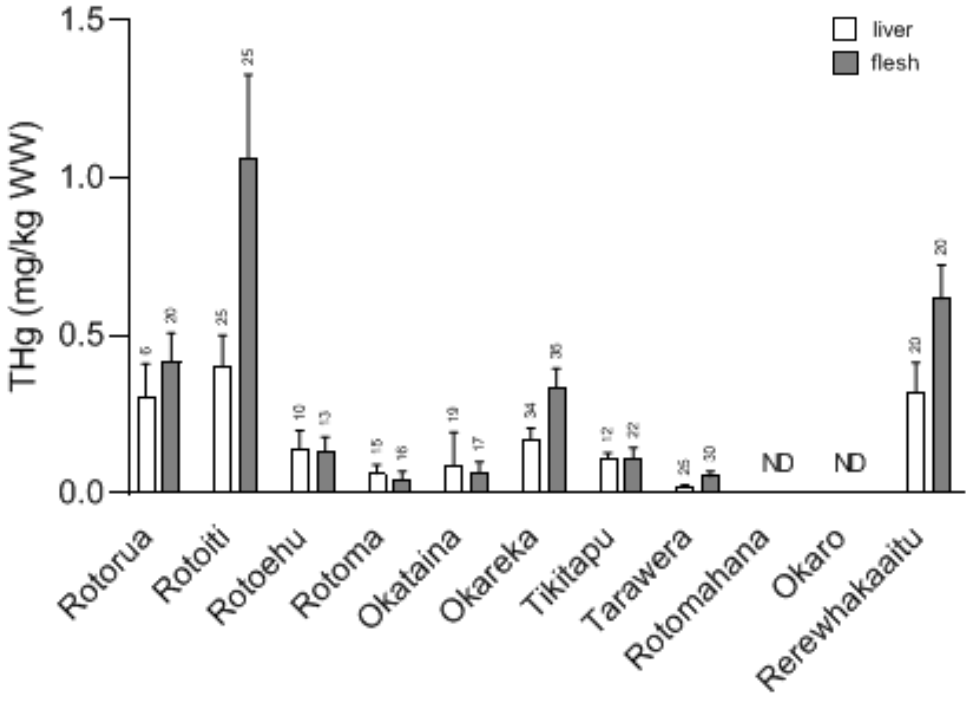

Figure 22. Total mercury concentrations in hepatopancreas and flesh for koura reported in 9 Rotorua lakes. Individual numbers represent sample size (n).

THg concentrations were measured in both the hepatopancreas and flesh of koura, revealing tissue-specific distribution patterns that differ from those observed in trout. Whereas trout generally showed higher THg concentrations in the liver, koura often exhibited greater THg concentrations in the flesh relative to the hepatopancreas. Koura collected from Lakes Rotorua, Rotoiti, Okareka, Tarawera, and Rerewhakaaitu showed higher THg concentrations in flesh than in hepatopancreas tissue, while individuals from Lakes Rotoehu, Rotoma, Okataina, and Tikitapu displayed broadly similar THg concentrations between the two tissues..

This differential partitioning of THg between liver and muscle tissues is noteworthy when comparing various species. For many fish species, such as those studied by Havelkova et al. (2008), Mieiro et al. (2009), and Guilherme et al. (2010), THg concentrations are typically higher in the liver than in the muscle tissue. However, Harley et al. (2015) reported significantly higher Hg concentrations in the muscle tissues of sculpins compared to their livers. Sculpins, like koura, are benthic organisms, suggesting that skeletal muscle may play a crucial role in Hg bioaccumulation within this tissue and contribute more substantially to overall body burden due to its larger mass.

The mechanism behind the different THg partitioning patterns observed in koura remains uncertain. It could be influenced by their bottom-dwelling habitat or unique tissue physiology. Giblin and Massaro (1973) determined that the rate of Hg elimination from muscle is much slower than from the liver, kidney, or heart in rainbow trout (*Oncorhynchus mykiss*), with most of the Hg distributed to the muscle still present after 100 days. This finding supports the idea that skeletal muscle serves as a long-term storage site for mercury.

Goldstein et al. (1996) found similar patterns in lower trophic level or benthic-dwelling fish species, where mercury concentrations were lower in the liver and significantly higher in the muscle tissue. In carp (*Cyprinus carpio*), which is a benthic omnivore with a hepatopancreas (a combined liver and pancreas) similar to that of koura, Goldstein reported THg levels of 0.31 µg/g ww in muscle compared to 0.11 µg/g ww in the hepatopancreas. This suggests that the hepatopancreas may process and store mercury differently than the liver of piscivorous fishes, which have a greater capacity for storing lipid-soluble mercury.

An interesting correlation emerged when comparing the THg concentrations in koura from different lakes. Specifically, koura from lakes Rotorua, Rotoiti, Okareka, and Rerewhakaaitu exhibited higher THg concentrations in their flesh compared to those from other lakes that were below the FDA advisory levels for mercury contamination (Figure 19). This finding is consistent with previous observations in trout, where MeHg was found to be more concentrated in the flesh than in the liver when THg levels were high. The observation that higher THg concentrations in koura are localized primarily in the flesh suggests that MeHg may constitute a significant portion of the total mercury content. This implication is supported by the fact that MeHg is known to accumulate predominantly in muscle tissues due to its lipophilic nature and the slower rate of elimination from these tissues compared to other organs such as the liver, kidney, or heart (Giblin & Massaro, 1973). However, it is important to note that attempts to reanalyse stored digested samples from koura collected ten years prior were unsuccessful. This failure suggests potential issues with sample stability and preservation over time, particularly regarding the possible loss or conversion of MeHg. MeHg can undergo various transformations in environmental conditions, leading to degradation or conversion into other forms that may not be detectable using standard analytical methods.

An analysis of MeHg in the digestive glands of kakahi revealed a significant inverse relationship between the percentage of MeHg and THg concentrations (Figure 24). Statistical evaluation indicated this inverse correlation was highly significant ($P < 0.0001$, Spearman's

rank correlation coefficient r = -0.6781). Lakes Rotorua and Rotoiti, characterized by high THg levels in kakahi digestive glands, exhibited a notably low percentage of MeHg relative to total mercury content, ranging from approximately 1.3% to less than 20%. Conversely, Lake Okareka, which had the lowest THg concentrations in the digestive glands of kakahi, displayed the highest percentage of MeHg (Figure 23).

This inverse relationship between MeHg and THg in the digestive gland indicates a shift in mercury partitioning with increasing mercury load. Similar patterns have been reported in previous studies (Havelková et al., 2008; Wiener et al., 2002), which show that at higher mercury burdens, detoxification organs such as the liver or digestive gland may retain proportionally less MeHg relative to total mercury. In this context, MeHg is more commonly observed in muscle tissue, where it binds strongly to sulfhydryl groups in proteins and contributes substantially to whole-body mercury burdens (Bloom, 1992; Jewett et al., 2003). The observed inverse association between MeHg and THg in the digestive gland is therefore consistent with documented tissue-specific distribution patterns in both trout and koura, where elevated THg concentrations are accompanied by increased MeHg accumulation in flesh. These findings reflect established physiological controls on mercury storage and distribution rather than indicating a single mechanistic pathway.

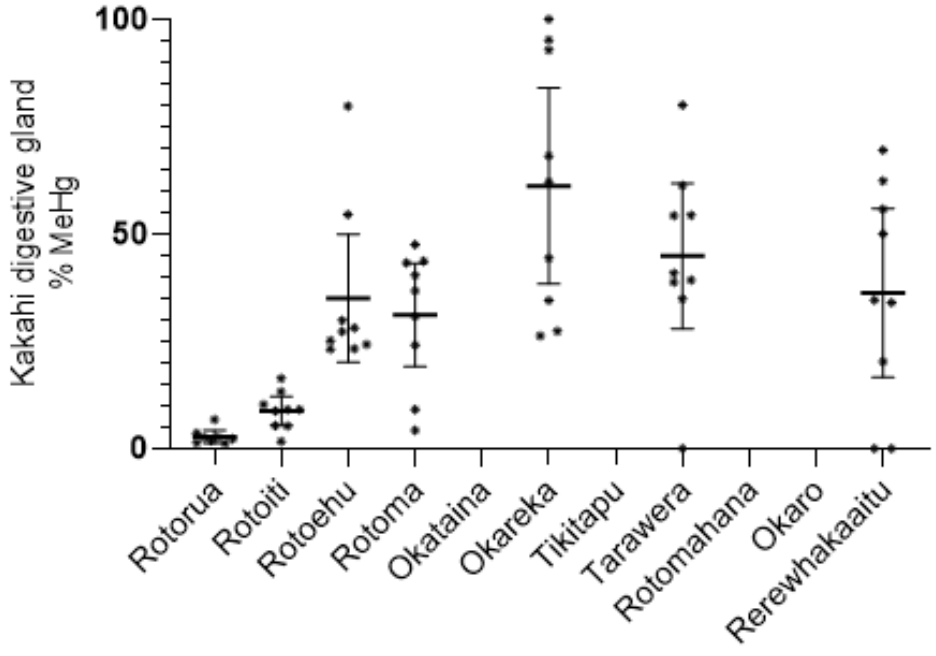

Figure 23. Percent MeHg of THg in kakahi digestive gland seen in 7 Rotorua lakes.

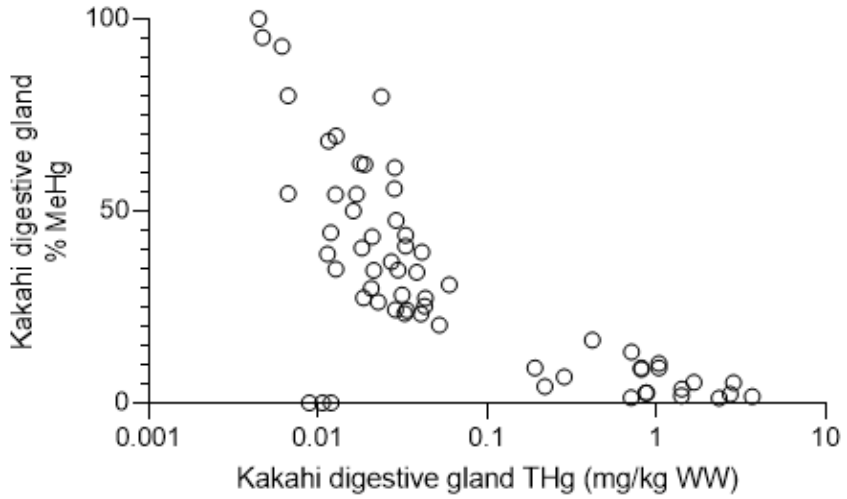

Figure 24. Percent MeHg (%) vs THg (mg/kg ww) in kakahi digestive gland.

Table 7. Sediment THg (mg/kg DW) for lakes around Rotorua. Data provided by D. Trolle (2006), pers. comm., unpublished data.

Lakes	**Sediment THg (mg/kg DW)**
Okareka	0.0751
Tarawera	0.2129
Rotoma	0.6038
Rotoehu	0.9668
Okataina	2.7905
Rerewhakaaitu	3.1240
Tikitapu	12.9071
Rotoiti	61.4102

Data on sediment THg concentrations were obtained from Trolle (2006) for eight lakes in the Rotorua region, as detailed in Table 7. Notably, Lake Rotoiti exhibited the highest sediment THg concentration at 61.4 mg/kg DW, which aligns with our findings that this lake also has one of the highest THg concentrations in its biota. To further investigate these relationships, linear regression analyses (Figure 25) were conducted between mean THg levels

in trout, koura (freshwater crayfish), and kakahi (mussels) and sediment THg concentrations. The results indicate statistically significant regressions for each biotic group:

- Trout: ($n = 8$), ($r^2 = 0.9004$), ($p < 0.05$)

- Koura: ($n = 8$), ($r^2 = 0.7295$), ($p < 0.05$)

- Kakahi: ($n = 8$), ($r^2 = 0.9966$), ($p < 0.05$)

These regressions suggest a strong positive relationship between sediment THg concentrations and THg levels in biota, although the analysis is heavily influenced by the high THg values observed in Lake Rotoiti. Unfortunately, Lake Rotorua was not included in Trolle's (2006) dataset, which limits our ability to draw comprehensive conclusions for all key lakes in the region.

Previous research by Kim and Burggraaf (1999) has also provided evidence that mean MeHg concentrations in trout linearly covary with THg levels in water for five Te Arawa lakes.They emphasized that THg concentrations in water are a critical factor in determining MeHg levels within the upper trophic levels of the aquatic food web. The presence of higher THg in lake waters, predominantly in labile inorganic forms, facilitates microbial methylation processes, leading to elevated bioaccumulation of MeHg in aquatic organisms (Jeong et al., 2024; Regnell & Tesson, 2024; Regnell & Watras, 2019).

The strong positive correlations observed between sediment THg and biota THg highlight the importance of understanding the transport mechanisms and transformation pathways of mercury within these ecosystems. Sediment serves as a significant sink for mercury, particularly in lakes with high levels of anthropogenic pollution. The release of labile forms of mercury from sediments can contribute to higher concentrations in the water column, thereby increasing the potential for methylation by microorganisms.

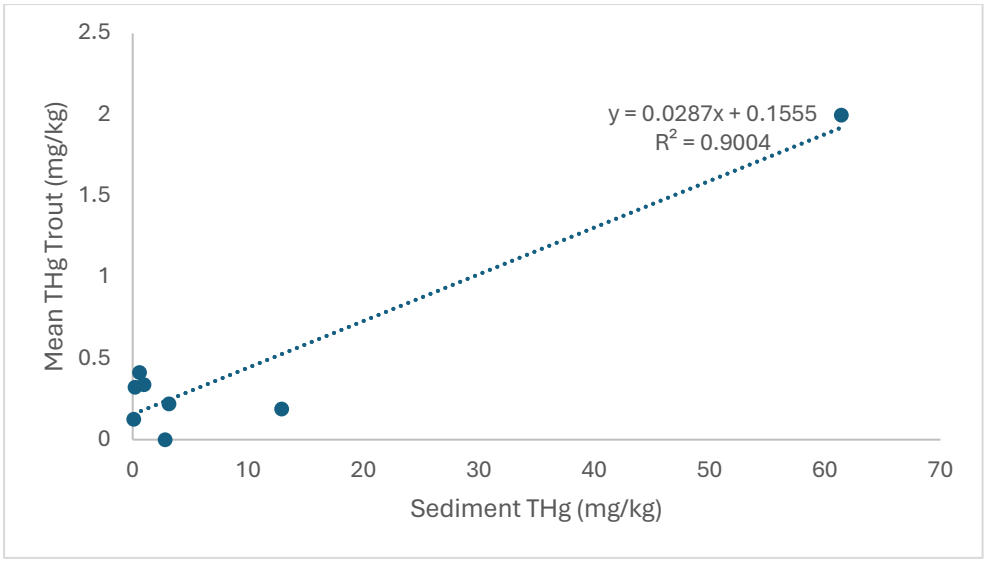

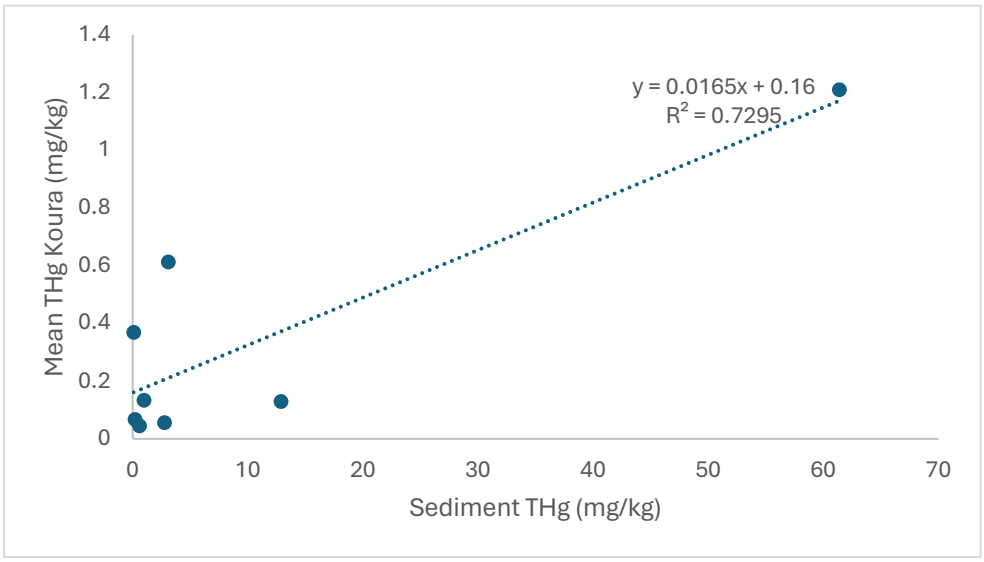

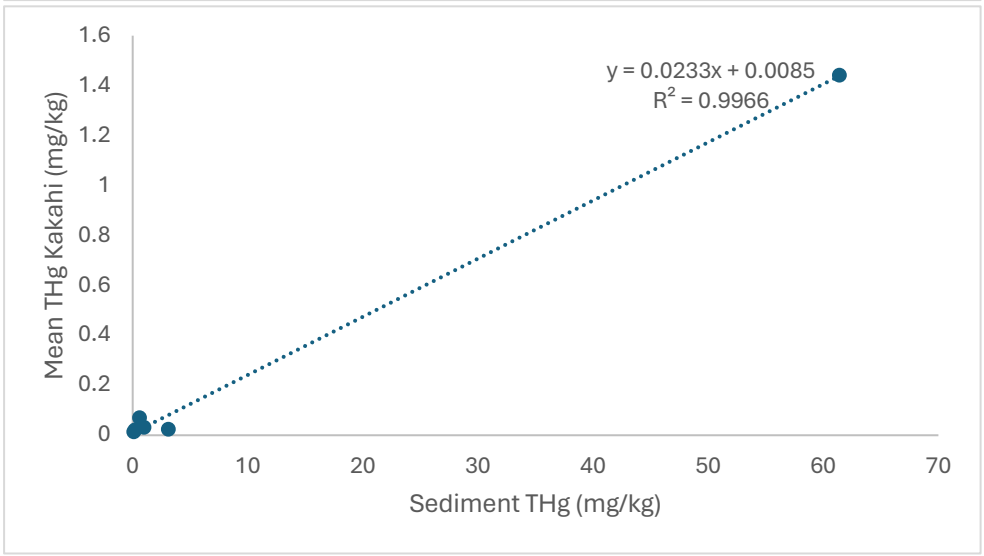

Figure 25. Mean THg concentration (mg/kg) in trout (2017-2019), koura (2007-2008) and kakahi (2017-2019) vs sediment THg (2006-2007) in eight lakes. Linear regression lines were also depicted in the Figure.

A bioaccumulation model (Figure 26) developed in this study provides a framework for understanding the magnification of THg across various trophic levels within the Rotorua lakes ecosystem. This model elucidates significant accumulation patterns that are particularly pronounced at lower trophic levels, especially among benthic invertebrates such as kakahi and koura. This model was constructed using data from this study, specifically by plotting linear regressions between mean THg concentrations in trout, koura (freshwater crayfish), and kakahi (mussels) against sediment THg concentrations reported by Trolle (2006). The bioaccumulation factors (BAFs) were derived to quantify the magnification of Hg across trophic levels.

Regression analysis between THg in trout and koura indicated a bioaccumulation factor of approximately 1.74 ($10^{0.24}$ between these trophic levels)., suggesting that mercury is bioaccumulated about 1.74 times between these two trophic levels. However, it should be noted that the diet of trout includes other species such as smelt and bullies, which might also contribute to THg bioaccumulation; data on these additional prey items were not available for this study. The BAFs calculated in this study are as follows:

- Trout and sediment: $10^{4.71}$

- Koura and sediment: $10^{4.47}$

- Kakahi and sediment: $10^{4.62}$

Notably, the greatest bioaccumulation of THg occurs at lower trophic levels, particularly between sediment and benthic invertebrates such as kakahi and koura. This rapid bioaccumulation is indicative of an equilibrium between uptake and elimination rates.

In Marziali and Valsecchi's (2021) work, sediment feeders like *Corbicula riparia* exposed to Hg-contaminated sediment exhibited mercury concentrations that exceeded the European Environmental Quality Standard (EQS) for biota. Similarly, numerous studies have highlighted the utility of benthic invertebrates as bioindicators of environmental contamination (Pisanello et al., 2016; Marziali & Valsecchi, 2021). The high BAFs observed in kakahi and koura correlate well with elevated THg levels in sediments. The proximity of benthic organisms to contaminated sediments facilitates significant uptake of mercury, which is often methylated by microorganisms in these environments (Compeau & Bartha, 1985; Gilmour et al., 1992; Xu et al., 2019). This process leads to the bioaccumulation of MeHg. Similarly, Kim and

Burggraaf's study reported that the greatest bioaccumulation of MeHg occurred between water and zooplankton, as well as between koura and trout.

In summary, the bioaccumulation model developed in this study highlights significant magnification of THg across various trophic levels within the Rotorua lakes ecosystem. Benthic invertebrates have been identified as crucial bioindicators of environmental mercury contamination due to their close association with sedimentary environments where mercury concentrations tend to be higher. The high bioaccumulation factors observed for these organisms underscore the importance of sediments as primary sources of THg uptake. Specifically, our analysis reveals that benthic invertebrates such as kakahi and koura exhibit a marked capacity for accumulating THg, indicating their role as sensitive indicators of environmental mercury contamination due to their close association with contaminated sediments.

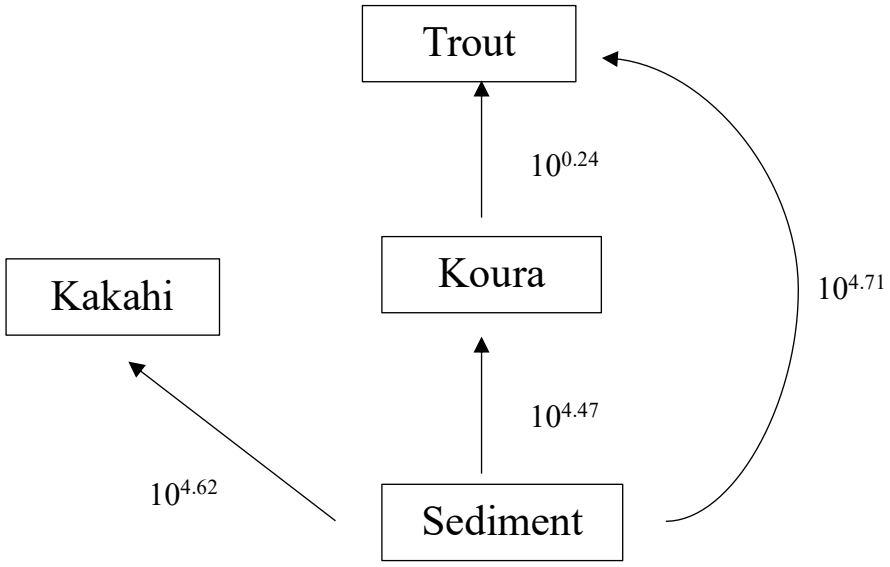

Figure 26: Bioaccumulation model for the trout food web. Bioaccumulation factors for Hg between each tropic level and sediment are shown in the figure.

4.5 Conclusion

This study revealed that trout sampled from Lakes Rotorua, Rotoiti, and Rotomahana exhibited THg and MeHg levels exceeding the World Health Organization (WHO) recommended safe thresholds. Similarly, koura sampled from Lakes Rotorua, Rotoiti, Okareka, and Rerewhakaaitu demonstrated Hg concentrations that surpassed WHO guidelines. Additionally, high mercury levels were detected in kakahi collected from Lakes Rotorua and Rotoiti. This study highlights significant disparities in THg and MeHg concentrations across different lake ecosystems. A notable concern is the concentration of MeHg present in trout flesh compared to liver tissue. Given that consumers typically preferentially consume the flesh rather than the liver, this finding highlights a significant risk. The correlation between elevated THg levels in koura flesh and specific lakes with higher mercury contamination highlights the need for continuous monitoring and assessment of mercury bioaccumulation patterns in benthic organisms. Understanding these patterns is crucial for assessing potential ecological impacts and human health risks associated with consumption of contaminated aquatic species. The significant inverse relationship between MeHg and THg in the digestive glands of kakahi also underscores a critical physiological process in mercury bioaccumulation. When THg levels are high, MeHg is likely to be transferred to muscle tissues where it can accumulate more significantly. This finding supports previous observations in trout and koura and highlights the need for comprehensive monitoring programs to assess mercury contamination levels across different aquatic ecosystems. Further research is necessary to elucidate the sources and mechanisms of mercury accumulation in these ecosystems, as well as to evaluate the broader implications for both ecological and human health. Understanding these dynamics can inform more effective strategies for mitigating mercury exposure through dietary intake, particularly in communities that rely on aquatic resources as a primary food source.

5 Correlation of methylmercury with elements characterizing geothermal and eutrophic influence

5.1 Introduction

The correlation between MeHg concentrations and elements characteristic of geothermal and eutrophic influences is a critical area of inquiry in aquatic environmental science because geothermal systems are recognized sources of inorganic mercury and other trace elements to aquatic environments, providing a substantial pool of bioavailable Hg that can subsequently be transformed into MeHg. At the same time, eutrophic conditions enhance microbial activity, particularly among sulfate-reducing bacteria, which are primary agents responsible for mercury methylation. The co-occurrence of geothermal inputs and elevated nutrient levels therefore creates physicochemical conditions that can promote both increased mercury availability and enhanced methylation efficiency. Geothermal influences stem from activities such as hot springs and volcanic vents, which introduce various trace elements, including sulfur, iron, manganese, selenium, mercury and other metals, into aquatic systems (Kaasalainen and Stefansson, 2012). These geochemical inputs, originating from subsurface geological formations, can substantially affect water chemistry. In contrast, eutrophic influences are driven by the enrichment of water bodies with nutrients such as nitrogen and phosphorus, typically resulting from anthropogenic sources like agricultural runoff and untreated sewage discharge. This nutrient enrichment fosters algal blooms and excessive aquatic plant growth, often leading to oxygen depletion and subsequent alterations in biogeochemical processes (Zhang et al., 2023).

Studies indicate that elements associated with both geothermal and eutrophic influences significantly affect MeHg production. Geothermal systems, characterized by elevated sulfur levels and trace metal concentrations, may enhance the methylation of inorganic mercury. Sulfur, in particular, plays a crucial role in this process, as sulfur compounds can serve as substrates or cofactors for mercury-methylating microorganisms (Manceau et al., 2015). Similarly, in eutrophic systems, increased organic matter and heightened microbial activity create favorable conditions for mercury methylation. Organic-rich environments provide both the carbon sources and

the microbial community structures necessary for the conversion of inorganic mercury into MeHg (Coelho et al., 2009). Moreover, the interaction of various elements within these systems influences MeHg bioavailability and transport. For example, sulfur compounds not only facilitate mercury methylation but also affect the solubility and speciation of mercury (Deonarine & Hsu-Kim, 2009). Concurrently, the binding of mercury to organic matter can modulate its mobility and ecological persistence, impacting its bioaccumulation in aquatic organisms (Kneer et al., 2020). The presence of DOM is particularly significant, as it can alter mercury speciation and enhance its bioavailability for methylation processes (Wu et al., 2022).

Research has extensively associated MeHg production with anaerobic microbial activity within lake sediments (Korthals & Winfrey, 1987; Gilmour & Henry, 1991). Sulfate-reducing bacteria (SRB) have been identified as the primary agents responsible for mercury methylation (Compeau & Bartha, 1985; King et al., 2000). Korthals and Winfrey (1987) reported that the highest methylation activity occurs just beneath the oxic/anoxic interface in sediments under oxygenated water, aligning with the zone of maximal sulfate reduction (King et al., 2000). In lakes and reservoirs, the primary source of MeHg is internal production (Watras et al., 2005). While many studies examining water column methylation have observed elevated MeHg concentrations in the anoxic hypolimnion of seasonally stratified waterbodies, they often fail to concurrently measure MeHg production in sediments (McCord et al., 2016; Watras et al., 1995). The hypolimnetic MeHg pool can arise from several sources, including sedimentary production followed by diffusion into overlying waters, or direct production within the water column itself (Eckley & Hintelmann, 2006; Watras et al., 1995).

The highest potential methylation rates (Km) in both sediments and the water column frequently, though not exclusively, occur near the redox boundary, where oxic and anoxic conditions meet. This is typically where electron acceptors like sulfur are actively cycled between their oxidized and reduced states (Watras et al., 1995). In well-oxygenated environments, this redox boundary is confined to the upper few centimeters of sediment or along the interface between terrestrial and aquatic zones (McClain et al., 2003). In seasonally stratified lakes, the oxic-anoxic boundary shifts between the sediment layer and the water column depending on seasonal thermal stratification (Watras et al., 1995). In this instance, Manganese (Mn) plays a significant

role as a redox-active element in the biogeochemical processes of eutrophic lakes, particularly in relation to oxygen dynamics, nutrient cycling, and the mobility of other trace metals, including mercury. Numerous studies (Vlassopoulos et al., 2018; Farrell et al., 1998; Jackson 1989) have demonstrated that Mn oxides exert an inhibitory effect on the production of MeHg. Their strong oxidative properties contribute to the suppression of mercury methylation by limiting the availability of Hg^{2+} for methylating microorganisms, thereby reducing MeHg formation and potential bioaccumulation in aquatic food webs. This sequestration limits the accessibility of Hg^{2+} to anaerobic methylating microorganisms, such as sulfate- and iron-reducing bacteria, which are responsible for MeHg formation. In addition, Mn oxides influence redox conditions by acting as alternative electron acceptors, thereby suppressing the development of strongly reducing environments that favour mercury methylation. Mn oxides may also compete with iron and sulfur phases for mercury binding, shifting Hg into less methylatable forms and further constraining MeHg production (Vlassopoulos et al., 2018). This study aimed to investigate a potential correlation between Mn concentrations and THg concentrations in trout liver.

Selenium (Se) is an essential element in biological systems, primarily due to its role in selenoenzymes such as glutathione peroxidases (GPX) and thioredoxin reductases (TXNRD), which are critical for cellular defense against oxidative stress (Lubos et al., 2011; Benhar, 2018). Although vital for numerous biological processes, selenium exhibits a narrow margin between beneficial and harmful concentrations, with toxicity occurring at relatively high levels (Surai, 2006). This dual nature underscores the complexity of selenium's interactions with mercury, as both elements have a strong mutual affinity that can influence each other's toxicological effects. Selenium compounds are believed to reduce human exposure to methylmercury (MeHg) by facilitating mercury detoxification (Dang et al., 2011; Luque-Garcia et al., 2013). The effectiveness of this protective action is dependent on selenium availability: research indicates that selenium must be present in tissues at a molar concentration exceeding that of mercury, typically requiring a Se:Hg ratio greater than 1:1, to counteract mercury toxicity effectively (Gochfeld et al., 2021). Therefore, this study also investigated the relationship of selenium concentrations in trout, koura and kakahi in the Te Arawa Lakes.

Understanding these complex interactions is essential for accurately predicting

the distribution and risks associated with MeHg in aquatic ecosystems. Mercury methylation and accumulation are governed by the interplay between geochemical inputs, redox conditions, microbial activity, and food-web dynamics. Geothermal inputs can elevate background concentrations of inorganic mercury and redox-active elements such as sulfur, iron, manganese, and selenium, which influence mercury speciation and bioavailability. Concurrently, eutrophic conditions promote high primary productivity and organic matter deposition, leading to hypolimnetic anoxia that enhances the activity of mercury-methylating microorganisms. The balance between processes that promote methylation (e.g., anoxia and microbial activity) and those that suppress it (e.g., metal oxide scavenging and selenium interactions) ultimately determines MeHg production and its transfer through aquatic food webs. Such insights are crucial for developing management strategies aimed at mitigating MeHg production and exposure, thereby protecting human and ecosystem health. By identifying the processes driving MeHg formation under geothermal and eutrophic conditions, researchers can inform policies to address mercury contamination effectively.

5.2 Literature Review

The Taupo Volcanic Zone (TVZ) is a geothermally active region of significant geological and ecological importance. Extending approximately 250 kilometers northeast from Mount Ruapehu in the south to White Island in the central North Island of New Zealand, the TVZ is characterized by its relatively narrow width of less than 50 kilometers and its complex geological features (Timperley & Vigor-Brown, 1986; Boothroyd, 2009). This area encompasses numerous water bodies, including major rivers and lakes such as Lake Taupo and the Waikato River system, which are heavily influenced by geothermal activity. Lake Taupo, the largest lake in New Zealand with an area of 616 square kilometers, and the 425-kilometer-long Waikato River serve as integral components of the region's hydrology, ecology, and cultural heritage.

The waters within the TVZ exhibit a remarkable range of chemical compositions, reflecting the interplay between typical rainfall contributions and geothermal influences. Some water bodies within the zone have highly saline geothermal waters with pH levels as low as 1.8 (Timperley & Vigor-Brown, 1986). These chemical characteristics set the lakes and rivers of the TVZ apart from other water systems in New Zealand. For example, concentrations of sodium and potassium

in these waters frequently exceed those of calcium and magnesium, a distinct chemical signature associated with geothermal contributions (Timperley, 1987). Smaller lakes and streams in the region often exhibit extreme temperatures and pH levels, conditions that can significantly constrain biological diversity and shape the composition of aquatic ecosystems (Boothroyd, 2009; Duggan et al., 2007).

Geothermal contaminants such as mercury present significant environmental and management challenges in the TVZ, as they can bioaccumulate in aquatic ecosystems, affecting both ecological health and human use of these waters. The concentration of MeHg in water, sediments, and aquatic organisms is influenced by microbial community composition, organic matter availability, pH, temperature, redox potential, sulfate and sulfide levels, and the presence of inorganic mercury (Hg(II)) (D'Itri, 1990). These factors collectively regulate mercury methylation, determining MeHg bioavailability and potential biomagnification in food webs. MeHg is rarely introduced directly into lake systems; it is primarily produced in situ through microbial methylation of Hg(II), particularly under anoxic conditions in sediments and water columns (Winfrey and Rudd, 1990). This methylation is one stage in a complex biogeochemical cycle of chemical, physical, and biological transformations. Once formed, MeHg can bioaccumulate and biomagnify through food webs, affecting species such as fish, crustaceans, and shellfish, which hold both ecological and human importance (Kim & Burggraaf, 1999).

Timperley and Vigor-Brown (1986) conducted a study on the contribution of geothermal inputs to the salt content of lakes in the TVZ. By analyzing the concentrations of major ions in 32 lakes, they categorized lake-water inputs into five primary sources: precipitation, weathering-basic minerals, weathering-acidic minerals, geothermal water, and geothermal steam. Their findings revealed that salts derived from geothermal water accounted for an average of 30% (ranging from 0% to 69%) of the salt content in larger lakes within the region. The study also documented considerable variability in total dissolved salts, bicarbonate, and calcium concentrations across the sampled lakes, with average values of 171 grams per cubic meter (range: 2.4–876 grams per cubic meter), 52.3 grams per cubic meter (range: 0–231 grams per cubic meter), and 4.5 grams per cubic meter (range: 0.08–18 grams per cubic meter), respectively.

Variations in water geochemistry, particularly hardness (calcium and

magnesium concentrations) and alkalinity (buffering capacity), strongly influence key ecological processes. These parameters affect sediment pH stability, which regulates microbial activities such as nitrification and mercury methylation (Winfrey and Rudd, 1990). Methylation occurring at the sediment-water interface and within the aerobic water column produces higher net MeHg than subsurface sediment exchange, likely due to reduced binding and precipitation with HgS. Dissolved organic carbon (DOC) further drives in-lake MeHg formation by binding Hg^{2+}, maintaining its bioavailability to methylating microbes, and providing a carbon source that stimulates microbial activity. Lower pH conditions, especially in acidic lakes, enhance methylation, increasing MeHg bioavailability and potential bioaccumulation in aquatic organisms. Together, these geochemical factors play a central role in controlling MeHg production and its ecological impact.

Efforts to monitor and assess the ecological health of lakes often rely on metrics such as the Trophic Level Index (TLI). The TLI (Burns et al, 1999) is a widely used tool in aquatic ecology that quantifies the trophic status of water bodies, ranging from oligotrophic (low nutrient levels) to hypertrophic (extremely high nutrient levels). It is calculated using a combination of biological and chemical parameters, including phytoplankton biomass (measured via chlorophyll-a concentration), submerged macrophyte abundance, Secchi depth (an indicator of water clarity), and concentrations of total phosphorus and total nitrogen. These parameters provide insights into the degree of eutrophication, a process driven by nutrient enrichment that can lead to excessive algal growth, reduced water clarity, and oxygen depletion. The calculation of the TLI typically involves assigning scores to each parameter based on its value relative to trophic state categories. These scores are then combined to produce an overall index, often using a weighted average. Low TLI scores (<30) indicate oligotrophic conditions, characterized by nutrient-poor, clear water with low primary productivity. Moderate scores (30–50) reflect mesotrophic lakes, which have moderate nutrient levels and productivity. High TLI values (50–70) correspond to eutrophic conditions, where nutrient enrichment leads to elevated phytoplankton biomass, reduced water clarity, and the potential for algal blooms. Very high scores (>70) indicate hypereutrophic lakes, with excessive nutrient concentrations, frequent algal blooms, and likely oxygen depletion in deeper waters. By integrating parameters such as total nitrogen, total phosphorus, chlorophyll-a, and water clarity, the TLI provides a useful tool for comparing lakes and monitoring changes in trophic status over time.

Submerged aquatic plants (Clayton and Edwards, 2006) are another important indicator of lake health. These plants play vital roles in nutrient cycling, habitat provision, and water quality maintenance, making them key components of lake ecosystems. High species diversity within submerged plant communities often signifies good water quality and ecological balance, whereas reduced diversity may indicate environmental stressors such as eutrophication or pollution. Similarly, plant abundance and spatial distribution can reflect the influence of factors such as nutrient availability, turbidity, and localized pollution sources. The health and distribution of submerged aquatic plants also provide critical insights into water quality and ecosystem services. Healthy plant populations support biodiversity by providing habitat for fish, invertebrates, and other organisms, while also contributing to oxygen production and carbon sequestration. Regular monitoring of these plants, through methods such as visual surveys, quantitative sampling, and tissue analysis, is essential for understanding and managing lake ecosystems. Such monitoring can inform strategies to address challenges such as nutrient enrichment, pollution, and habitat degradation. A good example would be the Lake SPI (Submerged Plant Indicators). Lake SPI conditions are assigned using a standardised assessment of submerged macrophyte communities, which serve as sensitive indicators of long-term ecological condition in lakes. The approach is based on the premise that submerged aquatic plants integrate the effects of water clarity, nutrient enrichment, and physical disturbance over time. Surveys are typically conducted using divers or underwater video along depth transects to document the distribution and composition of submerged vegetation. The assessment considers three main criteria. The first is the maximum depth of plant colonisation, which reflects light availability and water clarity. In clearer, less nutrient-enriched lakes, submerged plants are able to grow to greater depths, whereas increased turbidity and eutrophication restrict plant growth to shallower zones. The second criterion is species composition, with emphasis on the relative dominance of native versus invasive macrophytes. Lakes dominated by native species, such as charophytes, are considered to be in better ecological condition than those where invasive species prevail. The third criterion is lake bed occupancy, which evaluates the extent and continuity of plant cover across the lake bottom, providing insight into habitat quality and disturbance. Scores from these criteria are combined to generate a Lake SPI Index score, typically expressed as a percentage, which is then used to assign the lake to a condition category ranging from excellent to bad. High SPI (80-100) scores indicate deep, continuous plant beds dominated by native species and are characteristic of clear,

low-nutrient systems. Scores of 60–79 reflect good condition, with predominantly native species but minor ecological changes. Moderate scores (40–59) indicate a reduction in native species and a greater presence of tolerant species, signaling moderate ecological disturbance. Low scores (20–39) suggest poor condition, with few native plants and dominance of tolerant or invasive species, while very low scores (0–19) indicate extremely degraded lakes with minimal native vegetation.Lower scores are often associated with eutrophication and degraded ecological condition (Edwards et al., 2005).

Hypolimnetic volumetric oxygen depletion is another critical process influencing lake ecosystems. This phenomenon refers to the reduction in dissolved oxygen concentration in the hypolimnion, the cold, dense bottom layer of a stratified lake. Oxygen depletion in the hypolimnion (Eckley and Hintelmann, 2006) can result from biological activity, such as the decomposition of organic matter, as well as chemical processes like the oxidation of reduced substances in sediments. Stratification exacerbates this process by limiting oxygen replenishment from the atmosphere and photosynthesis. Hypolimnetic oxygen depletion can lead to hypoxia or anoxia, conditions that are detrimental to aquatic life and can mobilize contaminants from sediments. Hypolimnetic hypoxia in lakes is strongly associated with the accumulation of various toxic compounds in the hypolimnion, including phosphate, ammonia, iron, manganese, and MeHg (Beutel et al., 2014a; Watras, 2009; Golterman, 2001; Davison, 1993). Oxygen-deprived conditions facilitate the release of toxic substances from sediments, including MeHg, H_2S, ammonium (NH_4^+) and other redox-sensitive metals. These compounds accumulate in the hypolimnion and are transported vertically through diffusion, entrainment, and seasonal mixing processes such as autumn turnover. Once introduced into the photic zone, they can influence primary production, exacerbate oxygen depletion, and increase the bioavailability of toxic compounds to aquatic organisms (Welch & Cooke, 1995; Slotton et al., 1995). This process not only affects water quality but also contributes to the incorporation of MeHg into the aquatic food web and its subsequent biomagnification through trophic levels, as MeHg produced under anoxic conditions becomes available to primary producers and is transferred upward to higher trophic organisms (Watras et al., 1998). The persistence of internally recycled nutrients highlights the long-term impacts of hypolimnetic hypoxia on lake ecosystems and the challenges associated with water quality restoration efforts.

Manganese dioxide (MnO_2), specifically in the form of pyrolusite or birnessite, has been shown to significantly reduce MeHg concentrations in sediment porewater, with reductions ranging from 66% to 89%, depending on the specific MnO_2 type (Vlassopoulos et al., 2018). This effect was observed when MnO_2 was either mixed directly with Hg contaminated sediment or applied as a thin-layer amendment to the sediment surface (Vlassopoulos et al., 2018). Furthermore, experimental mesocosm studies confirmed that manganese reduction was the dominant redox process, suggesting that the presence of MnO_2 maintained redox conditions above those favorable for mercury methylation, such as those associated with Fe(III)-reducing and sulfate-reducing environments.

Zhang et al. (2023) demonstrated that trivalent manganese (Mn(III)) can degrade MeHg under a range of conditions, highlighting a potential mechanism by which manganese concentrations in aquatic systems may influence mercury accumulation in fish. In their study, Mn(III) on the surface of synthesized manganese dioxide (MnO_2-x) degraded approximately 28 ± 4% of MeHg, with low-molecular-weight organic acids like oxalate and citrate enhancing this process through the formation of soluble Mn(III)-ligand complexes. Because MeHg constitutes the majority of THg in fish, the oxidative breakdown of MeHg by Mn(III) could reduce the bioavailable mercury entering the food web. This suggests that environments with higher reactive Mn concentrations may partially mitigate MeHg uptake by trout, potentially contributing to lower THg concentrations, although the effect would interact with other factors such as DOC, pH, and microbial activity.

Selenium (Se) is an element of particular interest in aquatic ecosystems due to its complex chemistry and its influence on biogeochemical processes and bioaccumulation dynamics. Although selenium primarily originates from the weathering of rocks and soils, its uptake and toxicity are influenced by factors such as pH, water hardness, and concentrations of sulfur and phosphate (Rosenfeld & Beath, 1964). Selenium exists in multiple oxidation states, including selenium (VI), selenium (IV), and selenium (II), each of which exhibits distinct chemical behaviours. For instance, selenates and selenites, the oxyanions of selenium (VI) and selenium (IV), are soluble and readily accumulated by biota, particularly in alkaline and oxidizing conditions (CCREM, 1987). Conversely, under acidic and reducing conditions, selenium can be reduced to elemental selenium, which is insoluble and removed from

the water column.

The biological effects of selenium vary among its chemical forms, with organic selenium compounds such as selenomethionine being more toxic than inorganic forms like selenite and selenate (Fergusson, 1990). Selenium contamination can have significant ecological consequences, as demonstrated by studies in Lake Macquarie, New South Wales, where sediments were found to be a major source of selenium for benthic infauna and fish predators (Peters et al., 1999). Selenium can be bioconcentrated by aquatic organisms by factors ranging from 100 to 30,000, leading to reproductive failure in some species without visibly affecting adults (Lemly, 1999).

The uptake of inorganic selenium by organisms is influenced by water chemistry. For example, selenate uptake increases in the presence of calcium and magnesium, while the addition of sulfate ions can inhibit uptake by competing for cellular transport sites (Ogle & Knight, 1996; Williams et al., 1994). Interactions between selenium and other elements, such as mercury or copper, can further influence its toxicity. Complexation reactions between selenium and mercury, for instance, reduce the bioavailability of both elements, thereby mitigating their toxic effects (Raymond and Ralston 2020). These complex interactions underscore the need for a strategic approach to managing selenium contamination and its ecological impacts.

The relationship between Hg and Se is complex, as these two elements have a high mutual affinity and can influence each other’s toxicity. One of the primary mechanisms through which MeHg exerts its toxic effects is by causing oxidative stress (Sasaki et al., 2023), a condition in which the balance between reactive oxygen species (ROS) and the body's ability to neutralize them is disrupted. This oxidative stress is mainly caused by MeHg's ability to irreversibly bind to selenium in the form of selenocysteine (SeCys), a critical component of antioxidant enzymes such as glutathione peroxidase (GPX) and thioredoxin reductase (TXNRD) (Lubos et al., 2011). When mercury binds to SeCys, it inactivates these enzymes, impairing the body’s ability to manage oxidative stress (Ralston & Raymond, 2018; Spiller, 2018). However, interactions between mercury and selenium can lead to the formation of insoluble compounds such as mercury selenide (HgSe) or stable complexes, reducing selenium bioavailability (Gochfeld and Burger, 2021). This reduces the availability of selenium for the synthesis of SeCys and the replacement of the inactivated antioxidant enzymes. Consequently, mercury exposure can lead to a relative selenium deficiency,

further exacerbating oxidative stress. In addition to its impact on selenium, mercury also affects other antioxidant defense systems, such as superoxide dismutase (SOD) (Kumar et al., 2020) and catalase (Chen et al., 2015), which are enzymes responsible for neutralizing ROS. Although mercury exposure may cause selenium deficiency, the symptoms of mercury poisoning are not identical to those caused by selenium deficiency. This distinction suggests that while both elements interact in the context of oxidative stress, their toxic effects manifest through different biological mechanisms.

The relationship between selenium (Se) and Hg toxicity has been the subject of several studies, with Se often seen as a protective agent against Hg toxicity. The foundational work in this area was the Parizek and Ostadalova (1969) paper, which reported that the injection of sodium selenite (Na-selenite) shortly after exposure to mercury chloride ($HgCl_2$) reduced the toxic effects of mercury in rats. This protective role of selenium was later extended to the realm of fish consumption and its potential to mitigate MeHg toxicity. Ganther et al. (1972) conducted an experiment where Japanese Quail were fed MeHg in a diet containing either tuna or corn. The chicks fed tuna, which is rich in selenium, survived, while those on a corn-based diet did not. Further experiments confirmed that selenium, at levels equivalent to those found in the tuna diet, could protect against the toxicity of MeHg. Additionally, rats that were fed a diet containing 0.5 mg/L of selenium were able to survive exposure to MeHg in drinking water, whereas those on a selenium-deficient diet did not survive (Ganther et al., 1972). In Amazonian Brazil, where indigenous populations are exposed to mercury through gold mining and fish consumption, high dietary selenium was found to protect motor function, suggesting a similar protective role in humans (Lemire et al., 2011).

However, the protective effects of selenium against mercury toxicity are not universally observed. Some studies have confirmed selenium's protective role, while others have found little or no benefit, or even synergistic toxic effects (Penglase et al., 2014; Heinz et al., 2012). While some authors propose that selenium acts by sequestering mercury, others, such as Ralston and Raymond (2018), suggest that mercury may sequester selenium, leading to oxidative damage when selenium is insufficient. Selenium has a high affinity for sulfhydryl (-SH) groups and may inhibit enzymes by binding to cysteine (Cys). Excessive selenium has also been linked to lipid peroxidation, a process that can damage cellular membranes (Hoffman, 2002).

Furthermore, not all interactions between selenium and mercury are protective. For example, in an experiment where selenium-methionine (Se-met) and MeHg were injected into bird eggs, Se-met caused more deformities and hatching failure than MeHg alone. When the two were injected together, while the hatching rate improved, the deformity rate also increased. This paradoxical effect suggests that the interaction between selenium and mercury can sometimes exacerbate toxicity, particularly when both are present in certain forms (Heinz et al., 2012). The effects were more severe when the selenium was directly administered to the eggs, compared to when the selenium was transferred from the female bird. In summary, while selenium can offer protection against mercury toxicity in certain contexts, the relationship is complex, and in some cases, selenium may not provide protection or could even worsen toxicity, depending on the form and concentration of both elements. Incorporating Se measurements alongside Hg and MeHg provides a more complete understanding of potential ecological and human health risks in contaminated aquatic systems.

5.3 Materials and Methods

5.3.1 Study area

All eleven Te Arawa lakes located in the Bay of Plenty Region (Rotorua, Rotoiti, Rotoehu, Rotoma, Okataina, Okareka, Tikitapu, Tarawera, Rotomahana, Okaro, Rerewhakaaitu) were selected as part of the study area (Figure 27). These lakes lie within the Taupo Volcanic Zone (TVZ), which has existing natural geothermal activity. Physicochemical data for all lakes (2000-2015) were obtained from the Bay of Plenty Regional Council.

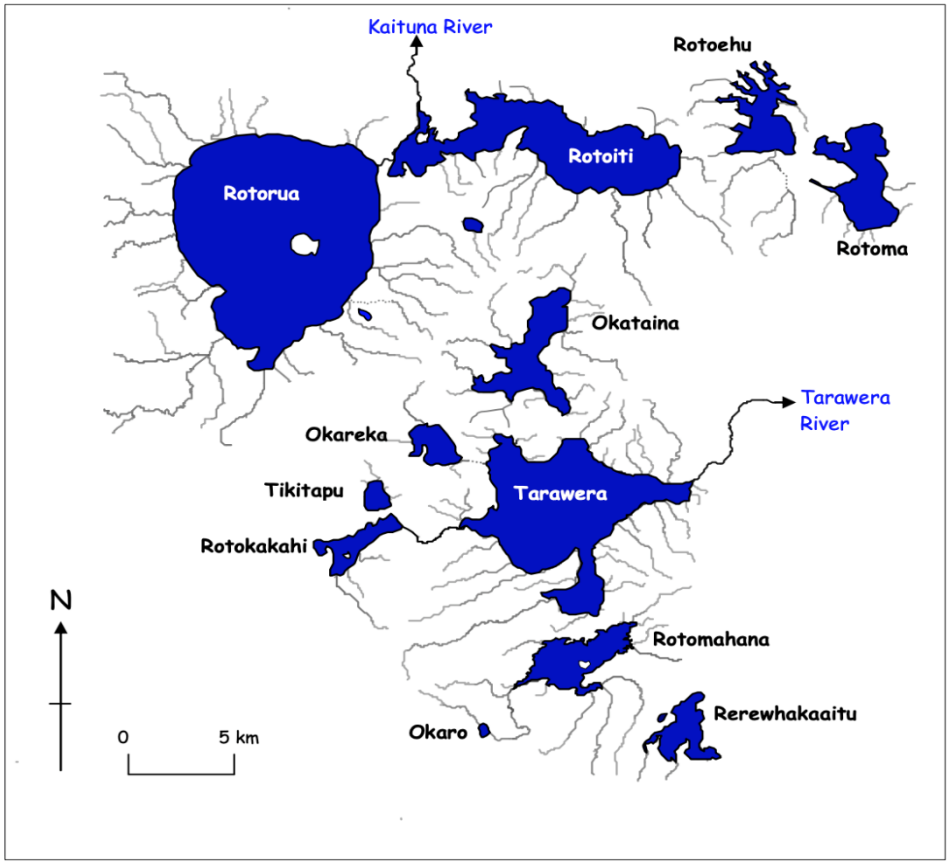

Figure 27. Map showing all Rotorua lakes.

5.3.2 Sample collection

Refer to section 4.3.2.

5.3.3 Sample analysis

5.3.3.1 Sample digestion

Refer to section 4.3.3.1.

5.3.3.2 Total mercury and Selenium analysis

Refer to section 4.3.3.2.

5.3.3.3 MeHg analysis

Refer to section 4.3.3.3.

5.3.3.4 Data analysis

Refer to section 4.3.4.

5.4 Results and Discussion

As mentioned in Chapter 4, trout that showed high levels of MeHg and elemental mercury came from Lakes Rotoiti, Rotomahana and Rotorua. A more in depth look into the lake chemistry and data regarding Lake SPI index as well trophic status were obtained from various NIWA reports (Table 8 and Table 9).

Over a period of 15 years from 2000 to 2015, Lake Rotoiti had changed from eutrophic to mesotrophic and once again back to eutrophic, while Lake Rotomahana and Lake Rotorua had remained constantly mesotrophic for the former and eutrophic for the latter. The Trophic Level Index (TLI) as seen in Figure 28 for Lake Rotoiti is at 4.0 while TLI for Lake Rotomahana is 3.9 and Lake Rotorua is 4.2. The Lake Submerged Plant Indicators (LakeSPI) (Table 9) for Lake Rotoiti from year 2000 to 2015 had remained poor throughout the period while LakeSPI for Lake Rotomahana had remained high throughout similar period. Lake Rotorua had a LakeSPI that was poor from 2000 to 2003 but improved to moderate from 2008 to 2015.

Table 8. Trophic condition of the 12 Rotorua lakes from year 2000-2015, based on TLI. Data compiled from various NIWA reports (Scholes & Hamil, 2016; Edwards et al., 2005).

Lake	**Trophic status (2000-2003)**	**Trophic status (2008-2009)**	**Trophic status (2014-2015)**
Okareka	Mesotrophic	Mesotrophic	Mesotrophic
Okaro	Supertrophic	Supertrophic	Eutrophic
Okataina	Oligotrophic	Oligotrophic	Oligotrophic
Rerewhakaaitu	Mesotrophic	Mesotrophic	Mesotrophic
Rotoehu	Eutrophic	Eutrophic	Mesotrophic
Rotoiti	Eutrophic	Mesotrophic	Eutrophic
Rotokakahi	Mesotrophic	Mesotrophic	Mesotrophic
Rotoma	Oligotrophic	Oligotrophic	Oligotrophic
Rotomahana	Mesotrophic	Mesotrophic	Mesotrophic
Rotorua	Eutrophic	Eutrophic	Eutrophic
Tarawera	Oligotrophic	Oligotrophic	Oligotrophic
Tikitapu	Mesotrophic	Oligotrophic	Oligotrophic

Table 9. Lake SPI condition of the 12 Rotorua lakes from year 2000- 2015. Data compiled from various NIWA reports (Scholes & Hamil, 2016; Edwards et al., 2005).

Lake	**Lake SPI condition (2000-2003)**	**Lake SPI condition (2008-2009)**	**Lake SPI condition (2014-2015)**
Okareka	Moderate	Moderate	High
Okaro	Poor	Poor	Moderate
Okataina	High	Moderate	Moderate
Rerewhakaaitu	Moderate	Moderate	Moderate
Rotoehu	Moderate	Poor	Poor
Rotoiti	Poor	Poor	Poor
Rotokakahi	Moderate	Moderate	Moderate
Rotoma	High	High	High
Rotomahana	High	High	High
Rotorua	Poor	Moderate	Moderate
Tarawera	Moderate	Moderate	Moderate
Tikitapu	High	Moderate	Moderate

The land cover characteristics within the catchments of Lakes Rotoiti, Rotomahana, and Rotorua vary significantly. Lake Rotorua, being the largest among these three lakes with an area of 80 km², is characterized by a land cover composition of 37% forest (a mix of predominantly exotic plantation and native bush), 47% pasture, and 8% urban areas, encompassing the city of Rotorua (Table 10). Conversely, Lakes Rotoiti and Rotomahana exhibited predominantly forested catchments with percentages of 79% and 40%, respectively; the remaining land is utilized as pasture while urban areas were minimal which constituted 2% and 1% respectively. Historical data indicated that these lakes shared similar trophic states between the decades of the 1950s to the 1970s (McColl, 1972; Livingston et al., 1986). In terms of limnological behavior, Lake Rotorua demonstrated polymictic characteristics, occasionally stratifying and experiencing deoxygenation during summer months. In contrast, Lakes Rotoiti and Rotomahana maintained their stratification throughout the summer season. Notwithstanding its larger size, Lake Rotorua is relatively shallower with its maximum depth at 45m compared to Lakes Rotoiti and Rotomahana, which are notably deeper at a maximum depth of 126m and 125m respectively.

Table 10. Water depth, catchment and land cover and types of mixing in Rotorua lakes. Data obtained from Rotorua Lakes Water Quality Report 2014/2015.

Lake	Max depth (m)	Lake area (km^2)	Topographical catchment area (km^2)	Mixing	% land cover			
					Native	Exotic	Pastoral	Urban
Okareka	33.5	3.43	19.6	Monomictic	44	8	37	3.0
Okaro	18	0.31	3.9	Monomictic	0	6	90	0
Okataina	78.5	10.8	60	Monomictic	79	8	8.0	0
Rerewhakaaitu	15.8	5.5	37	Polymictic	4	17	69	1.0
Rotoehu	13.5	7.9	36.7	Polymictic	31	30	34	0.6
Rotoiti	126	34.0	124.8	Monomictic	30	49	13	2.0
Rotokakahi	32	4.4	19.7	Monomictic	50	21	27	1.1
Rotoma	83	11.2	27.9	Monomictic	41	29	22	3.0
Rotomahana	125	9.1	83.0	Monomictic	23	17	40	1
Rotorua	45	80.97	597.4	Polymictic	19	18	47	8.0
Tarawera	87.5	41.5	143.3	Monomictic	60	15	17	1.0
Tikitapu	27.5	1.5	6.2	Monomictic	80	14	2.0	3

Geothermal inputs account for a substantial portion of the salts present in Lake Rotorua, Lake Rotoiti and Lake Rotomahana, with contributions from geothermal sources being approximately 107 g/m^3 of total dissolved salts for Lake Rotorua, 99.8 g/m^3 for Lake Rotoiti, and 876 g/m^3 for Lake Rotomahana (Timperley & Vigor-Brown, 1986).

Concentrations of THg and MeHg have been observed to be elevated in both the water bodies and trout populations across all three lakes, attributed primarily to geothermal influences (Weissberg & Zobel, 1973; Brooks et al., 1976; Kim & Burggraaf, 1999). This is in agreement with data obtained from this study (Figure 19 in chapter 4) where THg levels for Lakes Rotoiti (1.998 mg/kg flesh), Rotorua (1.763 mg/kg flesh) and Rotomahana (3.195 mg/kg flesh) were higher than the 1.0 mg/kg ww safe threshold level recommended by WHO. THg levels in koura were also elevated in these lakes where Lake Rotoiti had 1.211 mg/kg flesh while Lake Rotorua obtained 0.454 mg/kg flesh. No koura was found in Lake Rotomahana. For THg levels in kakahi digestive gland, Lake Rotoiti reported 1.441 mg/kg while Lake Rotorua had 1.323 mg/kg. No kakahi was found in Lake Rotomahana. In Figure 29, an average of THg (mg/kg WW) concentrations in trout flesh was plotted against Lake TLI. As can be seen, lakes Rotomahana, Rotoiti and Rotorua which had the three highest THg concentrations in trout had TLI scores of more than 4. A TLI score of more than 4 indicates that the lake water quality is poor; a lake that is eutrophic where it is characterised by murky water with high amounts of nutrients and algae. This result showed that eutrophication definitely had a part to play in THg bioaccumulation in

trout. In Figure 30, an increase in sediment THg (0-10 mg/kg DW) did not increase the THg (mg/kg WW) concentrations in trout flesh. However, when sediment THg in lake Rotoiti increased to almost 100 mg/kg DW, THg in trout flesh dramatically increased 4 times. Even so, there is no significant correlation between sediment THg levels and THg concentrations in trout.

Verburg et al. (2014) investigated Hg biomagnification in three New Zealand lakes namely Rotorua which is eutrophic, Rotomahana which is mesotrophic and finally Tarawera which is oligotrophic. Land use within the catchments of Lakes Rotorua, Rotomahana, and Tarawera differs markedly and provides important context for the contrasting trophic states and mercury biomagnification patterns observed by Verburg et al. (2014). The catchment of Lake Rotorua is heavily modified and dominated by agricultural land use, particularly pastoral farming, alongside urban development around Rotorua township. Extensive land clearance, fertiliser application, and livestock grazing have contributed to elevated nitrogen and phosphorus inputs through surface runoff, groundwater inflows, and stream discharges. These nutrient inputs have driven persistent eutrophication, promoting high primary productivity and periodic hypolimnetic anoxia. Such land-use pressures indirectly enhance mercury risks by creating physicochemical conditions; low dissolved oxygen, altered redox state, and increased microbial activity. These conditions favour mercury methylation and its subsequent transfer through the food web. In contrast, Lake Rotomahana catchment is less intensively farmed and is strongly influenced by geothermal activity and native vegetation, with limited agricultural development. Land use is characterised by a mix of conservation land, forested areas, and low-intensity pastoral farming. As a result, nutrient inputs are lower than those to Lake Rotorua, supporting its mesotrophic status. However, geothermal inflows contribute both mercury and dissolved solutes to the lake, and when combined with moderate nutrient enrichment, these conditions can still support enhanced methylation and bioaccumulation in higher trophic levels, as reflected in elevated mercury concentrations in trout. Lake Tarawera catchment is the least disturbed of the three and is dominated by exotic and native forestry, conservation land, and minimal urban or agricultural activity (Scholes & Hamil, 2016). Nutrient inputs are comparatively low, maintaining oligotrophic conditions, high water clarity, and well-oxygenated bottom waters. These land-use characteristics limit eutrophication-driven anoxia and reduce microbial methylation potential, contributing to lower mercury

bioavailability and reduced biomagnification in aquatic food webs relative to the more modified catchments. Overall, differences in land use across these catchments play a critical role in shaping nutrient status, oxygen dynamics, and microbial processes that indirectly control mercury cycling. While mercury sources in these lakes are largely natural, particularly geothermal, catchment land use influences the extent to which mercury is transformed into bioavailable methylmercury and accumulated in fish**,** helping to explain why eutrophic and mesotrophic systems pose greater risks to human and ecological health than oligotrophic lakes.

The study found that mercury concentrations in trout were highest in the eutrophic Lake Rotorua and mesotrophic Lake Rotomahana, exceeding international safety limits for human consumption by up to 440%. Verburg et al. (2014) also reported that physicochemical factors, such as lower pH, alkalinity, and dissolved oxygen, were associated with increased mercury concentrations and biomagnification in the eutrophic lake Rotorua. Periodic anoxic conditions in Lake Rotorua were shown to have enhanced mercury methylation and its transfer into the food web, contributing to higher bioaccumulation. Even so, while eutrophication generally reduces mercury concentrations in primary producers (phytoplankton), its impact on higher trophic levels is more complex, influenced by food web dynamics and environmental conditions.

The relationship between total mercury and MeHg accumulation in aquatic biota is intricately linked to the phenomenon of eutrophication, characterized by nutrient over-enrichment in aquatic ecosystems. Eutrophication primarily results from anthropogenic activities that increase nutrient inputs, particularly nitrogen and phosphorus, into water bodies. This nutrient influx can lead to excessive growth of algae, which subsequently influences the biogeochemical cycling of mercury and its transformation into MeHg, a more toxic form that bioaccumulates in aquatic food webs. Eutrophication can exacerbate mercury accumulation through several mechanisms. For instance, the increased productivity associated with eutrophication can enhance the microbial processes that convert inorganic mercury to MeHg. Orihel et al. (2008) highlighted that eutrophic conditions can mobilize soil-bound mercury, facilitating its transformation into MeHg. This transformation is critical as it leads to higher concentrations of MeHg in aquatic organisms, which can have detrimental effects on both aquatic life and human health. Moreover, the high productivity of

eutrophic waters can lead to oxygen depletion as algal blooms die off and decompose, creating hypoxic conditions that further stress aquatic ecosystems. This scenario is supported by Dodds et al. (2009), who discuss how eutrophication can lead to fish death and reduced biodiversity, which are compounded by the presence of MeHg. The interplay between eutrophication and mercury dynamics is particularly concerning in tropical and subtropical regions, where the natural processes of nutrient cycling and mercury methylation are often intensified due to climatic conditions and land use changes.

Fitzgerald and McCarty (2024) noted that in naturally oligotrophic catchments, where nutrient levels are typically low, increased eutrophication has led to elevated MeHg concentrations. Research conducted in northern Ontario has established a clear link between disturbances in primarily forested watersheds and increased eutrophication in lakes and rivers. When these watersheds are disrupted—whether through activities such as road construction, logging, or other human interventions—it can lead to more frequent algal blooms and an increased growth of aquatic plants (macrophytes) (Winter et al., 2011; Winter et al., 2002). This process is driven by the increased loading of total phosphorus (TP) into surface waters, a key nutrient that fuels eutrophication. One of the main pathways for this TP enrichment is the deposition of atmospheric dust and wood ash, which results from land disturbance (Meyers, 2006). As human activities disturb the landscape, they generate and mobilize fine particles that settle in nearby water bodies, increasing nutrient levels. This influx of phosphorus accelerates eutrophication, even in oligotrophic (nutrient-poor) watersheds, such as those found on the Canadian Shield. While these ecosystems are naturally low in nutrients, even a modest increase in phosphorus can have significant consequences. A critical and unexpected impact of this eutrophication is the enhanced transformation of inorganic mercury into its toxic form, MeHg. Fitzgerald and McCarty (2024) highlighted that the mean mercury tissue concentrations from trout flesh was between 0.4 -1.23 μg/g WW in the year 2010 to 2012 while in a span of five years, the mean mercury tissue concentrations had increased to 0.42 – 1.62 μg/g WW. This research underscored the unintended consequences of watershed disturbances, showing that even minor disruptions in forested regions can lead to significant ecological changes, including increased mercury contamination in aquatic food webs.

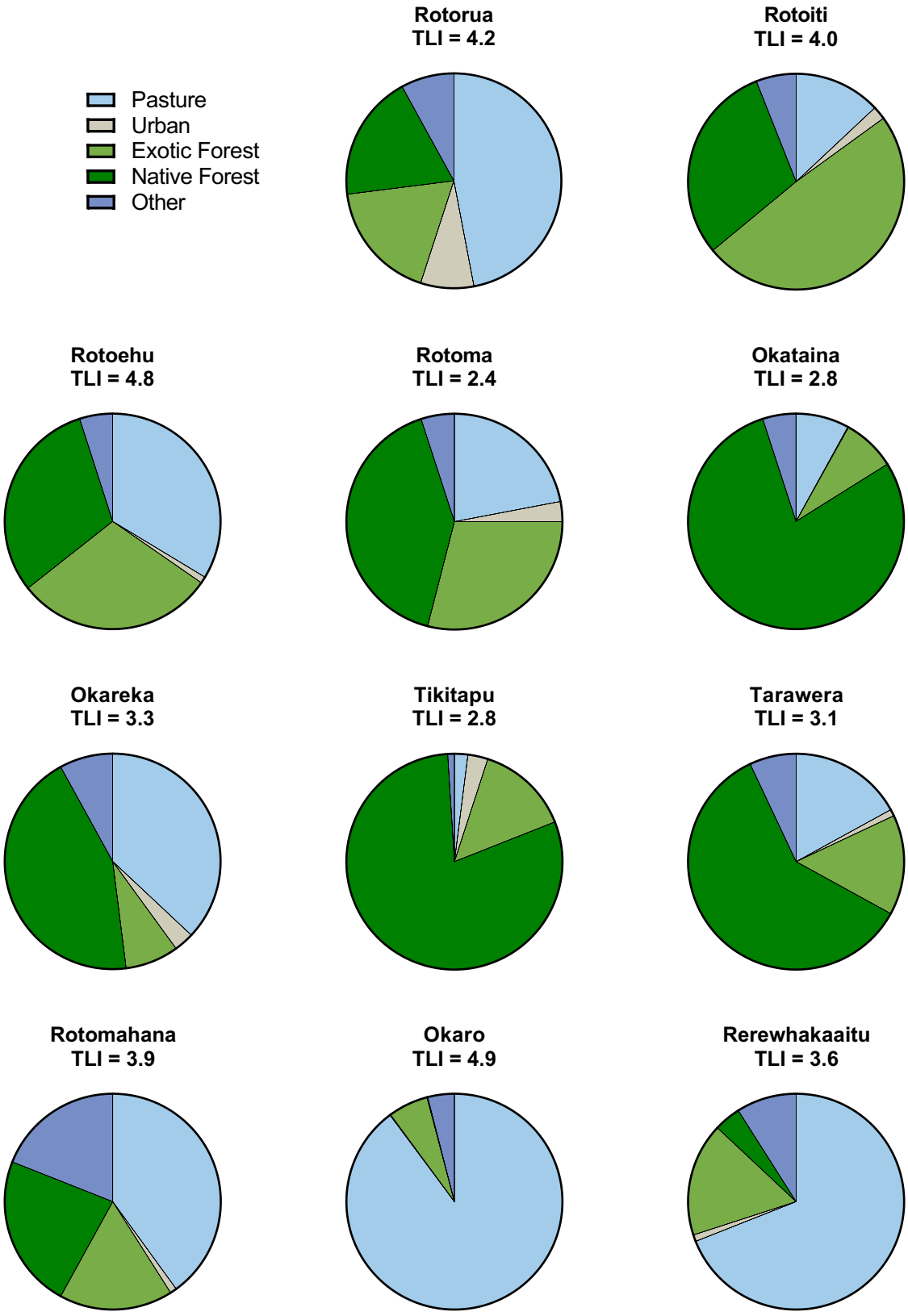

Figure 28. TLI results of the Rotorua lakes with percentages of land cover; pasture, urban, exotic forest, native forest and other. Data obtained from Rotorua Lakes Water Quality Report 2014/2015.

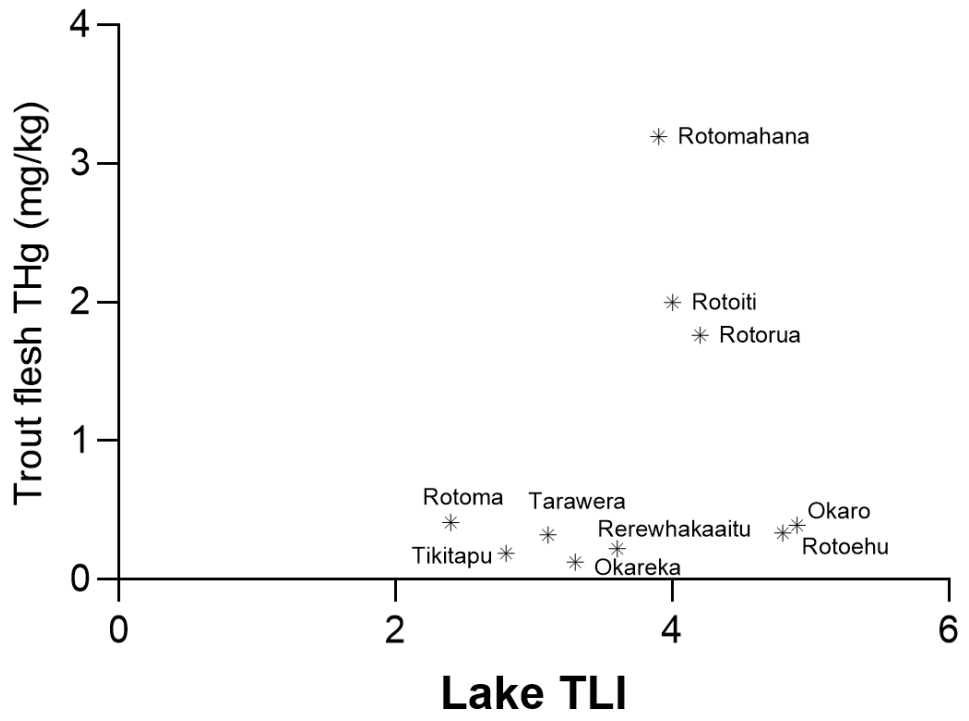

Figure 29. Average THg (mg/kg ww) in trout flesh versus Lake TLI.

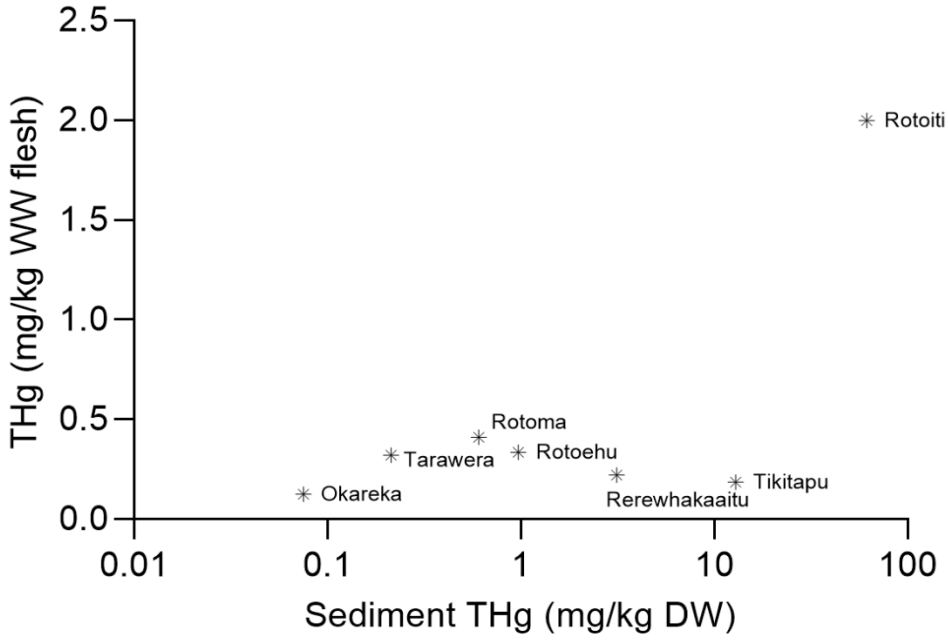

Figure 30. Average THg (mg/kg) in trout flesh versus sediment THg (mg/kg DW). D Data provided by D. Trolle (2006), pers. comm., unpublished data.

A more in-depth examination of Lake Rotoiti reveals a strong relationship between mercury bioaccumulation in trout and changes in lake water quality over time. Lake Rotoiti transitioned from eutrophic to mesotrophic and back to eutrophic. The increase in mercury concentration in trout over time in Lake Rotoiti coincides with the decline in water quality and also prolonged and severe period of hypolimnetic anoxia (Figure 31). Hypolimnetic volumetric oxygen depletion (HVOD) rate serves as a critical metric for assessing lake quality, particularly in stratified lakes during the summer months. Rapid oxygen depletion in the hypolimnion can have profound ecological impacts, as anoxic conditions facilitate the release of nutrients such as nitrogen and phosphorus as well as inorganic mercury from sediments (Eckley and Hintelmann, 2006; Orihel et al, 2007). These nutrients subsequently disperse throughout the water column during seasonal mixing, particularly at the onset of winter (Millard et al., 2023).

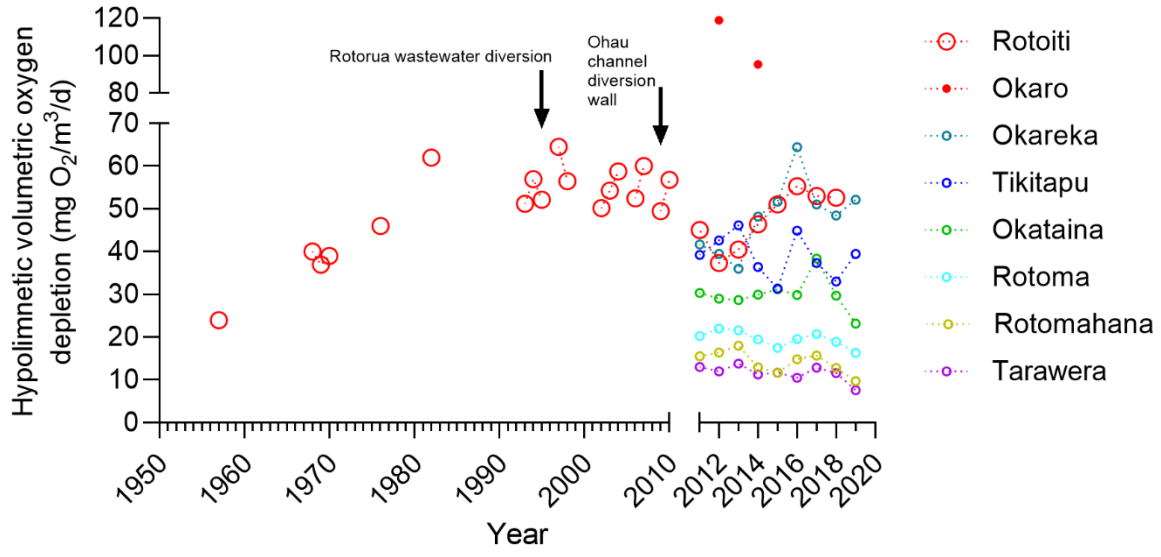

Figure 31. Hypolimnetic volumetric oxygen depletion (HVOD) in Lake Rotoiti from year 1955 to 2019.

As can be seen in Figure 31, the HVOD for Lake Rotoiti appeared to be increasing since the 1950s and reached its peak in year 1986 before slowly decreasing after the Rotorua wastewater diversion and the Ohau channel diversion wall was built. The water quality of Lake Rotoiti had been significantly influenced by the degradation of Lake Rotorua, primarily due to nutrient influxes from the Ohau Channel (Figure 33), septic systems, and agricultural activities. Historically, these inputs included

approximately 150 tonnes of nitrogen and 15 tonnes of phosphorus annually entering Lake Rotoiti's main body. Although nutrient contributions from septic tanks and farming are relatively minor compared to the Ohau Channel, the accumulated nutrients now reside within the lake's bottom sediments, perpetuating internal loading. To mitigate this issue, a diversion wall was constructed in 2008 to redirect nutrient-rich inflows from Lake Rotorua away from Lake Rotoiti and toward the Kaituna River (ISSN 1775 9372 Environmental Publication, 2009). Elevated nutrient concentrations in the water column promote excessive algal growth, which can lead to the development of toxic algal blooms under certain conditions. The decline in water quality has also had adverse effects on the habitat of aquatic species, particularly fish. As algae proliferate and subsequently die, their decomposition consumes dissolved oxygen in the water column. When stratification prevents the mixing of oxygen-rich surface waters with deeper layers, hypoxic or anoxic conditions develop in the hypolimnion. This oxygen depletion confines fish to the oxygenated upper layers of the lake, reducing the overall habitable area and potentially affecting fish populations. Anoxic hypolimnion creates an optimum condition whereby microbial processes dominate mercury methylation. Eckley and Hintelmann (2006) investigated the rates and conditions under which inorganic Hg is converted to MeHg in the water columns of five Canadian lakes. They found that mercury methylation was detected exclusively in anoxic hypolimnia, highlighting the role of anaerobic bacteria, particularly sulfate-reducing bacteria (SRB). Methylation rates also varied with depth and peaked just below the oxic/anoxic boundary (oxycline), indicating narrowly defined microbial zones. Millard et al. (2023) found that seasonal stratification significantly influenced mercury methylation rates. During warmer months, stratification led to reduced mixing in the water column, creating anoxic conditions that favored methylation processes. The study found that methylation rates were highest in the summer and early fall when stratification was most pronounced. Conversely, during winter and early spring, when the reservoir was well-mixed and oxygen levels were higher, methylation rates decreased significantly. The sediment also exhibited seasonal variability, with higher methylation rates observed during stratified conditions. He concurred with Eckley and Hintelmann (2006) that the anoxic conditions that develop during stratification periods promote microbial activity that facilitates the conversion of inorganic mercury to MeHg.

In comparing HVOD rates across stratified lakes over the past 9 years (Figure

32), Lakes Okaro, Rotoiti, Okareka, Tikitapu, and Okataina consistently exhibited elevated HVOD rates relative to other monomictic lakes. These lakes frequently experience hypolimnetic anoxia during summer stratification. Notably, Lake Okaro demonstrates a significantly more rapid depletion of dissolved oxygen in its hypolimnion, reaching anoxic conditions within two months—much faster than other lakes in the Rotorua Te Arawa region (BOPRC, 2016). This rapid oxygen depletion renders the calculation of HVOD rates using monthly monitoring data impractical. In contrast, Lake Rotoiti's hypolimnion remains oxygenated for a longer duration, taking approximately five months to reach anoxic conditions. Interestingly, Lakes Rotomahana and Tarawera, which are more oligotrophic, exhibit lower HVOD rates compared to Lakes Okataina and Rotoma. Despite their larger hypolimnetic volumes, Rotomahana and Tarawera experience slower oxygen depletion. The shallower average depth and smaller hypolimnetic volume of Okataina and Rotoma contribute to their higher HVOD rates, likely driven by a combination of higher abundance of oxygen-consuming organisms and inflows of groundwater.

Polymictic lakes, such as Rotorua and Rotoehu, also experience episodes of oxygen depletion in bottom waters, though these events are typically linked to intermittent thermal stratification. Such stratification occurs during periods of warm, calm weather, cutting off bottom waters from atmospheric oxygen replenishment. An example of this phenomenon occurred in late 2014, when a stable anticyclonic weather system established prolonged stratification in the Rotorua region. Both Lakes Rotorua and Rotoehu experienced rapid oxygen depletion in their bottom waters, leading to anoxia for nearly a month before mixing resumed. This simultaneous depletion in both lakes reflects the widespread influence of the anticyclonic conditions during that period, as graphically depicted in monitoring data from late 2014 and early 2015. These findings highlight the intricate interactions between meteorological conditions, lake morphometry, and biological processes in determining hypolimnetic oxygen dynamics. Such insights are essential for managing the ecological health and nutrient cycling of stratified lakes.

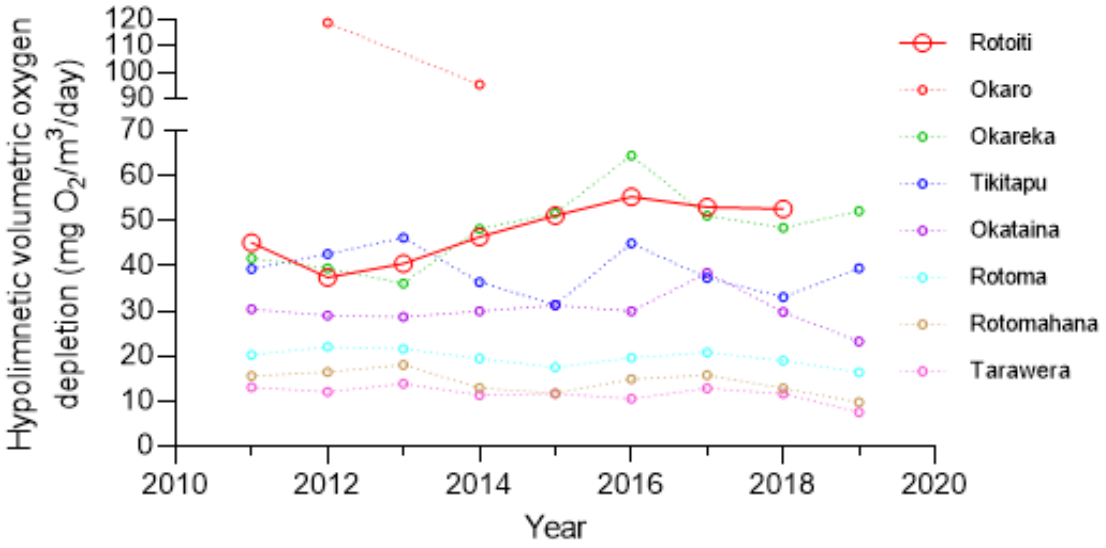

Figure 32. Hypolimnetic volumetric oxygen depletion (HVOD) in Lakes Rotoiti, Okaro, Okareka, Tikitapu, Okataina, Rotoma, Rotomahana and Tarawera from year 2011 to 2019. Data obtained from Bay of Plenty Regional Council, 2019.

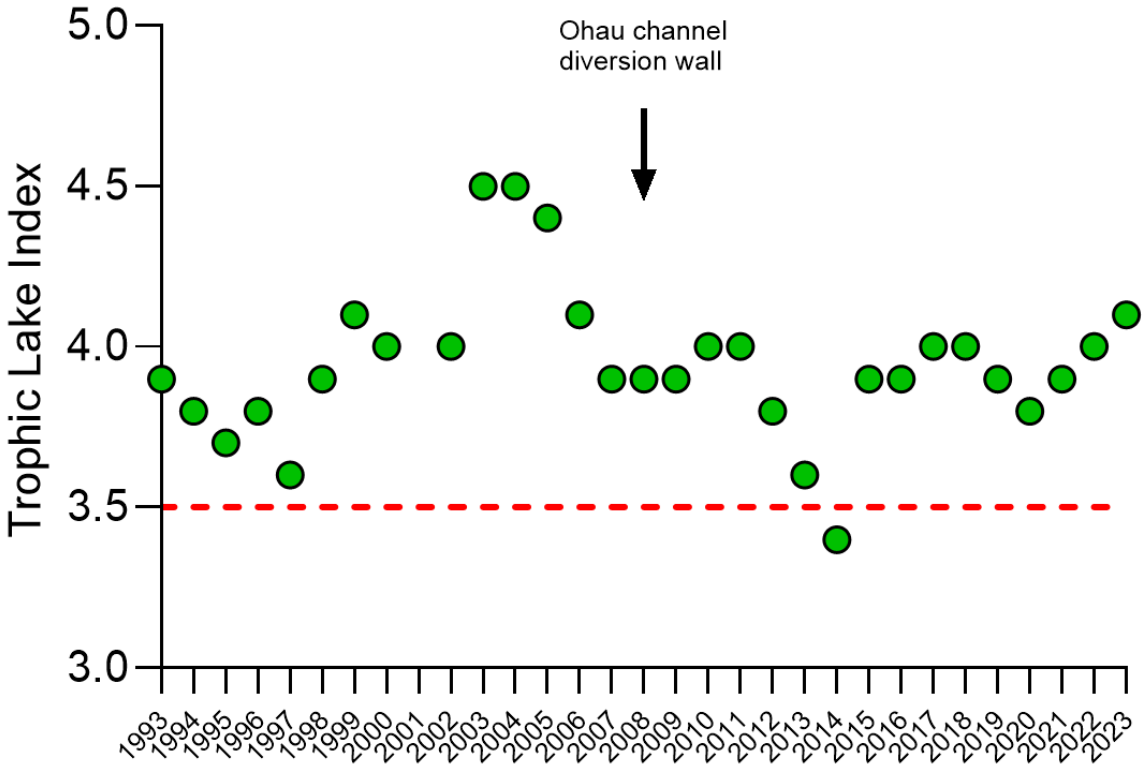

Figure 33. Lake Rotoiti TLI from 1993 to 2023.

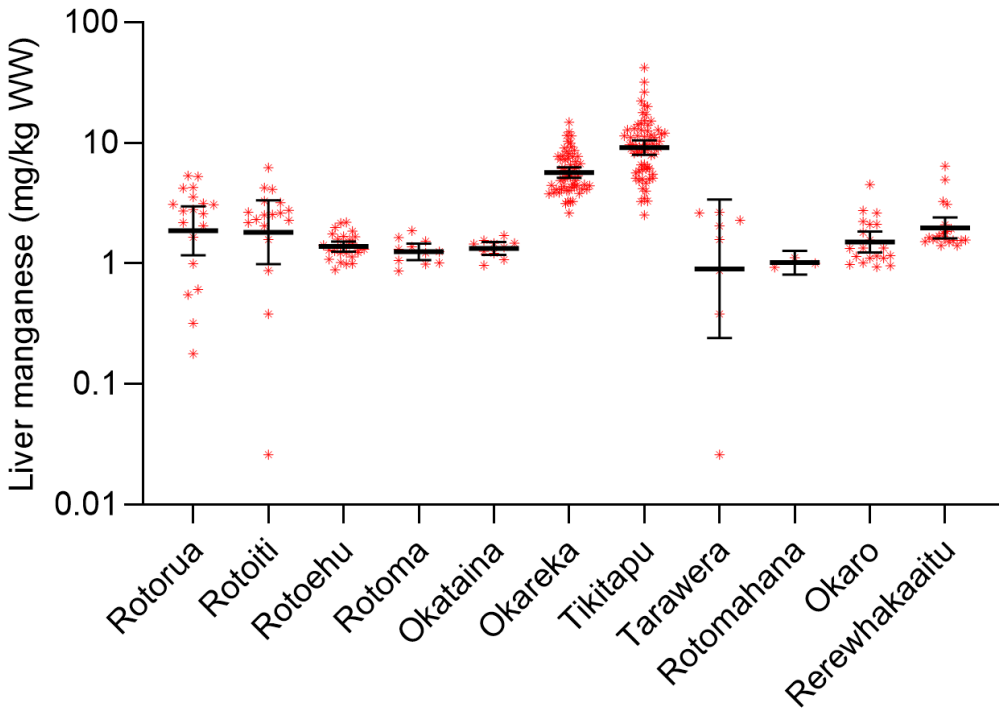

Figure 34. Manganese concentrations (mg/kg WW) in trout liver in 11 Rotorua Lakes.

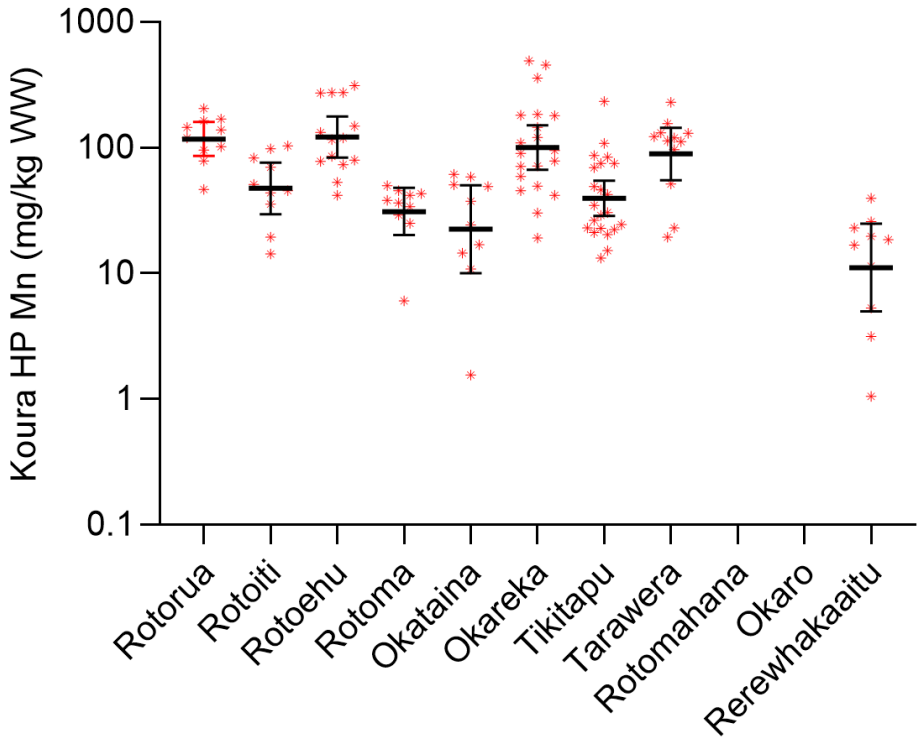

Figure 35. Manganese concentrations (mg/kg WW) in koura hepatopancreas in 9 Rotorua Lakes.

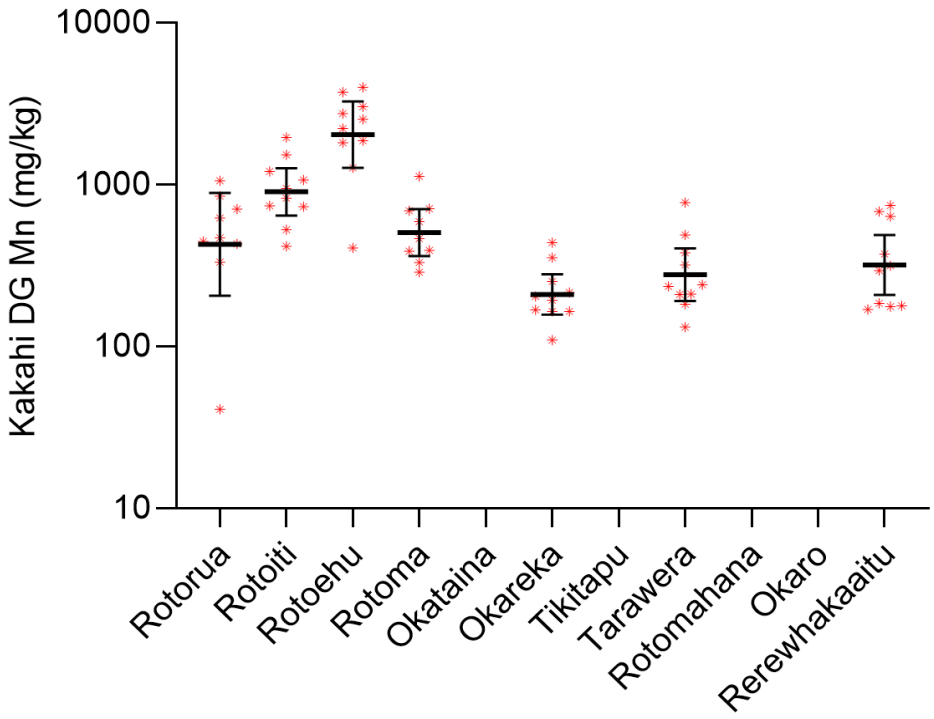

Figure 36. Manganese concentrations (mg/kg WW) in kakahi digestive gland in 7 Rotorua Lakes.

The analysis of manganese (Mn) in trout liver across 11 Rotorua lakes (Figure 34) showed concentrations ranging between 1 and 10 mg/kg WW. In contrast, Mn concentrations in koura hepatopancreas (Figure 35) were notably higher, ranging from 10 to 100 mg/kg WW across nine Rotorua lakes. A similar observation was seen in kakahi digestive glands (Figure 36), where Mn concentrations ranged from 100 to 1000 mg/kg WW across seven Rotorua lakes. While Mn concentrations exhibited minimal variation across different lakes, a distinct pattern emerged, showing a tenfold increase in Mn concentrations at lower trophic levels within the food chain. These findings align with the research conducted by Niemiec and Wiśniowska-Kielian (2015), which reported significantly higher Mn concentrations in benthic organisms, specifically *Diptera Chironomidae* larvae, compared to carp sampled from a fish pond. Their study found that Mn concentrations in benthic organisms ranged from 19.27 to 33.88 mg/kg dry mass, whereas Mn concentrations in carp liver ranged between 1.876 and 10.50 mg/kg dry mass. Additionally, they reported that Mn concentrations in sediment were approximately 2210 times higher than those in the surrounding water. Benthic organisms exhibit a heightened sensitivity to Mn accumulation, as its concentrations are significantly elevated in sediments. The high levels of Mn in these

organisms are primarily attributed to its substantial accumulation in sedimentary deposits. Manganese, as a trace element, demonstrates a strong tendency for bioconcentration, particularly in aquatic organisms occupying lower trophic levels within the food chain (Oweson and Hernroth, 2009). These findings suggest that Mn accumulates more readily in sediment and benthic organisms, leading to a higher bioavailability of Mn at lower trophic levels in aquatic ecosystems.

As illustrated in Figure 37, the analysis revealed no significant correlation ($p = 0.780$) between Mn and THg concentrations in trout. Additionally, to further explore potential interactions, Mn concentrations in trout liver were plotted against % MeHg (Figure 38). However, the results indicated no significant relationship ($p = 0.757$) between these variables, suggesting that Mn accumulation in trout liver does not influence mercury speciation or bioaccumulation in the studied population.

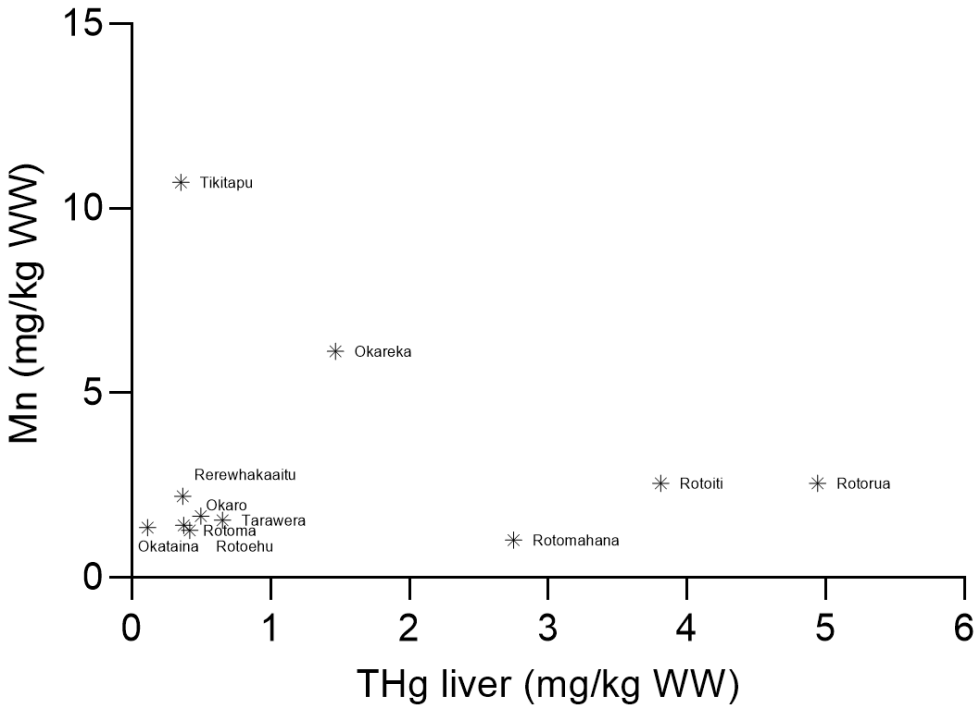

Figure 37. Manganese concentrations (mg/kg WW) versus THg concentrations (mg/kg WW) in trout liver.

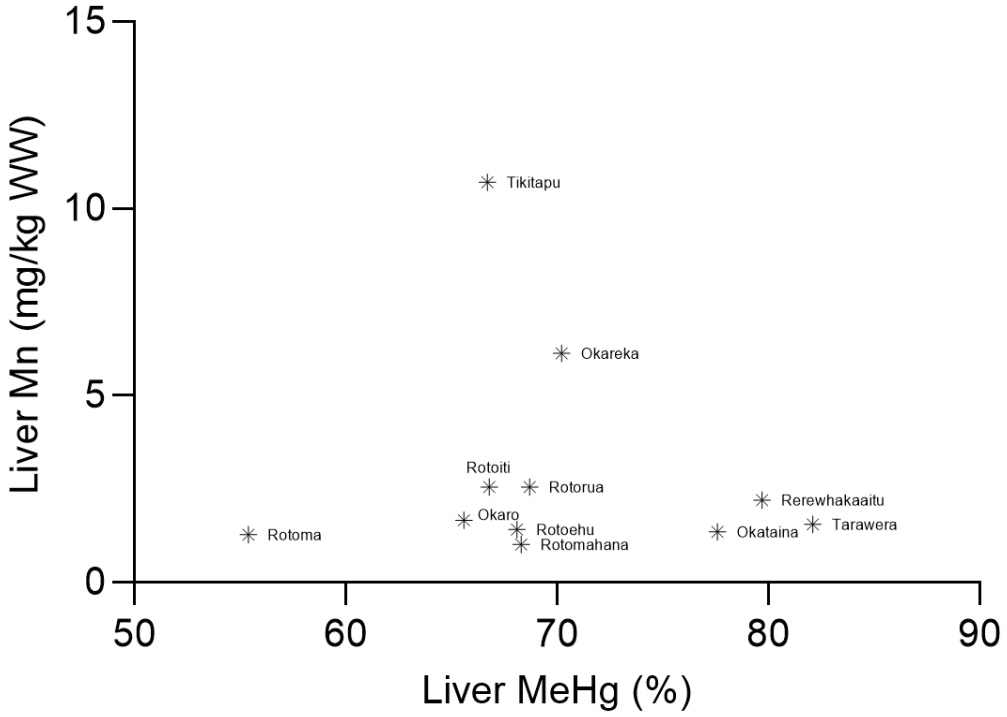

Figure 38. Manganese concentrations (mg/kg WW) versus % MeHg concentrations in trout liver.

This study also examined selenium (Se) concentrations in trout, koura, and kakahi across multiple Rotorua lakes. As illustrated in Figure 39, Se concentrations in trout liver ranged from 0.2 to 100 mg/kg wet weight (WW) across 11 Rotorua lakes, with the majority of samples exhibiting Se concentrations between 1 and 10 mg/kg WW. Similarly, Se concentrations in koura hepatopancreas (Figure 40) varied between 0.3 and 2.3 mg/kg WW across nine Rotorua lakes. In contrast, Se concentrations in kakahi digestive glands (Figure 41) displayed a broader range, spanning from 0.002 to 10 mg/kg WW. While Se concentrations in trout liver and koura hepatopancreas were relatively consistent across the sampled lakes, a notable variation was observed in kakahi digestive glands. Specifically, selenium concentrations in Lake Rotorua and Lake Rotoiti were significantly elevated compared to the other lakes, with levels approximately 1000-fold and 100-fold higher, respectively. This distinct variation in Se distribution suggests potential differences in bioavailability, trophic transfer, or environmental factors influencing Se accumulation in these aquatic ecosystems. While mercury has been relatively well studied in the Rotorua lakes, data on Se concentrations in fish, koura, and kakahi remain scarce in the published literature. Additionally, no studies have been conducted to investigate the presence or

distribution of Se in the lake water of this region.

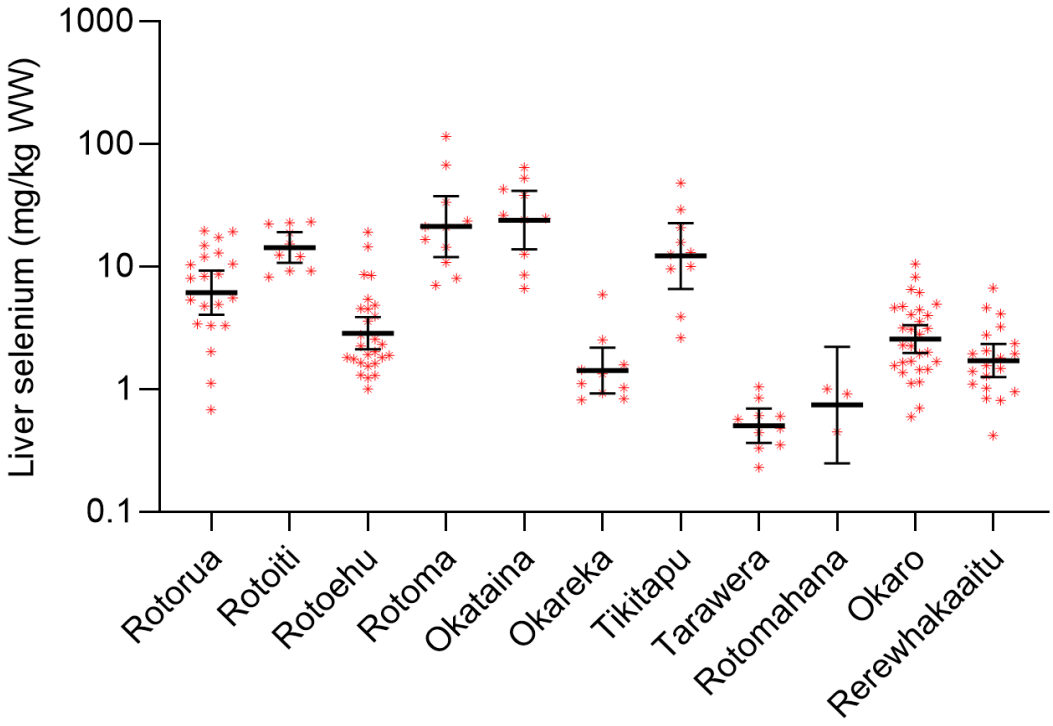

Figure 39. Selenium concentrations (mg/kg WW) in trout liver in 11 Rotorua Lakes.

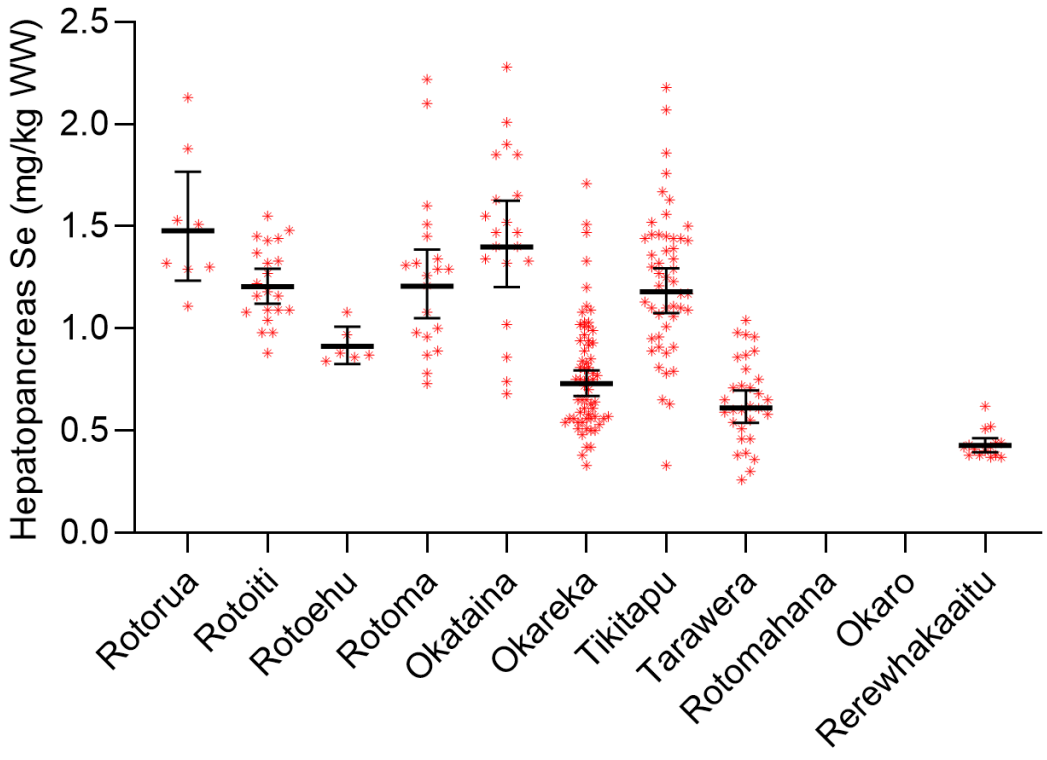

Figure 40. Selenium concentrations (mg/kg WW) in koura hepatopancreas in 9 Rotorua Lakes.

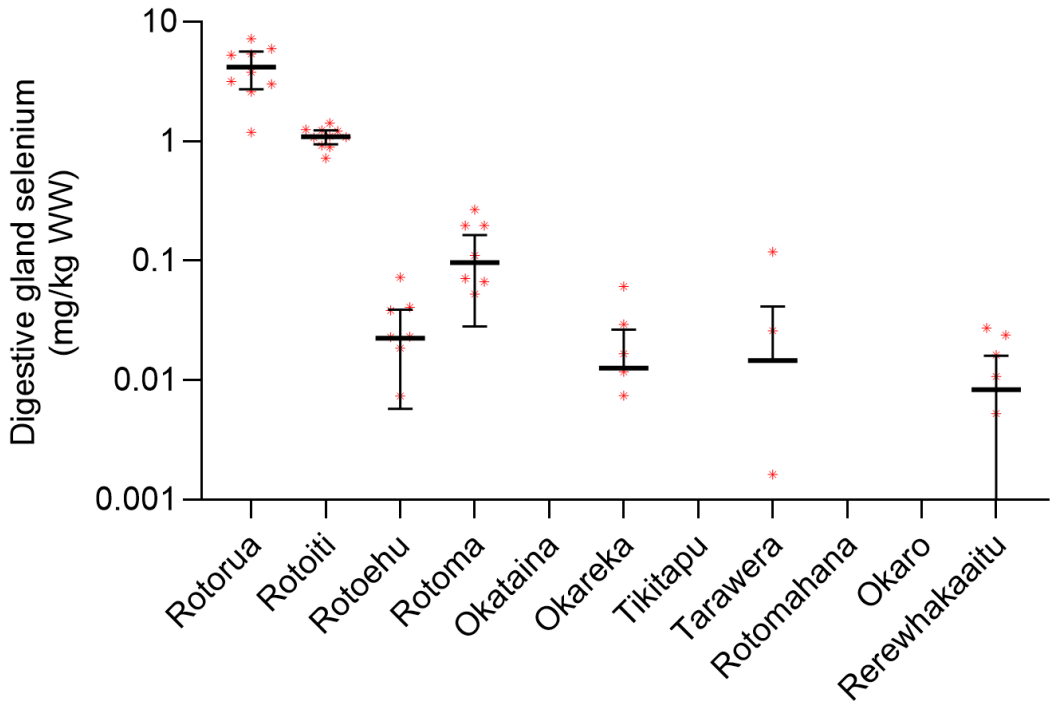

Figure 41. Selenium concentrations (mg/kg WW) in kakahi digestive gland in 7 Rotorua Lakes.

This study also aimed to examine the relationship between THg concentrations in trout flesh and liver. As illustrated in Figure 42, a strong positive correlation was observed between THg levels in trout flesh and liver, with a Pearson correlation coefficient of $r = 0.8146$ ($P < 0.0001$). This indicates that an increase in THg concentration in trout flesh is significantly associated with an increase in THg concentration in the liver. However, the relationship is non-linear, as THg concentrations in trout flesh appear to reach a maximum threshold. Additionally, this study also examined the relationship between % MeHg and THg concentrations in trout liver. As presented in Figure 43, the results indicate no significant correlation between % MeHg and THg in trout liver.

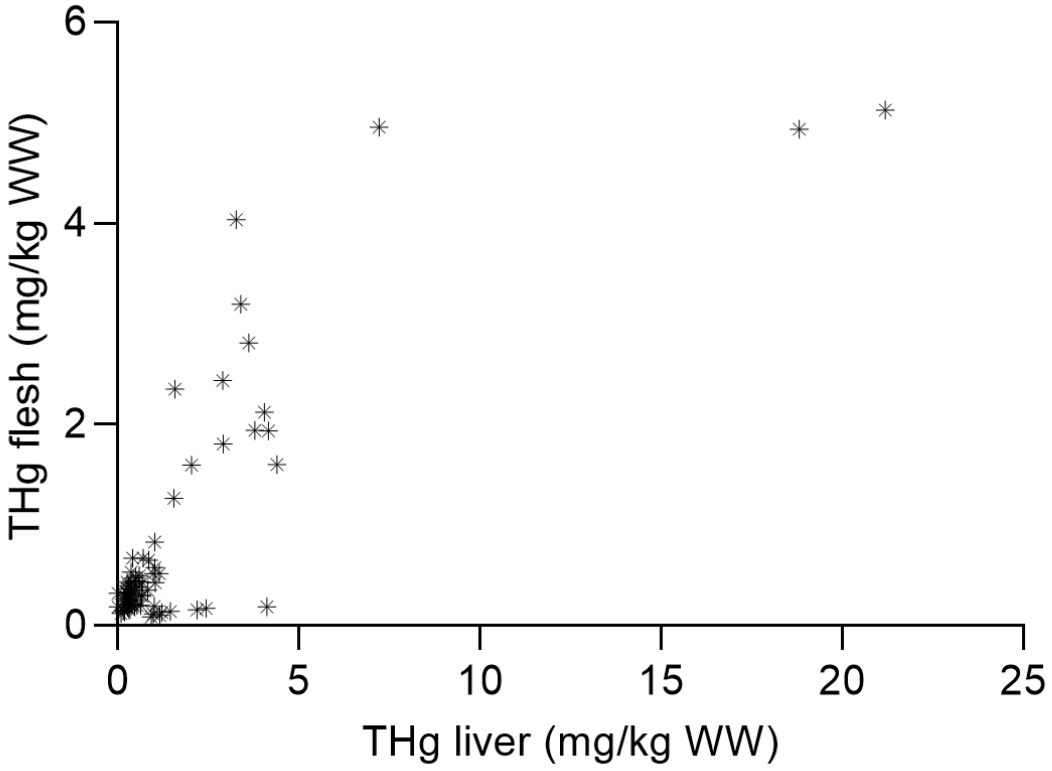

Figure 42. THg concentrations (mg/kg WW) in trout flesh versus liver

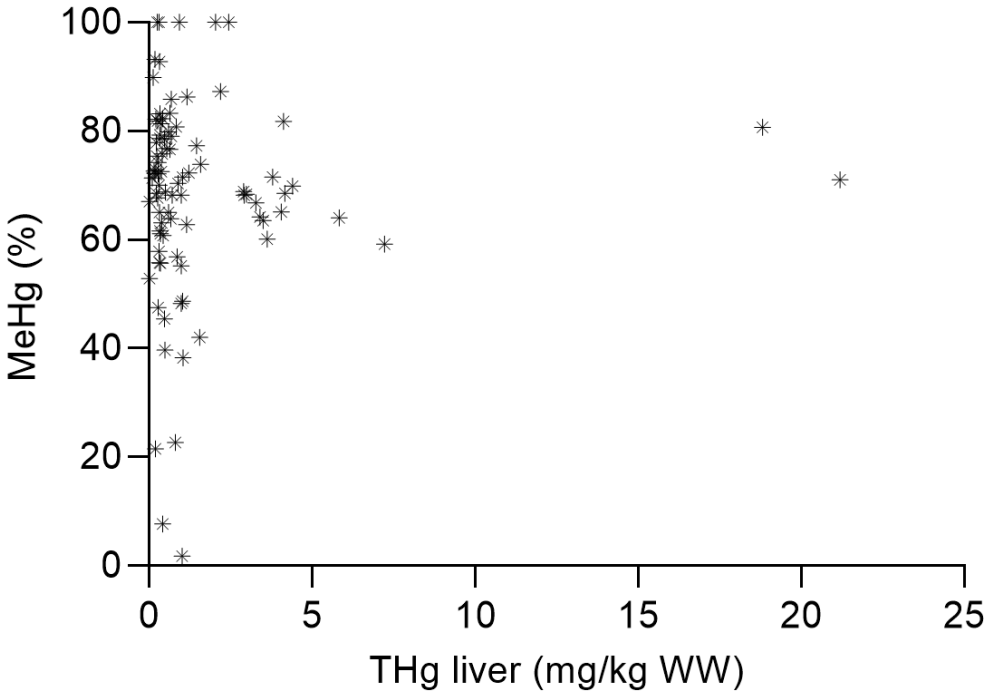

Figure 43. % MeHg versus THg concentrations (mg/kg WW) in trout liver.

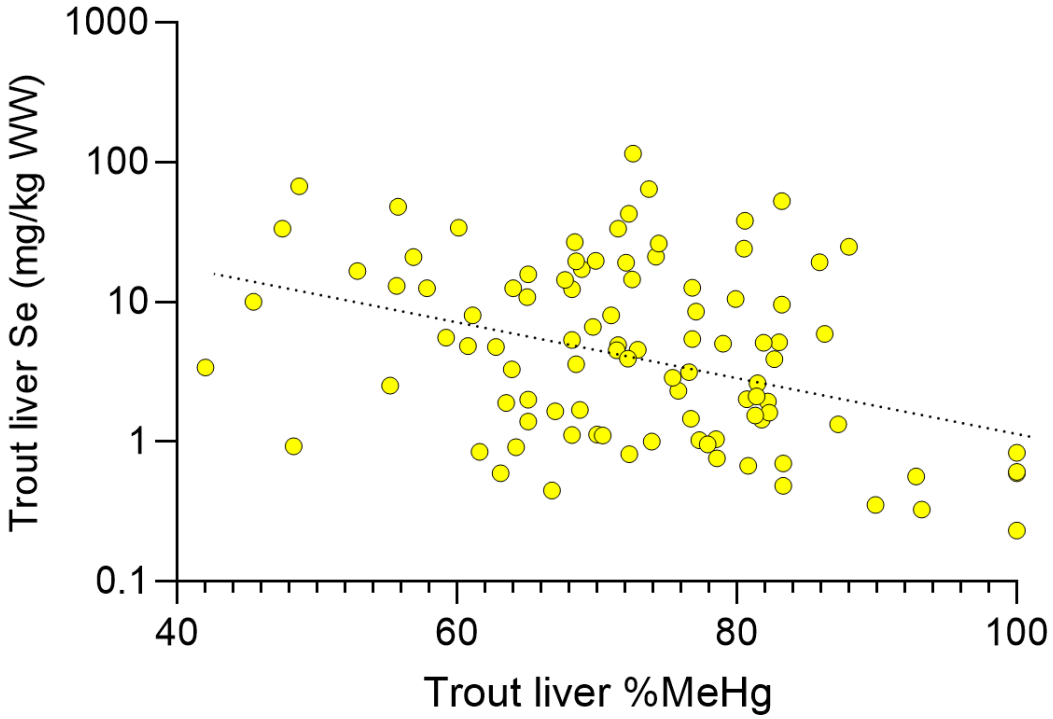

Figure 44. The graph above illustrates the relationship between selenium (mg/kg WW) and % MeHg in trout liver.

This study demonstrated a significant correlation between liver selenium (log Se) concentrations and % MeHg in trout liver, as shown in Figure 44. The Pearson correlation coefficient was r = -0.3496 (p = 0.0004), indicating that higher levels of selenium in the liver are associated with a decrease in % MeHg, while lower selenium levels correspond with increased % MeHg. These findings suggest that the liver may be the primary site for selenium-induced demethylation of MeHg in fish, as compared to the flesh, which is supported by previous literature. Afonso et al. (2008) observed similar results in deep-water fish off the coast of Portugal, where higher selenium concentrations were associated with reduced mercury toxicity, particularly in the liver. Their study indicated that selenium accumulates predominantly in the liver, with lower % MeHg in the liver compared to the muscle tissue. These findings align with the present study, reinforcing the idea that selenium exerts protective effects against MeHg toxicity in the liver. Additionally, research on freshwater lake trout from Argentina by Arribere et al. (2008) showed that elevated selenium levels in muscle tissues were linked to reduced mercury concentrations, suggesting that a selenium-rich

diet may facilitate mercury detoxification. Furthermore, it is possible that interactions between selenium and mercury in the aquatic environment could lead to the formation of insoluble compounds, reducing mercury bioavailability to organisms. This mechanism, as described by Belzile et al. (2006), may contribute to lower mercury concentrations in organisms exposed to elevated selenium levels. Together, these findings highlight the potential role of selenium in mitigating mercury toxicity in aquatic organisms, particularly within the liver.

The study also investigated the correlation between selenium concentrations and THg in koura hepatopancreas. As shown in Figure 45, no significant relationship ($p = 0.897$) was observed between these two variables. Figure 46 illustrates a strong negative correlation between % MeHg and THg concentrations in kakahi digestive gland. Pearson correlation analysis confirms this relationship, with a coefficient of $r = -0.518$, indicating statistical significance ($p < 0.0001$). This negative correlation suggests that as the proportion of MeHg in kakahi digestive gland increases, the concentration of total mercury decreases. The percentage of MeHg relative to THg indicates that MeHg constitutes the majority of the total mercury present in the trout tissue. In addition, a strong positive correlation was observed between THg concentrations and tissue Se concentrations (mg/kg wet weight). Pearson correlation analysis yielded a coefficient of $r = 0.645$, with $p < 0.0001$, signifying a statistically significant relationship. This positive correlation implies that as THg concentrations increase, tissue selenium levels also rise. In contrast, %MeHg in the kakahi digestive gland was negatively correlated with tissue selenium concentrations, with a Pearson correlation coefficient of $r = -0.4847$ ($p < 0.0001$). These findings are consistent with previous studies that have shown selenium in fish tissues to have protective effects against MeHg uptake (Bidon et al., 2023; Rudershausen et al., 2023; Ribeiro et al., 2022).

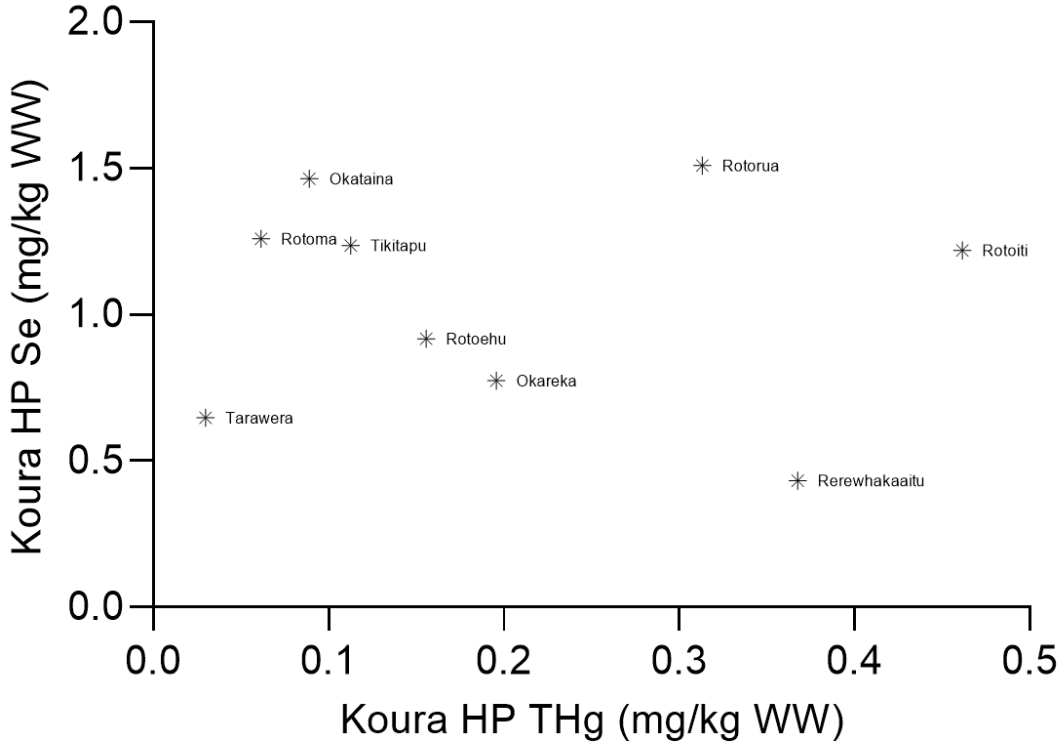

Figure 45. The graph above illustrates the relationship between selenium (mg/kg WW) and THg (mg/kg WW) in koura hepatopancreas.

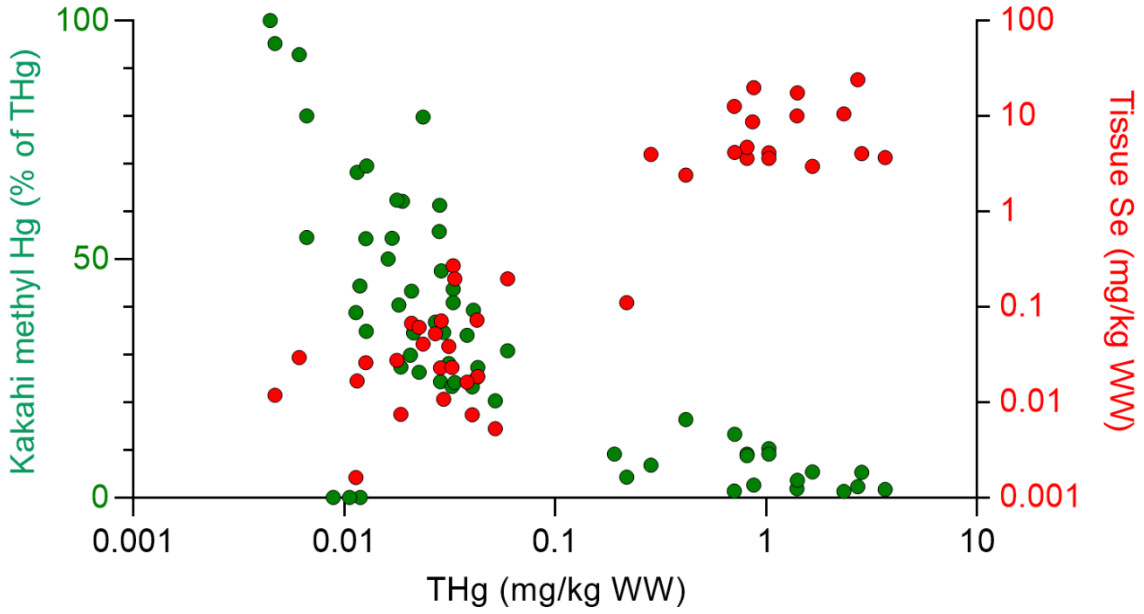

Figure 46. The graph illustrates the relationship between % MeHg relative to THg, THg (mg/kg wet weight) and tissue selenium in kakahi (mg/kg wet weight).

The complex pathways involved in mercury transport, binding, and excretion help explain the tissue-specific patterns observed in this study and underscore the importance of Hg-Se interactions. Differences in Se availability among water, fish, and benthic invertebrates such as koura and kakahi may influence mercury speciation, the proportion of MeHg retained in tissues, and associated toxicological responses, including oxidative stress. The negative associations observed between Se and %MeHg in selected tissues suggest a potential moderating role of Se on Hg bioavailability and toxicity. These findings highlight the need to consider Se alongside Hg when interpreting bioaccumulation dynamics and assessing ecological and human health risks in the Rotorua lakes.

5.5 Conclusion

In summary, the geochemical characteristics of lakes exert a strong influence on the concentrations of THg and MeHg within aquatic ecosystems. Geothermal inputs, along with anthropogenic factors such as eutrophication and hypolimnetic anoxia, collectively create conditions conducive to the accumulation of THg and MeHg in aquatic organisms. Seasonal stratification in lakes further exacerbates these effects by promoting oxygen depletion in the hypolimnion, a process that catalyzes the microbial methylation of inorganic mercury to MeHg. This study demonstrated that the aforementioned factors observed in Lakes Rotorua, Rotoiti, and Rotomahana were associated with elevated concentrations of THg and MeHg in trout, which occupy the highest trophic level in these ecosystems. Mn had been shown to concentrate in the lower trophic organisms due to high sediment concentrations. There was no relationship observed between Mn and THg, and also Mn and % MeHg.

Notably, the findings also revealed the protective role of selenium (Se) against MeHg toxicity in trout, specifically within the liver. However, this protective effect was shown to be contingent upon the molar ratio of Hg to Se. A ratio exceeding 1:1 is necessary to mitigate MeHg toxicity effectively. Conversely, deviations from this balance may result in synergistic toxicity, wherein the combined effects of Hg and Se amplify their harmful impact on the organism. This underscores the delicate interplay between these elements and highlights the need for further investigation into their biogeochemical interactions, particularly in ecosystems influenced by geothermal activity and anthropogenic stressors. These findings contribute to a deeper understanding of mercury and selenium dynamics in aquatic ecosystems, with

implications for the management of freshwater resources and the health of trophic food webs.

6 Conclusions and Future Work

6.1 Conclusions

This study represents a pioneering effort to systematically investigate elemental mercury and MeHg using advanced sampling technologies such as 3-MFSG DGT combined with ecological assessments in the context of Rotorua's unique freshwater environments. Through rigorous methodological development, this study had overcome obstacles in handling the silica resin gel as well as the implementation of the HPLC-ICPMS to separate and identify MeHg. It is a first in New Zealand to implement a method that is able to identify and quantify MeHg using the above instrumentation instead of the usual atomic absorbance spectrometer (AAS). The study managed to deploy the 3-MFSG DGT in three Te Arawa lakes with much seasonal variability in that period of time. Mercury and MeHg were detected at higher levels in the hypolimnion of Lakes Okaro and Rotoiti as compared to the epilimnion. The data obtained confirmed that lake stratification which occur in warmer months had hypolimnetic anoxia which promotes conditions that favour MeHg production.

Through gathered data analysis from 11 Te Arawa Lakes, this study analysed and compiled the THg and MeHG concentrations across three different species namely, trout, koura and kakahi. This research compared THg data from past five studies (1976 to 2019) with data obtained from this research and found that THg concentrations had been consistently high (above 1 mg/kg WW as advised by the WHO advisory) in trout found in Lakes Rotorua, Rotoiti, and Rotomahana. The three species sampled also showed high THg concentrations in the aforementioned lakes. This study found that MeHg accounts for 86-96.9% of THg found in trout flesh while THg is mostly concentrated in the liver. The distribution of MeHg and THg between liver and flesh remains uncertain for different species as when THg levels are high, the liver's capacity for metal detoxification may be overloaded and may prompt a transfer of MeHg to other tissues. It is a complex interplay between the physical environment and biological ability within these organisms. This study also noted that bioaccumulation of THg occur between the sediment and benthic organisms.

This study concluded that eutrophication and hypolimnetic anoxia in lakes are key factors influencing the production and bioaccumulation of THg and MeHg in aquatic organisms. Although manganese (Mn) concentrations were found to be

elevated in the kakahi digestive gland, no significant correlation was observed between Mn uptake and THg or %MeHg in trout, koura, or kakahi. In contrast, selenium (Se) concentrations in trout liver exhibited a negative correlation with %MeHg, suggesting a potential mitigating effect of Se on MeHg accumulation. This inverse relationship was further supported by data from the kakahi digestive gland, reinforcing the hypothesis that Se may confer protective effects against MeHg toxicity.

6.2 Recommendations for Future Work

1. **Longitudinal Monitoring of Mercury Levels**
    - Conduct long-term studies to track temporal variations in THg and MeHg concentrations in fish, koura, and kakahi across multiple seasons and hydrological cycles.
    - Investigate potential changes in mercury bioaccumulation due to climate change, eutrophication, and alterations in land use.
2. **Expanded Species and Ecosystem Studies**
    - Include a wider range of aquatic species, including primary producers and lower trophic level organisms, to assess the full extent of mercury bioaccumulation and biomagnification in food webs.
    - Investigate mercury dynamics in different lake ecosystems with varying levels of anthropogenic influence and natural geochemical conditions.
3. **Sediment and Water Column Interactions**
    - Conduct in-depth studies on mercury and MeHg cycling in lake sediments and their flux into the water column.
    - Assess how environmental factors such as redox conditions, microbial activity, and organic matter influence Hg methylation rates.
4. **Role of Hypolimnetic Anoxia and Eutrophication**
    - Investigate the relationship between lake trophic status, hypoxia, and Hg methylation rates to better understand the impact of eutrophication on mercury bioavailability.
    - Assess how hypolimnetic oxygenation strategies could potentially mitigate Hg methylation and bioaccumulation.

5. **Mercury-Selenium Interactions**
    - Further explore the protective role of selenium against MeHg toxicity across different species and tissues.
    - Examine how dietary Se intake and environmental Se concentrations influence mercury detoxification mechanisms in aquatic organisms.
6. **Isotopic Analysis of Mercury Sources**
    - Utilize mercury stable isotope analysis to differentiate between natural and anthropogenic sources of mercury contamination.
    - Investigate atmospheric deposition and watershed inputs to determine the primary contributors to mercury loading in lake ecosystems.
7. **Human and Wildlife Health Risk Assessments**
    - Conduct risk assessments based on mercury concentrations in fish species consumed by local communities to establish safe consumption guidelines.
    - Assess potential sublethal effects of mercury exposure on fish health, reproduction, and behaviour.
8. **Source Identification and Pathway Analysis of Mercury Inputs**
    - Conduct targeted investigations of Hg sources**,** including geothermal inputs, atmospheric deposition, catchment runoff, and internal sediment recycling.
    - Combine Hg stable isotopes, elemental ratios (e.g. Hg:Mn, Hg:Se), and geochemical tracers to distinguish between natural geothermal versus anthropogenic contributions**.**
    - Assess how lake morphology and hydrodynamics influence retention, redistribution, and transformation of Hg once it enters the system.
9. **Evolutionary and Adaptive Toxicology in Geothermal Systems**
    - Investigate whether long-term exposure to elevated Hg and trace metals has driven physiological or biochemical adaptations in resident species such as trout, koura, and kakahi.
    - Examine variation in detoxification pathways (e.g. Hg–Se complex formation, antioxidant enzyme activity, metal-binding proteins) among populations inhabiting geothermal versus non-geothermal lakes.
    - Explore the potential for local adaptation or tolerance thresholds, providing insight into how chronic exposure shapes species responses to contaminant stress over evolutionary timescales.

10. **Otolith-Based Reconstruction of Mercury Exposure**
    - Utilize otolith microchemistry to reconstruct lifetime exposure histories of mercury and associated trace elements in fish.
    - Combine otolith Hg, Mn, and Se profiles with stable isotope data to identify exposure pathways, habitat use, and potential geothermal source signatures.
    - Apply otolith-derived timelines to assess chronic exposure and potential adaptive responses to long-term mercury stress in geothermal lake systems.

By addressing these research gaps, future studies can enhance understanding of mercury dynamics in freshwater ecosystems and inform more effective management strategies to mitigate mercury contamination and its ecological and human health risks.

7 References

Abreu, S., Pereira, E., Vale, C., & Duarte, Ac. (2000). Accumulation of mercury in sea bass from a contaminated lagoon (Ria de Aveiro, Portugal). *Marine Pollution Bulletin*, *40*(4), 293–297.

Amde, M., Yin, Y., Zhang, D., & Liu, J. (2016). Methods and recent advances in speciation analysis of mercury chemical species in environmental samples: A review. *Chemical Speciation & Bioavailability*, *28*(1–4), 51–65.

Amirbahman, A., Massey, D. I., Lotufo, G., Steenhaut, N., Brown, L. E., Biedenbach, J. M., & Magar, V. S. (2013). Assessment of mercury bioavailability to benthic macroinvertebrates using diffusive gradients in thin films (DGT). *Environmental Science: Processes & Impacts*, *15*(11), 2104–2114.

Ariya, P. A., Amyot, M., Dastoor, A., Deeds, D., Feinberg, A., Kos, G., Poulain, A., Ryjkov, A., Semeniuk, K., Subir, M., & Toyota, K. (2015). Mercury Physicochemical and Biogeochemical Transformation in the Atmosphere and at Atmospheric Interfaces: A Review and Future Directions. *Chemical Reviews*, *115*(10), 3760–3802. https://doi.org/10.1021/cr500667e

Armstrong, G. J., Janssen, S. E., Lepak, R. F., Rosera, T. J., Peterson, B. D., Cushing, S. T., Tate, M. T., & Hurley, J. P. (2025). Seasonal Stratification Drives Bioaccumulation of Pelagic Mercury Sources in Eutrophic Lakes. *ACS ES&T Water*, *5*(5), 2444–2454. https://doi.org/10.1021/acsestwater.5c00028

Arrighi, S., Franceschini, F., Petrini, R., Fornasaro, S., & Ghezzi, L. (2024). The Legacy of Hg Contamination in a Past Mining Area (Tuscany, Italy): Hg Speciation and Health Risk Assessment. *Toxics*, *12*(6), 436. https://doi.org/10.3390/toxics12060436

Atkinson, C. A., Jolley, D. F., & Simpson, S. L. (2007). Effect of overlying water pH, dissolved oxygen, salinity and sediment disturbances on metal release and sequestration from metal contaminated marine sediments. *Chemosphere*, *69*(9), 1428–1437.

Balshaw, S., Edwards, J. W., Ross, K., & Daughtry, B. (2008). Mercury distribution in the muscular tissue of farmed southern bluefin tuna (Thunnus maccoyii) is inversely related to the lipid content of tissues. *Food Chemistry*, *111*(3), 616–621.

Barkay, T., & Gu, B. (2022). Demethylation─The Other Side of the Mercury Methylation Coin: A Critical Review. *ACS Environmental Au*, *2*(2), 77–97. https://doi.org/10.1021/acsenvironau.1c00022

Basu, N., Bastiansz, A., Dórea, J. G., Fujimura, M., Horvat, M., Shroff, E., Weihe, P., & Zastenskaya, I. (2023). Our evolved understanding of the human health risks of mercury. *Ambio*, *52*(5), 877–896. https://doi.org/10.1007/s13280-023-01831-6

Bates, M. N. (2006). Mercury amalgam dental fillings: An epidemiologic assessment. *International Journal of Hygiene and Environmental Health*, *209*(4), 309–316. https://doi.org/10.1016/j.ijheh.2005.11.006

Baya, P. A., Gosselin, M., Lehnherr, I., St. Louis, V. L., & Hintelmann, H. (2015). Determination of monomethylmercury and dimethylmercury in the Arctic marine boundary layer. *Environmental Science & Technology*, *49*(1), 223–232.

Benoit, J. M., Gilmour, C. C., & Mason, R. P. (2001). The Influence of Sulfide on Solid-Phase Mercury Bioavailability for Methylation by Pure Cultures of *Desulfobulbus propionicus* (1pr3). *Environmental Science & Technology*, *35*(1), 127–132. https://doi.org/10.1021/es001415n

Benoit, J. M., Gilmour, C. C., Mason, R. P., & Heyes, A. (1999). Sulfide Controls on Mercury Speciation and Bioavailability to Methylating Bacteria in Sediment Pore Waters. *Environmental Science & Technology*, *33*(6), 951–957. https://doi.org/10.1021/es9808200

Berg, V., Ugland, K. I., Hareide, N. R., Groenningen, D., & Skaare, J. U. (2000). Mercury, cadmium, lead, and selenium in fish from a Norwegian fjord and off the coast, the importance of sampling localityPresented at QUASIMEME–QUASH 1999, Egmond aan Zee, The Netherlands, October 6–9, 1999. *Journal of Environmental Monitoring*, *2*(4), 375–377.

Berlin, M., Zalups, R., & Fowler, B. (2007). Mercury. Handbook on the toxicology of metals. *Elsevier*, *10*, B978-012369413.

Bloom, N. S. (1992). On the Chemical Form of Mercury in Edible Fish and Marine Invertebrate Tissue. *Canadian Journal of Fisheries and Aquatic Sciences*, *49*(5), 1010–1017. https://doi.org/10.1139/f92-113

Bloom, N. S., Gill, G. A., Cappellino, S., Dobbs, C., McShea, L., Driscoll, C., Mason, R., & Rudd, J. (1999). Speciation and cycling of mercury in Lavaca Bay, Texas, sediments. *Environmental Science & Technology*, *33*(1), 7–13.

Blum, J. D., Popp, B. N., Drazen, J. C., Anela Choy, C., & Johnson, M. W. (2013). Methylmercury production below the mixed layer in the North Pacific Ocean. *Nature Geoscience*, *6*(10), 879–884.

Boening, D. W. (2000). Ecological effects, transport, and fate of mercury: A general review. *Chemosphere*, *40*(12), 1335–1351.

Boudou, A., & Ribeyre, F. (1985). Experimental study of trophic contamination of Salmogairdneri by two mercury compounds—HgCl 2 and CH 3 HgCl—Analysis at the organism and organ levels. *Water, Air, and Soil Pollution*, *26*, 137–148.

Bowles, K. C., Apte, S. C., Maher, W. A., Kawei, M., & Smith, R. (2001). Bioaccumulation and biomagnification of mercury in lake Murray, Papua New Guinea. *Canadian Journal of Fisheries and Aquatic Sciences*, *58*(5), 888–897.

Bratkič, A., Klun, K., & Gao, Y. (2019). Mercury speciation in various aquatic systems using passive sampling technique of diffusive gradients in thin-film. *Science of the Total Environment*, *663*, 297–306.

Bretier, M., Dabrin, A., Billon, G., Mathon, B., Miege, C., & Coquery, M. (2020). To what extent can the biogeochemical cycling of mercury modulate the measurement of dissolved mercury in surface freshwaters by passive sampling? *Chemosphere*, *248*, 126006.

Britannica, E. (2025). Mercury. In *Encyloperdia Britannica*. https://www.britannica.com/science/mercury-chemical-element

Brooks, R., Lewis, J., & Reeves, R. (1976). Mercury and other heavy metals in trout of Central North Island, New Zealand. *New Zealand Journal of Marine and Freshwater Research*, *10*(2), 233–244.

Brown, J., Mercier, L., & Pinnavaia, T. J. (1999). Selective adsorption of Hg 2+ by thiol-functionalized nanoporous silica. *Chemical Communications*, *1*, 69–70.

Budtz-Jørgensen, E., Grandjean, P., Keiding, N., White, R. F., & Weihe, P. (2000). Benchmark dose calculations of methylmercury-associated neurobehavioural

deficits. *Toxicology Letters*, *112–113*, 193–199. https://doi.org/10.1016/S0378-4274(99)00283-0

Cabana, G., & Rasmussen, J. B. (1994). Modelling food chain structure and contaminant bioaccumulation using stable nitrogen isotopes. *Nature*, *372*(6503), 255–257.

Cantwell, M. G., Burgess, R. M., & Kester, D. R. (2002). Release and phase partitioning of metals from anoxic estuarine sediments during periods of simulated resuspension. *Environmental Science & Technology*, *36*(24), 5328–5334.

Cappuyns, V., & Swennen, R. (2005). Kinetics of element release during combined oxidation and pHstat leaching of anoxic river sediments. *Applied Geochemistry*, *20*(6), 1169–1179.

Cattani, I., Spalla, S., Beone, G., Del Re, A., Boccelli, R., & Trevisan, M. (2008). Characterization of mercury species in soils by HPLC–ICP-MS and measurement of fraction removed by diffusive gradient in thin films. *Talanta*, *74*(5), 1520–1526.

Cattani, I., Zhang, H., Beone, G. M., Del Re, A. A. M., Boccelli, R., & Trevisan, M. (2009). The role of natural purified humic acids in modifying mercury accessibility in water and soil. *Journal of Environmental Quality*, *38*(2), 493–501.

Chang, L.-Y., Davison, W., Zhang, H., & Kelly, M. (1998). Performance characteristics for the measurement of Cs and Sr by diffusive gradients in thin films (DGT). *Analytica Chimica Acta*, *368*(3), 243–253.

Chen, C. Y., & Folt, C. L. (2005). High plankton densities reduce mercury biomagnification. *Environmental Science & Technology*, *39*(1), 115–121.

Chen, C. Y., Stemberger, R. S., Kamman, N. C., Mayes, B. M., & Folt, C. L. (2005). Patterns of Hg bioaccumulation and transfer in aquatic food webs across multi-lake studies in the northeast US. *Ecotoxicology*, *14*, 135–147.

Chen, M.-L., Ma, H.-J., Zhang, S.-Q., & Wang, J.-H. (2011). Mercury speciation with L-cysteine functionalized cellulose fibre as adsorbent by atomic fluorescence spectrometry. *Journal of Analytical Atomic Spectrometry*, *26*(3), 613–617.

Chen, Y.-C., Chen, C.-Y., Hwang, H.-J., Chang, W.-B., Yeh, W.-J., & Chen, M.-H. (2004). Comparison of the metal concentrations in muscle and liver tissues of fishes from the Erren River, southwestern Taiwan, after the restoration in 2000. *Journal of Food and Drug Analysis*, *12*(4), 8.

Chess, T. W. (2010). *Laboratory optimization and field demonstration of diffusive gradients in thin films for in-situ mercury measurements of river sediments*.

Choi, S.-C., Chase Jr, T., & Bartha, R. (1994). Enzymatic catalysis of mercury methylation by Desulfovibrio desulfuricans LS. *Applied and Environmental Microbiology*, *60*(4), 1342–1346.

Chrystall, L., & Rumsby, A. (2009). Mercury Inventory for New Zealand 2008. *Ministry for the Environment*. https://environment.govt.nz/assets/Publications/Files/mercury-inventory-new-zealand-2008.pdf

Cizdziel, J., Hinners, T., Cross, C., & Pollard, J. (2003). Distribution of mercury in the tissues of five species of freshwater fish from Lake Mead, USA. *Journal of Environmental Monitoring*, *5*(5), 802. https://doi.org/10.1039/b307641p

Clarisse, O., & Hintelmann, H. (2006). Measurements of dissolved methylmercury in natural waters using diffusive gradients in thin film (DGT). *Journal of Environmental Monitoring*, *8*(12), 1242–1247.

Clarkson, T. W., Magos, L., & Myers, G. J. (2003). The Toxicology of Mercury—Current Exposures and Clinical Manifestations. *New England Journal of Medicine*, *349*(18), 1731–1737. https://doi.org/10.1056/NEJMra022471

Colaco, C. D., Yabuki, L. N. M., Rolisola, A. M., Menegário, A. A., de Almeida, E., Suárez, C. A., Gao, Y., Corns, W. T., & do Nascimento Filho, V. F. (2014). Determination of mercury in river water by diffusive gradients in thin films using P81 membrane as binding layer. *Talanta*, *129*, 417–421.

Coleman Wasik, J. K., Mitchell, C. P. J., Engstrom, D. R., Swain, E. B., Monson, B. A., Balogh, S. J., Jeremiason, J. D., Branfireun, B. A., Eggert, S. L., Kolka, R. K., & Almendinger, J. E. (2012). Methylmercury Declines in a Boreal Peatland When Experimental Sulfate Deposition Decreases. *Environmental Science & Technology*, *46*(12), 6663–6671. https://doi.org/10.1021/es300865f

Compeau, G., & Bartha, R. (1985). Sulfate-reducing bacteria: Principal methylators of mercury in anoxic estuarine sediment. *Applied and Environmental Microbiology*, *50*(2), 498–502.

Coulibaly, M., Bamba, D., Yao, N. A., Zoro, E. G., & El Rhazi, M. (2016). Some aspects of speciation and reactivity of mercury in various matrices. *Comptes Rendus. Chimie*, *19*(7), 832–840. https://doi.org/10.1016/j.crci.2016.02.005

Craig, P. (1986). Organomercury compounds in the environment. In *Organometallic compounds in the environment* (pp. 65–110). Longman Harlow.

Craig, P., Eng, G., & Jenkins, R. (1986). Occurrence and pathways of organometallic compounds in the environment—General considerations. *Organometallic Compounds in the Environment*, 1–55.

Davison, W., & Zhang, H. (1994). In situ speciation measurements of trace components in natural waters using thin-film gels. *Nature*, *367*(6463), 546–548.

Davison, W., & Zhang, H. (2012a). Progress in understanding the use of diffusive gradients in thin films (DGT) – back to basics. *Environmental Chemistry*, *9*(1), 1–13. https://doi.org/10.1071/EN11084

Davison, W., & Zhang, H. (2012b). Progress in understanding the use of diffusive gradients in thin films (DGT)–back to basics. *Environmental Chemistry*, *9*(1), 1–13.

Diviš, P., Szkandera, R., BRULíK, L., Dočekalová, H., MATúš, P., & Bujdoš, M. (2009). Application of new resin gels for measuring mercury by diffusive gradients in a thin-films technique. *Analytical Sciences*, *25*(4), 575–578.

Diviš, P., Szkandera, R., & Dočekalová, H. (2010). Characterization of sorption gels used for determination of mercury in aquatic environment by diffusive gradients in thin films technique. *Open Chemistry*, *8*(5), 1105–1109.

Dočekalová, H., & Diviš, P. (2005). Application of diffusive gradient in thin films technique (DGT) to measurement of mercury in aquatic systems. *Talanta*, *65*(5), 1174–1178.

Donovan, C. L., Donovan, W. F., Bioresearches (Firm), Ltd, B., & Plenty, B. of P. (N Z. : R. E. B. of. (2003). *Estimate of the Geothermal Nutrient Inputs to Twelve Rotorua Lakes*. Bioresearches, Consulting Biologists & Archaeologists. https://books.google.co.nz/books?id=qPwZRQAACAAJ

Downs, S., Macloed, C., & Lester, J. (1998). Mercury in precipitation and its relation to bioaccumulation in fish: A literature review. J Water Air Soil Pollut 108: 149–187. *Find This Article Online*.

Driscoll, C. T., Han, Y.-J., Chen, C. Y., Evers, D. C., Lambert, K. F., Holsen, T. M., Kamman, N. C., & Munson, R. (2007). Mercury contamination in remote forest and aquatic ecosystems in the northeastern US: sources, transformations and management options. *Bioscience*, *57*(1), 17–28.

Driscoll, C. T., Mason, R. P., Chan, H. M., Jacob, D. J., & Pirrone, N. (2013). Mercury as a global pollutant: Sources, pathways, and effects. *Environmental Science & Technology*, *47*(10), 4967–4983. https://doi.org/10.1021/es305071v

Drott, A., Lambertsson, L., Björn, E., & Skyllberg, U. (2008). Do potential methylation rates reflect accumulated methyl mercury in contaminated sediments? *Environmental Science & Technology*, *42*(1), 153–158.

Dus, L., Svobodová, Z., Janous, D., Vykusová, B., Jarkovskỳ, J., Šmíd, R., Pavlis, P., & others. (2005). Bioaccumulation of mercury in muscle tissue of fish in the Elbe River (Czech Republic): Multispecies monitoring study 1991–1996. *Ecotoxicology and Environmental Safety*, *61*(2), 256–267.

Edwards, T., Clayton, J., & de Winton, M. (2005). *The Condition of Lakes in the Waikato Region Using LakeSPi* (Nos 1172–4005; Environment Waikato Technical Report 2006/13). National Institute of Water and Atmostpheric Research Ltd.

Effler, S. W., & Bloom, N. S. (1990). Seasonal variability in the mercury speciation of Onondaga Lake (New York). *Water, Air, and Soil Pollution*, *53*, 251–265.

Ehrlich, H. L., & Newman, D. K. (Eds). (2008). *Geomicrobiology* (0 edn). CRC Press. https://doi.org/10.1201/9780849379079

Elinder, C., Friberg, L., Nordberg, G., & Vouk, V. (1986). Handbook on the toxicology of metals. *Amsterdam. Elsevier Science Publishers*, *2*, 664–679.

Essington, T. E., & Houser, J. N. (2003). The effect of whole-lake nutrient enrichment on mercury concentration in age-1 yellow perch. *Transactions of the American Fisheries Society*, *132*(1), 57–68.

Farkas, A., Salanki, J., & Varanka, I. (2000). Heavy metal concentrations in fish of Lake Balaton. *Lakes & Reservoirs: Research & Management*, *5*(4), 271–279.

Fatin-Rouge, N., Starchev, K., & Buffle, J. (2004). Size effects on diffusion processes within agarose gels. *Biophysical Journal*, *86*(5), 2710–2719.

Feng, X., Fryxell, G. E., Wang, L.-Q., Kim, A. Y., Liu, J., & Kemner, K. M. (1997). Functionalized monolayers on ordered mesoporous supports. *Science*, *276*(5314), 923–926.

Fergusson, J. E. (1990). *The Heavy Elements: Chemistry, Environmental Impact and Health Effects* (1st edn). Pergamon Press.

Fernández-Gómez, C., Bayona, J. M., & Díez, S. (2012). Laboratory and field evaluation of diffusive gradient in thin films (DGT) for monitoring levels of dissolved mercury in natural river water. *International Journal of Environmental Analytical Chemistry*, *92*(15), 1689–1698.

Fernández-Gómez, C., Dimock, B., Hintelmann, H., & Díez, S. (2011). Development of the DGT technique for Hg measurement in water: Comparison of three different types of samplers in laboratory assays. *Chemosphere*, *85*(9), 1452–1457.

Fitz, W. J., Wenzel, W. W., Zhang, H., Nurmi, J., Štipek, K., Fischerova, Z., Schweiger, P., Köllensperger, G., Ma, L. Q., & Stingeder, G. (2003). Rhizosphere characteristics of the arsenic hyperaccumulator Pteris vittata L. and monitoring of phytoremoval efficiency. *Environmental Science & Technology*, *37*(21), 5008–5014.

Fitzegerald, W. (1989). *Atmospheric and oceanic cycling of mercury. Chemical Oceanography, vol. 10*. Academic Press, London.

Fitzgerald, W. F., & Clarkson, T. W. (1991). Mercury and monomethylmercury: Present and future concerns. *Environmental Health Perspectives*, *96*, 159–166.

Fitzgerald, W. F., Engstrom, D. R., Mason, R. P., & Nater, E. A. (1998). The case for atmospheric mercury contamination in remote areas. *Environmental Science & Technology*, *32*(1), 1–7.

Fitzgerald, W. F., Lamborg, C. H., & Hammerschmidt, C. R. (2007). Marine biogeochemical cycling of mercury. *Chemical Reviews*, *107*(2), 641–662.

Fleming, E. J., Mack, E. E., Green, P. G., & Nelson, D. C. (2006). Mercury methylation from unexpected sources: Molybdate-inhibited freshwater sediments and an iron-reducing bacterium. *Applied and Environmental Microbiology*, *72*(1), 457–464.

Fowler, S. W. (1990). Critical review of selected heavy metal and chlorinated hydrocarbon concentrations in the marine environment. *Marine Environmental Research*, *29*(1), 1–64.

Friberg, L., & Vostal, J. (1972). *Mercury in the environment: A toxicological and epidemiological appraisal*.

Gao, Y., De Canck, E., Leermakers, M., Baeyens, W., & Van Der Voort, P. (2011). Synthesized mercaptopropyl nanoporous resins in DGT probes for determining dissolved mercury concentrations. *Talanta*, *87*, 262–267.

Garmo, Ø. A., Davison, W., & Zhang, H. (2008). Effects of binding of metals to the hydrogel and filter membrane on the accuracy of the diffusive gradients in thin films technique. *Analytical Chemistry*, *80*(23), 9220–9225.

Garmo, Ø. A., Røyset, O., Steinnes, E., & Flaten, T. P. (2003). Performance study of diffusive gradients in thin films for 55 elements. *Analytical Chemistry*, *75*(14), 3573–3580.

Gill, G. A., & Bruland, K. W. (1990). Mercury speciation in surface freshwater systems in California and other areas. *Environmental Science & Technology*, *24*(9), 1392–1400.

Gilmour, C. C., Henry, E. A., & Mitchell, R. (1992). Sulfate stimulation of mercury methylation in freshwater sediments. *Environmental Science & Technology*, *26*(11), 2281–2287.

Goldstein, R. M., Brigham, M. E., & Stauffer, J. C. (1996). Comparison of mercury concentrations in liver, muscle, whole bodies, and composites of fish from the Red River of the North. *Canadian Journal of Fisheries and Aquatic Sciences*, *53*(2), 244–252. https://doi.org/10.1139/f95-203

Gonzalez, P., Dominique, Y., Massabuau, J.-C., Boudou, A., & Bourdineaud, J.-P. (2005). Comparative effects of dietary methylmercury on gene expression in liver, skeletal muscle, and brain of the zebrafish (Danio rerio). *Environmental Science & Technology*, *39*(11), 3972–3980.

Grandjean, P., Weihe, P., White, R. F., Debes, F., Araki, S., Yokoyama, K., Murata, K., Sørensen, N., Dahl, R., & Jørgensen, P. J. (1997). Cognitive Deficit in 7-Year-Old Children with Prenatal Exposure to Methylmercury. *Neurotoxicology and Teratology*, *19*(6), 417–428. https://doi.org/10.1016/S0892-0362(97)00097-4

Harley, J., Lieske, C., Bhojwani, S., Castellini, J. M., López, J. A., & O'Hara, T. M. (2015). Mercury and methylmercury distribution in tissues of sculpins from the Bering Sea. *Polar Biology*, *38*, 1535–1543.

Hatch, W. R., & Ott, W. L. (1968). Determination of submicrogram quantities of mercury by atomic absorption spectrophotometry. *Analytical Chemistry*, *40*(14), 2085–2087.

Havelková, M., Dušek, L., Némethová, D., Poleszczuk, G., & Svobodová, Z. (2008). Comparison of Mercury Distribution Between Liver and Muscle – A Biomonitoring of Fish from Lightly and Heavily Contaminated Localities. *Sensors*, *8*(7), 4095–4109. https://doi.org/10.3390/s8074095

Hintelmann, H., Evans, R. D., & Villeneuve, J. Y. (1995). Measurement of mercury methylation in sediments by using enriched stable mercury isotopes combined with methylmercury determination by gas chromatography–inductively coupled plasma mass spectrometry. *Journal of Analytical Atomic Spectrometry*, *10*(9), 619–624.

Honda, K., Sahrul, M., Hidaka, H., & Tatsukawa, R. (1983). Organ and tissue distribution of heavy metals, and their growth-related changes in Antarctic fish, Pagothenia borchgrevinki. *Agricultural and Biological Chemistry*, *47*(11), 2521–2532.

Hong, Y. S., Kinney, K. A., & Reible, D. D. (2011). Effects of cyclic changes in pH and salinity on metals release from sediments. *Environmental Toxicology and Chemistry*, *30*(8), 1775–1784.

Hong, Y. S., Rifkin, E., & Bouwer, E. J. (2011). Combination of diffusive gradient in a thin film probe and IC-ICP-MS for the simultaneous determination of CH3Hg+ and Hg2+ in oxic water. *Environmental Science & Technology*, *45*(15), 6429–6436.

Houserova, P., Kuban, V., Spurny, P., Habarta, P., & others. (2006). Determination of total mercury and mercury species in fish and aquatic ecosystems of Moravian rivers. *VETERINARNI MEDICINA-PRAHA-*, *51*(3), 101.

Hsu-Kim, H., Kucharzyk, K. H., Zhang, T., & Deshusses, M. A. (2013). Mechanisms regulating mercury bioavailability for methylating microorganisms in the aquatic environment: A critical review. *Environmental Science & Technology*, *47*(6), 2441–2456.

Jackson, T. A. (1997). Long-range atmospheric transport of mercury to ecosystems, and the importance of anthropogenic emissions—A critical review and evaluation of the published evidence. *Environmental Reviews*, *5*(2), 99–120. https://doi.org/10.1139/a97-005

Jeong, H., Ali, W., Zinck, P., Souissi, S., & Lee, J.-S. (2024). Toxicity of methylmercury in aquatic organisms and interaction with environmental factors and coexisting pollutants: A review. *Science of The Total Environment*, *943*, 173574. https://doi.org/10.1016/j.scitotenv.2024.173574

Jewett, S. C., Zhang, X., Naidu, A. S., Kelley, J. J., Dasher, D., & Duffy, L. K. (2003). Comparison of mercury and methylmercury in northern pike and Arctic grayling from western Alaska rivers. *Chemosphere*, *50*(3), 383–392.

Johnels, A., & Westermark, T. (1969). Mercury contamination of the environment in Sweden. *Chemical Fallout: Current Research on Persistent Pesticides.*, 221–241.

Johnson, F. O., & Atchison, W. D. (2009). The role of environmental mercury, lead and pesticide exposure in development of amyotrophic lateral sclerosis. *Neurotoxicology*, *30*(5), 761–765.

Kamman, N. C., Lorey, P. M., Driscoll, C. T., Estabrook, R., Major, A., Pientka, B., & Glassford, E. (2004). Assessment of mercury in waters, sediments, and biota of New Hampshire and Vermont lakes, USA, sampled using a geographically randomized design. *Environmental Toxicology and Chemistry: An International Journal*, *23*(5), 1172–1186.

Kannan, K., Smith, R., Jr, Lee, R., Windom, H., Heitmuller, P., Macauley, J., & Summers, J. (1998). Distribution of total mercury and methyl mercury in water, sediment, and fish from south Florida estuaries. *Archives of Environmental Contamination and Toxicology*, *34*, 109–118.

Keating, M. H., Mahaffey, K., Schoeny, R., Rice, G., & Bullock, O. (1997). *Mercury study report to Congress. Volume 1. Executive summary*. Environmental Protection Agency, Research Triangle Park, NC (United States).

Kennedy, C. J. (2003). Uptake and accumulation of mercury from dental amalgam in the common goldfish, Carassius auratus. *Environmental Pollution*, *121*(3), 321–326.

Kim, J. P. (1995). Methylmercury in rainbow trout (Oncorhynchus mykiss) from Lakes Okareka, Okaro, Rotomahana, Rotorua and Tarawera, North Island, New Zealand. *Science of the Total Environment*, *164*(3), 209–219.

Kim, J. P., & Burggraaf, S. (1999). Mercury bioaccumulation in rainbow trout (Oncorhynchus mykiss) and the trout food web in lakes Okareka, Okaro, Tarawera,

Rotomahana and Rotorua, New Zealand. *Water, Air, and Soil Pollution*, *115*, 535–546.

KIYOURA, R. (1964). Water pollution and Minamata disease. In *Advances in Water Pollution Research* (pp. 291–308). Elsevier.

Krabbenhoft, D. P., & Babiarz, C. L. (1992). The role of groundwater transport in aquatic mercury cycling. *Water Resources Research*, *28*(12), 3119–3128.

Lacerda, L. D., & Salomons, W. (1998). *Mercury from Gold and Silver Mining: A Chemical Time Bomb?* Springer Berlin Heidelberg. https://doi.org/10.1007/978-3-642-58793-1

Lawrence, A., & Mason, R. (2001). Factors controlling the bioaccumulation of mercury and methylmercury by the estuarine amphipod Leptocheirus plumulosus. *Environmental Pollution*, *111*(2), 217–231.

Lead, J., Hamilton-Taylor, J., Hesketh, N., Jones, M., Wilkinson, A., & Tipping, E. (1994). A comparative study of proton and alkaline earth metal binding by humic substances. *Analytica Chimica Acta*, *294*(3), 319–327.

Lee, B. J., Kwon, S. Y., Yin, R., Li, M., Jung, S., Lim, S. H., Lee, J. H., Kim, K. W., Kim, K. D., & Jang, J. W. (2020). Internal dynamics of inorganic and methylmercury in a marine fish: Insights from mercury stable isotopes. *Environmental Pollution*, *267*, 115588. https://doi.org/10.1016/j.envpol.2020.115588

Li, W., Teasdale, P. R., Zhang, S., John, R., & Zhao, H. (2003). Application of a poly (4-styrenesulfonate) liquid binding layer for measurement of Cu2+ and Cd2+ with the

diffusive gradients in thin-films technique. *Analytical Chemistry*, *75*(11), 2578–2583.

Li, Y., Mao, Y., Liu, G., Tachiev, G., Roelant, D., Feng, X., & Cai, Y. (2010). Degradation of Methylmercury and Its Effects on Mercury Distribution and Cycling in the Florida Everglades. *Environmental Science & Technology*, *44*(17), 6661–6666. https://doi.org/10.1021/es1010434

Liu, A., Hidajat, K., Kawi, S., & Zhao, D. (2000). A new class of hybrid mesoporous materials with functionalized organic monolayers for selective adsorption of heavy metal ions. *Chemical Communications*, *13*, 1145–1146.

Luengen, A. C., & Russell Flegal, A. (2009). Role of phytoplankton in mercury cycling in the San Francisco Bay estuary. *Limnology and Oceanography*, *54*(1), 23–40.

Makar, A. B., McMartin, K. E., Palese, M., & Tephly, T. R. (1975). Formate assay in body fluids: Application in methanol poisoning. *Biochemical Medicine*, *13*(2), 117–126. https://doi.org/10.1016/0006-2944(75)90147-7

Marrugo-Madrid, S., Salas-Moreno, M., Gutiérrez-Mosquera, H., Salazar-Camacho, C., Marrugo-Negrete, J., & Díez, S. (2022). Assessment of dissolved mercury by diffusive gradients in thin films devices in abandoned ponds impacted by small scale gold mining. *Environmental Research*, *208*, 112633.

Maršálek, P., Svobodová, Z., & Randák, T. (2007). The content of total mercury and methylmercury in common carp from selected Czech ponds. *Aquaculture International*, *15*, 299–304.

Mason, R. P., Fitzgerald, W. F., & Morel, F. M. (1994). The biogeochemical cycling of elemental mercury: Anthropogenic influences. *Geochimica et Cosmochimica Acta*, *58*(15), 3191–3198.

Mason, S., Hamon, R., Nolan, A., Zhang, H., & Davison, W. (2005). Performance of a mixed binding layer for measuring anions and cations in a single assay using the diffusive gradients in thin films technique. *Analytical Chemistry*, *77*(19), 6339–6346.

Mierle, G., & Ingram, R. (1991). The role of humic substances in the mobilization of mercury from watersheds. *Water Air & Soil Pollution*, *56*, 349–357.

Minamata Convention on Mercury: Text and annexes. (2024). In *Minamata Convention on Mercury*. Minamata Convention.

Miskimmin, B. (1991). Effect of natural levels of dissolved organic carbon (DOC) on methyl mercury formation and sediment-water partitioning. *Bulletin of Environmental Contamination and Toxicology;(United States)*, *47*(5).

Mongin, S., Uribe, R., Puy, J., Cecília, J., Galceran, J., Zhang, H., & Davison, W. (2011). Key role of the resin layer thickness in the lability of complexes measured by DGT. *Environmental Science & Technology*, *45*(11), 4869–4875.

Monnet-Tschudi, F., Zurich, M.-G., Boschat, C., Corbaz, A., & Honegger, P. (2006). Involvement of environmental mercury and lead in the etiology of neurodegenerative diseases. *Reviews on Environmental Health*, *21*(2), 105–118.

Morel, F. M., Kraepiel, A. M., & Amyot, M. (1998). The chemical cycle and bioaccumulation of mercury. *Annual Review of Ecology and Systematics*, *29*(1), 543–566.

Morita, M., Yoshinaga, J., & Edmonds, J. S. (1998). The determination of mercury species in environmental and biological samples (Technical report). *Pure and Applied Chemistry*, *70*(8), 1585–1615.

Murdock, C., Kelly, M., Chang, L.-Y., Davison, W., & Zhang, H. (2001). DGT as an in situ tool for measuring radiocesium in natural waters. *Environmental Science & Technology*, *35*(22), 4530–4535.

Mutter, J., Curth, A., Naumann, J., Deth, R., & Walach, H. (2010). Does inorganic mercury play a role in Alzheimer's disease? A systematic review and an integrated molecular mechanism. *Journal of Alzheimer's Disease*, *22*(2), 357–374.

Nooney, R. I., Kalyanaraman, M., Kennedy, G., & Maginn, E. J. (2001). Heavy metal remediation using functionalized mesoporous silicas with controlled macrostructure. *Langmuir*, *17*(2), 528–533.

Nriagu, J. O. (1989). A global assessment of natural sources of atmospheric trace metals. *Nature*, *338*(6210), 47–49. https://doi.org/10.1038/338047a0

Ogle, R. S., & Knight, A. W. (1996). Selenium bioaccumulation in aquatic ecosystems: 1. Effects of sulfate on the uptake and toxicity of selenate in Daphnia magna. *Archives of Environmental Contamination and Toxicology*, *30*(2), 274–279. https://doi.org/10.1007/BF00215808

Pak, K.-R., & Bartha, R. (1998). Mercury methylation and demethylation in anoxic lake sediments and by strictly anaerobic bacteria. *Applied and Environmental Microbiology*, *64*(3), 1013–1017.

Pan, F., Huang, J., & Feng, X. (2024). Sources, Fates, and Geochemical Cycling of Mercury in Geothermal Fields: Insights From Mercury Isotopes. *Geophysical Research Letters*, *51*(9), e2023GL107384. https://doi.org/10.1029/2023GL107384

Paquette, K., & Helz, G. (1995). Solubility of cinnabar (red HgS) and implications for mercury speciation in sulfidic waters. *Water, Air, and Soil Pollution*, *80*, 1053–1056.

Pickhardt, P. C., Folt, C. L., Chen, C. Y., Klaue, B., & Blum, J. D. (2002). Algal blooms reduce the uptake of toxic methylmercury in freshwater food webs. *Proceedings of the National Academy of Sciences*, *99*(7), 4419–4423.

Pirrone, N., Cinnirella, S., Feng, X., Finkelman, R. B., Friedli, H. R., Leaner, J., Mason, R., Mukherjee, A. B., Stracher, G. B., Streets, D. G., & Telmer, K. (2010). Global mercury emissions to the atmosphere from anthropogenic and natural sources. *Atmospheric Chemistry and Physics*, *10*(13), 5951–5964. https://doi.org/10.5194/acp-10-5951-2010

Polak-Juszczak, L. (2018). Distribution of organic and inorganic mercury in the tissues and organs of fish from the southern Baltic Sea. *Environmental Science and Pollution Research*, *25*(34), 34181–34189. https://doi.org/10.1007/s11356-018-3336-9

Pullout guide to food safety in pregnancy. (2023, May). [Ministry for Primary Industries]. New Zealand Food Safety. https://www.mpi.govt.nz/food-safety-home/food-pregnancy/list-safe-food-pregnancy#mercury-intake

Quevauviller, P. (1996). CRMs for quality control of determinations of chemical forms of elements in support to EU legislation. *Fresenius' Journal of Analytical Chemistry*, *354*, 515–520.

Ralston, N. V. C., & Raymond, L. J. (2018). Mercury's neurotoxicity is characterized by its disruption of selenium biochemistry. *Biochimica et Biophysica Acta (BBA) - General Subjects*, *1862*(11), 2405–2416. https://doi.org/10.1016/j.bbagen.2018.05.009

Ravichandran, M. (2004). Interactions between mercury and dissolved organic matter—-A review. *Chemosphere*, *55*(3), 319–331.

Regnell, O., & Tesson, SylvieV. M. (2024). Total mercury and methylmercury in lake water in years before and after removal of mercury-polluted pulp fiber sediment. *Environmental Pollution*, *362*, 125011. https://doi.org/10.1016/j.envpol.2024.125011

Regnell, O., & Watras, Carl. J. (2019). Microbial Mercury Methylation in Aquatic Environments: A Critical Review of Published Field and Laboratory Studies. *Environmental Science & Technology*, *53*(1), 4–19. https://doi.org/10.1021/acs.est.8b02709

Reza, A. S., Jean, J.-S., Lee, M.-K., Liu, C.-C., Bundschuh, J., Yang, H.-J., Lee, J.-F., & Lee, Y.-C. (2010). Implications of organic matter on arsenic mobilization into groundwater: Evidence from northwestern (Chapai-Nawabganj), central (Manikganj) and southeastern (Chandpur) Bangladesh. *Water Research*, *44*(19), 5556–5574.

Scally, S., Davison, W., & Zhang, H. (2006). Diffusion coefficients of metals and metal complexes in hydrogels used in diffusive gradients in thin films. *Analytica Chimica Acta*, *558*(1–2), 222–229.

Schintu, M., Marrucci, A., Marras, B., Atzori, M., & Pellegrini, D. (2018). Passive sampling monitoring of PAHs and trace metals in seawater during the salvaging of the Costa Concordia wreck (Parbuckling Project). *Marine Pollution Bulletin*, *135*, 819–827.

Scholes, P., & Hamil, K. (2016). *Rotorua Lakes Water Quality Report 2014/2015* (Environmental Publication Nos 1179–9471). Bay of Plenty Regional Council.

Shade, C. W. (2008). Automated simultaneous analysis of monomethyl and mercuric Hg in biotic samples by Hg-thiourea complex liquid chromatography following acidic thiourea leaching. *Environmental Science & Technology*, *42*(17), 6604–6610.

Shade, C. W., & Hudson, R. J. (2005). Determination of MeHg in environmental sample matrices using Hg- Thiourea complex ion chromatography with on-line cold vapor generation and atomic fluorescence spectrometric detection. *Environmental Science & Technology*, *39*(13), 4974–4982.

Si, L., Branfireun, B. A., & Fierro, J. (2022). Chemical Oxidation and Reduction Pathways of Mercury Relevant to Natural Waters: A Review. *Water*, *14*(12), 1891. https://doi.org/10.3390/w14121891

Simpson, S. L., Apte, S. C., & Batley, G. E. (1998). Effect of short-term resuspension events on trace metal speciation in polluted anoxic sediments. *Environmental Science & Technology*, *32*(5), 620–625.

Spiller, H. A. (2018). Rethinking mercury: The role of selenium in the pathophysiology of mercury toxicity. *Clinical Toxicology*, *56*(5), 313–326. https://doi.org/10.1080/15563650.2017.1400555

Storm, D. L. (2020). Chemical monitoring of California's public drinking water sources: Public exposures and health impacts. In *Water contamination and health* (pp. 67–124). CRC Press.

Suárez-Criado, L., Queipo-Abad, S., Rodríguez-Cea, A., Rodríguez-González, P., & García Alonso, J. I. (2022). Comparison of GC-ICP-MS, GC-EI-MS and GC-EI-MS/MS for the determination of methylmercury, ethylmercury and inorganic mercury in biological samples by triple spike species-specific isotope dilution mass spectrometry. *Journal of Analytical Atomic Spectrometry*, *37*(7), 1462–1470. https://doi.org/10.1039/D2JA00086E

Teasdale, P. R., Hayward, S., & Davison, W. (1999). In situ, high-resolution measurement of dissolved sulfide using diffusive gradients in thin films with computer-imaging densitometry. *Analytical Chemistry*, *71*(11), 2186–2191.

Timperley, M. H., & Hill, L. F. (1997). Discharge of mercury from the Wairakei geothermal power station to the Waikato River, New Zealand. *New Zealand Journal of Marine and Freshwater Research*, *31*(3), 327–336. https://doi.org/10.1080/00288330.1997.9516770

Turull, M., Komarova, T., Noller, B., Fontàs, C., & Díez, S. (2018). Evaluation of mercury in a freshwater environment impacted by an organomercury fungicide using diffusive gradient in thin films. *Science of the Total Environment*, *621*, 1475–1484.

Van de Weerd, H., Van Riemsdijk, W., & Leijnse, A. (1999). Modeling the dynamic adsorption/desorption of a NOM mixture: Effects of physical and chemical heterogeneity. *Environmental Science & Technology*, *33*(10), 1675–1681.

Van Der Veeken, P. L., Pinheiro, J. P., & Van Leeuwen, H. P. (2008). Metal speciation by DGT/DET in colloidal complex systems. *Environmental Science & Technology*, *42*(23), 8835–8840.

Van Griethuysen, C., Luitwieler, M., Joziasse, J., & Koelmans, A. A. (2005). Temporal variation of trace metal geochemistry in floodplain lake sediment subject to dynamic hydrological conditions. *Environmental Pollution*, *137*(2), 281–294.

Verburg, P., Hickey, C. W., & Phillips, N. (2014). Mercury biomagnification in three geothermally-influenced lakes differing in chemistry and algal biomass. *Science of the Total Environment*, *493*, 342–354.

Vieira, E. F., Simoni, J. de A., & Airoldi, C. (1997). Interaction of cations with SH-modified silica gel: Thermochemical study through calorimetric titration and direct extent of reaction determination. *Journal of Materials Chemistry*, *7*(11), 2249–2252.

Vigh, P., Mastala, Z., Katalin, V., & others. (1996). Comparison of heavy metal concentration of grass carp (Ctenopharyngodon idella Cuv. Et Val.) in a shallow eutrophic lake and a fish pond (possible effects of food contamination). *Chemosphere*, *32*(4), 691–701.

Vlassopoulos, D., Kanematsu, M., Henry, E. A., Goin, J., Leven, A., Glaser, D., Brown, S. S., & O'Day, P. A. (2018). Manganese(IV) oxide amendments reduce methylmercury concentrations in sediment porewater. *Environmental Science: Processes & Impacts*, *20*(12), 1746–1760. https://doi.org/10.1039/C7EM00583K

Wang, N., Zhu, Y., Sheng, L., & Meng, D. (2005). Mercury pollution in Rana Chensinensis in Weisha River reach, in the upstream region of Songhua River. *Chinese Science Bulletin*, *50*, 2166–2170.

Wang, R., Feng, X.-B., & Wang, W.-X. (2013). In Vivo Mercury Methylation and Demethylation in Freshwater Tilapia Quantified by Mercury Stable Isotopes. *Environmental Science & Technology*, *47*(14), 7949–7957. https://doi.org/10.1021/es3043774

Wang, W.-X., Stupakoff, I., Gagnon, C., & Fisher, N. S. (1998). Bioavailability of inorganic and methylmercury to a marine deposit-feeding polychaete. *Environmental Science & Technology*, *32*(17), 2564–2571.

Wang, X., & Wang, W.-X. (2017). Selenium induces the demethylation of mercury in marine fish. *Environmental Pollution*, *231*, 1543–1551. https://doi.org/10.1016/j.envpol.2017.09.014

Ward, D. M., Nislow, K. H., Chen, C. Y., & Folt, C. L. (2010). Rapid, efficient growth reduces mercury concentrations in stream-dwelling Atlantic salmon. *Transactions of the American Fisheries Society*, *139*(1), 1–10.

Warner, K. A., Roden, E. E., & Bonzongo, J.-C. (2003). Microbial mercury transformation in anoxic freshwater sediments under iron-reducing and other electron-accepting conditions. *Environmental Science & Technology*, *37*(10), 2159–2165.

Warnken, K. W., Davison, W., Zhang, H., Galceran, J., & Puy, J. (2007). In situ measurements of metal complex exchange kinetics in freshwater. *Environmental Science & Technology*, *41*(9), 3179–3185.

Warnken, K. W., Zhang, H., & Davison, W. (2004). Performance characteristics of suspended particulate reagent-iminodiacetate as a binding agent for diffusive gradients in thin films. *Analytica Chimica Acta*, *508*(1), 41–51.

Warnken, K. W., Zhang, H., & Davison, W. (2006). Accuracy of the diffusive gradients in thin-films technique: Diffusive boundary layer and effective sampling area considerations. *Analytical Chemistry*, *78*(11), 3780–3787.

Watras, C., Back, R., Halvorsen, S., Hudson, R., Morrison, K., & Wente, S. (1998). Bioaccumulation of mercury in pelagic freshwater food webs. *Science of the Total Environment*, *219*(2–3), 183–208.

Weber, J. H. (1993). Review of possible paths for abiotic methylation of mercury (II) in the aquatic environment. *Chemosphere*, *26*(11), 2063–2077.

Weissberg, B., & Zobel, M. (1973). Geothermal mercury pollution in New Zealand. *Bulletin of Environmental Contamination and Toxicology*, *9*, 148–155.

Westöö, G. (1973). Methylmercury as Percentage of Total Mercury in Flesh and Viscera of Salmon and Sea Trout of Various Ages. *Science*, *181*(4099), 567–568. https://doi.org/10.1126/science.181.4099.567

WHO, I. (1990). Environmental health criteria 101: Methylmercury. *World Heal. Organ. Geneva*, *144*.

Wiener, J., Krabbenhoft, D., Heinz, G., & Scheuhammer, A. (2002). Ecotoxicology Of Mercury. In D. Hoffman, B. Rattner, G. Allen Burton Jr, & J. Cairns Jr (Eds), *Handbook of Ecotoxicology, Second Edition*. CRC Press. https://doi.org/10.1201/9781420032505.ch16

Williams, M. J., Ogle, R. S., Knight, A. W., & Burau, R. G. (1994). Effects of sulfate on selenate uptake and toxicity in the green alga Selenastrum capricornutum. *Archives of Environmental Contamination and Toxicology*, *27*(4). https://doi.org/10.1007/BF00214834

Wood, J. M., Kennedy, F. S., & Rosen, C. (1968). Synthesis of methyl-mercury compounds by extracts of a methanogenic bacterium. *Nature*, *220*(5163), 173–174.

Wu, T., Wang, G., Zhang, Y., Kong, M., & Zhao, H. (2017). Determination of mercury in aquatic systems by DGT device using thiol-modified carbon nanoparticle suspension as the liquid binding phase. *New Journal of Chemistry*, *41*(18), 10305–10311.

Yao, H., Zhao, Y., Lin, C.-J., Yi, F., Liang, X., & Feng, X. (2020). Development of a novel composite resin for dissolved divalent mercury measurement using diffusive gradients in thin films. *Chemosphere*, *251*, 126231.

Young, R. (2009). Life in fresh water—Fish. In *The Encyclopedia of New Zealand*. Te Ara. https://teara.govt.nz/en/life-in-fresh-water/page-4

Yu, X., Driscoll, C. T., Montesdeoca, M., Evers, D., Duron, M., Williams, K., Schoch, N., & Kamman, N. C. (2011). Spatial patterns of mercury in biota of Adirondack, New York lakes. *Ecotoxicology*, *20*, 1543–1554.

Zhang, H., & Davison, W. (1999). Diffusional characteristics of hydrogels used in DGT and DET techniques. *Analytica Chimica Acta*, *398*(2–3), 329–340.

Zhang, H., & Davison, W. (2000). Direct in situ measurements of labile inorganic and organically bound metal species in synthetic solutions and natural waters using diffusive gradients in thin films. *Analytical Chemistry*, *72*(18), 4447–4457.

Zhang, H., Davison, W., Gadi, R., & Kobayashi, T. (1998). In situ measurement of dissolved phosphorus in natural waters using DGT. *Analytica Chimica Acta*, *370*(1), 29–38.

Zhang, H., Davison, W., Miller, S., & Tych, W. (1995). In situ high resolution measurements of fluxes of Ni, Cu, Fe, and Mn and concentrations of Zn and Cd in porewaters by DGT. *Geochimica et Cosmochimica Acta*, *59*(20), 4181–4192.